sid.inpe.br/mtc-m21c/2021/02.24.17.54-TDI

AMAZONIAN JURUÁ RIVER MEANDER MIGRATION IMPACT ON RIVERINE COMMUNITIES: A CASE OF STUDY USING REMOTE SENSING TIME SERIES AND CLOUD COMPUTING

Gustavo Willy Nagel

Master's Dissertation of the Graduate Course in Remote Sensing, guided by Drs. Evlyn Márcia Leão de Moraes Novo, and Vitor Souza Martins, approved in February 25, 2021.

URL of the original document:
<http://urlib.net/8JMKD3MGP3W34R/448DFQL>

INPE
São José dos Campos
2021

PUBLISHED BY:

Instituto Nacional de Pesquisas Espaciais - INPE
Coordenação de Ensino, Pesquisa e Extensão (COEPE)
Divisão de Biblioteca (DIBIB)
CEP 12.227-010
São José dos Campos - SP - Brasil
Tel.:(012) 3208-6923/7348
E-mail: pubtc@inpe.br

sid.inpe.br/mtc-m21c/2021/02.24.17.54-TDI

AMAZONIAN JURUÁ RIVER MEANDER MIGRATION IMPACT ON RIVERINE COMMUNITIES: A CASE OF STUDY USING REMOTE SENSING TIME SERIES AND CLOUD COMPUTING

Gustavo Willy Nagel

Master's Dissertation of the Graduate Course in Remote Sensing, guided by Drs. Evlyn Márcia Leão de Moraes Novo, and Vitor Souza Martins, approved in February 25, 2021.

URL of the original document:
<http://urlib.net/8JMKD3MGP3W34R/448DFQL>

INPE
São José dos Campos
2021

Cataloging in Publication Data

Nagel, Gustavo Willy.

N131a Amazonian Juruá river meander migration impact on riverine communities: a case of study using remote sensing time series and cloud computing / Gustavo Willy Nagel. – São José dos Campos : INPE, 2021.

xiv + 101 p. ; (sid.inpe.br/mtc-m21c/2021/02.24.17.54-TDI)

Dissertation (Master in Remote Sensing) – Instituto Nacional de Pesquisas Espaciais, São José dos Campos, 2021.

Guiding : Drs. Evlyn Márcia Leão de Moraes Novo, and Vitor Souza Martins.

1. Google Earth Engine. 2. Floodplains. 3. Landsat. I.Title.

CDU 528.8(282.281.3)

MINISTÉRIO DA CIÊNCIA, TECNOLOGIA E INOVAÇÕES

INSTITUTO NACIONAL DE PESQUISAS ESPACIAIS

Serviço de Pós-Graduação - SEPGR

DEFESA FINAL DE DISSERTAÇÃO DE GUSTAVO WILLY NAGEL

BANCA Nº 022/2021, REG 14077/2019

No dia 25 de fevereiro de 2021, as 09h, por teleconferência, o(a) aluno(a) mencionado(a) acima defendeu seu trabalho final (apresentação oral seguida de arguição) perante uma Banca Examinadora, cujos membros estão listados abaixo. O(A) aluno(a) foi APROVADO(A) pela Banca Examinadora, por unanimidade, em cumprimento ao requisito exigido para obtenção do Título de Mestre em Sensoriamento Remoto. O trabalho precisa da incorporação das correções sugeridas pela Banca Examinadora e revisão final pelo(s) orientador(es).

Título: "AMAZONIAN JURUÁ RIVER MEANDER MIGRATION IMPACT ON RIVERINE COMMUNITIES: A CASE OF STUDY USING REMOTE SENSING TIME SERIES AND CLOUD COMPUTING"

Eu, Cláudio Clemente Faria Barbosa, como Presidente da Banca Examinadora, assino esta ATA em nome de todos os membros.

Dr. Cláudio Clemente Faria Barbosa - Presidente - INPE

Dra. Evlyn Márcia Leão de Moraes Novo - Orientadora - INPE

Dr. Vitor Souza Martins - Orientador - Michigan State University

Dr. João Vitor Campos e Silva - Convidado - Norwegian University of Life Sciences

Dr. Marie Paule Bonnet - Convidada - Institut de Recherche pour le Développement

Documento assinado eletronicamente por **Cláudio Clemente Faria Barbosa**, **Tecnologista**, em 01/03/2021, às 09:19 (horário oficial de Brasília), com fundamento no art. 6º do Decreto nº 8.539, de 8 de outubro de 2015.

A autenticidade deste documento pode ser conferida no site http://sei.mctic.gov.br/verifica.html, informando o código verificador **6555076** e o código CRC **72AB5402**.

Referência: Processo nº 01340.001196/2021-02 SEI nº 6555076

AGRADECIMENTOS

Eu gostaria de agradecer a meus pais Osvaldo Willy Nagel e Mary Ana da Silva Nagel que sempre me apoiaram e incentivaram a estudar. A meu irmão Frederico Nagel, pelos incentivos na realização dessa dissertação.

Gostaria de agradecer à minha namorada Valéria Cabreira Cabrera, pelo carinho e valiosos conselhos durante esse período.

Aos meus orientadores Dr. Evlyn Novo e Dr. Vitor Martins, pela amizade, confiança, dedicação, debates e conselhos que foram fundamentais para o desenvolvimento dessa dissertação e para a minha formação como cientista.

Aos meus colegas e amigos do Laboratório de Instrumentação em Sistemas Aquáticos (LabISA) e do curso de mestrado em Sensoriamento Remoto do INPE.

Aos colegas do projeto BONDS (Balancing biOdiversity coNservation with Development in Amazonian wetlandS) e ao Dr. João Vitor Campos e Silva, que contribuiu imensamente com a sua experiência nas comunidades do Juruá.

Agradeço ao Programa de Pós-Graduação do Instituto Nacional de Pesquisas Espaciais (INPE), aos professores do SERE, e à Coordenação de Aperfeiçoamento de Pessoal de Nível Superior (CAPES) pela bolsa de mestrado.

ABSTRACT

River meander migration promotes the formation of exceedingly sinuous rivers resulting in oxbow floodplain lakes. These riparian environments support communities that live along the river banks by providing reliable fishery and thus economic and food security. Meander migration results from erosion, sedimentation, and cutoffs that naturally change the floodplain geomorphology affects the dynamic of local communities and ultimately forces them to move to other banks or nearby cities. The erosion process, for example, might promote the loss of land on community shores and increase the risk of inundation frequency and severity. Sedimentation might gradually increase the distance between the river channel and communities' settlements, reducing their access to the river. Moreover, cutoff events, when the river favors a shorter path, might reduce the community access to the main river, and with time, totally isolate the population. In this context, communities that live along the Amazonian Juruá River banks, one of the most sinuous rivers on Earth, are vulnerable to the negative effects of the meander migration. Giving the size of the Amazon Basin rivers, it is not easy to monitor this process to prevent damages to the riverine population. Although not properly explored, remote sensing and cloud computing are promising for the study of the floodplains dynamics and their relationship with residents. In this research, we investigated the river meander impacts on local communities along the main Juruá Basin river channels. For that, the study consisted in (i) the development of an automatic algorithm to measure the river meander migration using cloud computing and Landsat time series, (ii) the identification of the number of communities affected by erosion and sedimentation along the Juruá River, (iii) the development of an easy-to-use methodology to predict the year of neck cutoff occurrence using remote sensing time series. (i) The Water Surface Change Detection Algorithm (WSCDA) identified meander migration areas along the Juruá River, with omission and commission errors lower than 13.44% and 7.08%, respectively. (ii) There are 369 rural communities without road access along the Juruá banks, the majority of which located in stable regions (58.8%). Those located on unstable reaches represent almost 40 %, divided into communities living in sedimentation (26.02%), and erosion areas (15.18%). This result suggests that the riverine population can make decisions based on their empirical knowledge and develop successful adaptations to the environment. Furthermore, larger communities (more than 20 houses), tend to live in more stable locations (70% of the total large communities), when compared to middle size (11-20 houses = 63.2%) and small communities (1-10 houses = 55.6%). (iii) The methodology for predicting the year of neck cutoff occurrence was accurate (R^2 =0.79 and MAPE = 13%) within 20 years. We identified migration rates previous to cutoffs ranging from 3 to 29 m/year along the Juruá Basin. The cutoff prediction methodology was then applied in river sections with potential community impact. The results in all sections promote essential knowledge about the relationship between local communities and the river meander migration and aim to support local planning to improve communities' resilience. Furthermore, the proposed WSCDA might be used to measure river morphology dynamics of water resources in different regions, with the potential to assess the impact on different riverine communities worldwide.

Key Words: Google Earth Engine, floodplains, Landsat.

IMPACTO DA MIGRAÇÃO DO RIO AMAZÔNICO JURUÁ EM COMUNIDADES RIBEIRINHAS: UM ESTUDO DE CASO USANDO SÉRIES TEMPORAIS DE SENSORIAMENTO REMOTO E COMPUTAÇÃO EM NUVEM.

RESUMO

O processo de migração de rios promove a formação de canais extremamente sinuosos e lagos de várzea. Esses ambientes fluviais sustentam comunidades ribeirinhas por meio da pesca, garantindo segurança econômica e alimentar. A migração de meandros dos rios é resultado de processos de erosão, sedimentação e corte de meandros (do inglês cutoff) que mudam naturalmente a geomorfologia da planície de inundação, afetando a dinâmica das comunidades locais e, por fim, forçando-as a se deslocarem para outras margens ou cidades próximas. O processo de erosão, por exemplo, pode promover a perda de terras nas margens da comunidade e aumentar o risco, frequência e severidade das inundações. A sedimentação, por outro lado, pode aumentar gradualmente a distância entre o canal do rio e os assentamentos das comunidades, reduzindo o acesso ao rio. Além disso, eventos de corte de meandro, quando o rio favorece um caminho mais curto, podem reduzir o acesso da comunidade ao rio principal e, com o tempo, isolar totalmente a população. Nesse contexto, as comunidades que vivem ao longo das margens do rio Juruá, um dos rios mais sinuosos do planeta, são altamente vulneráveis aos efeitos negativos da migração de meandros. Dadas as dimensões dos rios da Bacia Amazônica, acompanhar esses processos de forma a evitar danos à população ribeirinha é complexo e dispendioso. Embora não sejam devidamente explorados, a combinação de sensoriamento remoto e computação em nuvem é promissora para estudar planícies aluviais dinâmicas e sua relação com os ribeirinhos. Nesta pesquisa, investigaram-se os impactos do meandramento dos rios nas comunidades locais ao longo dos principais canais da Bacia do Juruá. Para tanto, o estudo consistiu no (i) desenvolvimento de um algoritmo automático para medir a migração do meandro do rio usando computação em nuvem e séries temporais Landsat, (ii) identificação do número de comunidades afetadas pela erosão e sedimentação ao longo do rio Juruá, (iii) desenvolvimento de uma metodologia de fácil uso para prever o ano de ocorrência de cutoff usando séries temporais de sensoriamento remoto. (i) O Algoritmo de Detecção de Mudança da Superfície da Água (do inglês WSCDA) identificou áreas de migração de meandros ao longo do rio Juruá, com erros de omissão e comissão inferiores a 13,44% e 7,08%, respectivamente. (ii) Foram mapeados 369 comunidades rurais sem acesso rodoviário ao longo das margens do Juruá, a maioria localizada em regiões geomorfologicamente estáveis (58,8%). Aqueles localizados em trechos instáveis representam quase 40%, e podem ser divididos em comunidades vivendo em áreas de sedimentação (26,02%) e em áreas de erosão (15,18%). Esse resultado sugere que a população ribeirinha toma decisões com base em seu conhecimento empírico da planície e desenvolve adaptações bem-sucedidas ao meio ambiente. Além disso, comunidades maiores (mais de 20 casas) tendem a viver em locais mais estáveis (70% das maiores comunidades), quando comparadas a comunidades de tamanho médio (11-20 casas = 63,2%) e comunidades pequenas (1-10 casas = 55,6%). (iii) A metodologia para prever o ano de ocorrência do corte de meandro teve boa acurácia (R^2 = 0,79 e MAPE = 13%) para cutoffs previstos num período de 20 anos. Taxas de migração anteriores a cutoff variam de 3 a 29 m / ano ao longo da Bacia do Juruá. A

metodologia de previsão de corte foi então aplicada em seções de rio com potencial impacto na comunidade. Os resultados em todas as seções promovem essencial conhecimento sobre a relação entre as comunidades locais e a migração dos meandros do rio e podem apoiar o planejamento local para melhorar a resiliência dessas comunidades. Além disso, o WSCDA proposto pode ser usado para medir a dinâmica da morfologia de rios em diferentes regiões, com o potencial de avaliar o impacto em diferentes comunidades ribeirinhas em todo o mundo.

Palavras-chave: Google Earth Engine, várzeas, Landsat.

LIST OF FIGURES

CONTENTS

1. INTRODUCTION

1.1 Overview

Amazonian floodplains are lively environments with high complex interactions among physical, hydrological, and biological patterns and with the riverine communities living along the river banks (JUNK et al., 2012). The intense water level fluctuation known as flood pulse (JUNK et al., 2012; CAMPOREALE et al., 2008) is the main force connecting the river water to the floodplain, a process that shapes the exchange of sediments and nutrients between them. This constant Amazonian floodplain dynamic might explain its high biodiversity (WARD et al., 1999), with approximately one-third of the Earth's known species within the Amazon basin (HECKENBERGER et al., 2007). This Amazonian high biodiversity supports local and riverine communities with access to fish and other animals that provide income and food security (CAMPOS-SILVA; PERES, 2016). Furthermore, the river-floodplain interactions provide local communities with fertile soils, waterway transport, and productive lakes for the fishery, conditions that explain the huge human concentration in pre-colonial and current times in those regions (FRAXE et al., 2007).

Concerns over biological conservation are widespread due to the high Amazonian biodiversity, regarding the region as a critical ‘tipping point’ to the Earth's climate and ecology (HECKENBERGER et al., 2007). The empirical ecological knowledge developed by trial and error was accumulated throughout generations by traditional and indigenous communities and is being recognized as essential for the protection and sustainable management of ecosystems (CEBRIÁN-PIQUERAS et al., 2020; LEITHÄUSER; HOLZHACKER, 2020; EARLY-CAPISTRÁN et al., 2020; BERKSTRÖM et al., 2019; TOMASINI et al., 2019; KOTHARI et al., 2013). In a recent paper, Ogar et al. (2020), reported that their traditional knowledge is deep and highly related to their natural ecosystem, resulting from a learning process built and adapted over a long period. Therefore, the preservation of the local communities and their culture is essential to preserve the high biodiversity of Amazonian floodplains (FRAINER et al., 2020; DAVIS, 2009).

The flood pulse in Amazonian floodplains also influences the river meander migration, another important factor that changes the floodplain landscape over time. The high sediment concentration of Amazonian white-rivers during the flooding season and the deposition of these sediments along floodplains favor the rivers meandering processes and thus their sinuosity (AHMED et al., 2019; CONSTANTINE et al., 2014; JUNK et al., 2011). The river meander migration is formed when the helical-flow circulation along a channel bend leads to the outer bank erosion (concave relative to the channel centerline) and inner bank sedimentation (convex relative to the channel centerline), forming point bars (IELPI; LAPÔTRE, 2020). Furthermore, the erosion promoted by the channel kinetic energy might lead to a cutoff event, whenever a change in the meander loop occurs to favor a shorter path, forming an oxbow lake (CAMPOREALE et al., 2008). The constant transformation of Amazonian floodplains forces a constant biota and local human communities' adaptation along the river banks.

As informed, the floodplain dynamics are essential for the survival of the local communities. The river meander migration, for example, produces areas of sedimentation (sandbanks) that are used by locals to collect turtles and for fishery (STANFORD et al., 2020). In the same way, cutoff events produce oxbow lakes that are used by the communities for fishing. Along the Middle Juruá River, for instance, the fish sustainable management on oxbow lakes is securing food and economic security for riverine communities, while protecting the arapaima fish (CAMPOS-SILVA; PERES, 2016). Furthermore, these Cutoff events reduce the river sinuosity, increasing the navigation access for nearby communities. As a result, all these floodplain characteristics are important for community culture maintenance, while ensuring economic stability, and food security.

However, although floodplain dynamics benefit local communities, some natural processes might disturb their lives. The river meander migration, for example, might erode or sediment community shores, increasing frequency and severity of inundation in the case of bank erosion and access to the river channel in the case of both sedimentation and erosion. Furthermore, a cutoff event might cause communities from an abandoned reach (transformed in an oxbow lake), to lose the connectivity to the river. Coomes et al. (2005), reported that a cutoff event in the Peruvian Amazon affected many communities living nearby, including a city of 3500 inhabitants. Nevertheless, the authors identified

that upstream communities were benefited from the shorter distance to other river regions (the cutoff reduced the river path by 64 km), showing the cutoff dual influences on communities. These impacts are well documented in floodplains in countries such as Bangladesh (ISLAM et al., 2020; FERDOUS et al., 2019; MONIRUL et al., 2017), but remains incipient in Amazonian regions.

Remote Sensing is particularly crucial to study large and inaccessible regions in the Amazon. This technology has been providing quantitative information about water dynamics, flooded forests, and sediment exchanges in Amazon floodplains (FASSONI-ANDRADE; PAIVA, 2019; MELACK et al., 1994). The long Landsat historical database (since 1984) of high-quality images makes this satellite capable of monitoring large areas over long periods (NGUYEN et al., 2019; ACHARYA et al., 2016; LIU et al., 2016; XIE et al., 2016; DU et al., 2014; YANG et al., 2015; PARDO-PASCUAL et al., 2012). These characteristics are also useful to study river morphodynamics and the river meandering process in floodplains (MUKHERJEE et al., 2017; SHAHROOD et al., 2020; SYLVESTER et al., 2019; MONEGAGLIA et al., 2018). Sylvester et al. (2019), for example, used Landsat imagery to study the relationship between the river curvature and the rate of migration in the remote Amazonian Juruá River.

However, while a large number of satellite images benefit the historical assessment of water conditions, the information processing becomes computationally a challenge. In this context, Google Earth Engine (GEE), a cloud-based platform, has improved the processing of large amounts of datasets using thousands of computers working in parallel (GORELICK et al., 2017; XIONG et al., 2017). In this sense, analyzing long historical radiometric data using GEE capabilities is promising to monitor floodplain variabilities and meander migration processes (BOOTHROYD et al., 2020; HIRD et al., 2017). However, although the GEE offers high processing capacity, the use of this cloud platform is still limited to study river morphology dynamics. Schwenk et al. (2017) and Isikdogan et al. (2017), for example, have developed automatic algorithms to detect meander migration using cloud computing. Nevertheless, the authors applied GEE just to download Landsat images, under-exploiting the platform processing capacity.

In this context, the use of remote sensing and cloud computing is a powerful instrument to monitor and analyze the impacts of the river meander migration over riparian rural

communities in the Amazon. The Amazonian Juruá basin is still well preserved and thus presents an opportunity to study the natural river meander migration dynamics without, so far, major engineering projects that are planned along the Amazon basin (LATRUBESSE et al., 2017). Moreover, the Juruá River is one of the most sinuous rivers on Earth and is home to many local communities that live along the river banks and suffer the intense Juruá migration rate. Preserve and protect these communities is a way to guarantee their cultural heritage and their knowledge about the environment and biodiversity. The combination of technology derived from scientific information and local knowledge developed throughout generations may empower local communities to become more resilient to local and global environmental changes (FRANZOLIN et al., 2020).

1.2 Objective

The objective of this research is to understand the interrelationship between the river meander migration in the Juruá Basin and the communities that live along their banks. Although this is a common process along the Amazonian rivers, the literature is scarce about the meander impacts on specific communities along the Amazon river. For this reason, further research can be proposed to explore remote sensing time series and cloud computing in the evaluation of meander dynamics and their influences on the remote riverine communities along Amazonian Juruá river. Remote sensing time series and cloud computing, by contrast, are useful to represent spatially and temporarily dynamic floodplains, capabilities that are promising to study remote rural communities in the Amazon and their relationship with the surrounding environment.

Based on these objectives, the following research questions are addressed in this dissertation:

1. *Is cloud computing effective to automatically detect erosion and sedimentation processes using remote sensing image time series? What are the main advantages and restraints when compared to traditional algorithms?*

2. *What is the proportion of riverine communities living in areas subject to the meandering of the Juruá River? How are these communities affected by erosion and sedimentation processes along their shores?*

3. *Can satellite river meander monitoring be applied to predict neck cutoffs? How can this forecast be used to improve inundation hazard mitigation actions and community safety?*

1.3 Outline

This paper-based master thesis is organized as follows:

Chapter 1 Introduces the topic of Amazonian high biodiversity and how local communities are important for their conservation. The chapter also explains the floodplain dynamics and their influence on riparian communities and how this relationship can be addressed using remote sensing.

Chapter 2 Presents the theoretical background of Amazonian floodplains and the formation of meanders and oxbow lakes. This chapter also explains the use of Landsat and cloud computing to study water resources and river meander migration.

Chapter 3 Presents the development of the automatic algorithm Water Surface Change Detection Algorithm (WSCDA) to identify areas of erosion and sedimentation along the Juruá River. This chapter also informs how this information was used to systematically map riparian communities that are affected by the river meander migration.

Chapter 4 This chapter describes a methodology to predict the neck cutoff year of occurrence. This chapter presents the validation using past cutoffs and the application of the cutoff methodology in imminent cutoff locations along the Juruá Basin.

Chapter 5 Summarizes the main findings of this dissertation.

2. LITERATURE REVIEW

2.1 Amazonian floodplains

The Amazon River system is the largest source of fresh water on the planet, accounting for approximately 16% of the river global discharge and 39% of sediment discharge in South America (FAGUNDES et al. 2020; OKI; KANAE, 2006; DAI; TRENBERTH, 2002). Before reaching the ocean, this huge amount of water interacts with the environment, producing wetlands and floodplains on the Amazon basin. Hess et al. (2015) have estimated that 14% of the Amazon Basin can be classified as wetlands, from which 9% represents open water areas during flooding seasons. As a result, wetlands and floodplains are a common feature on the Amazon basin, serving as important ecological habitat (JUNK et al., 1997), storing sediments (BOURGOIN et al., 2007), altering river paths (RICHEY, et al., 1989), retarding flood waves, and producing a substrate for chemical and biological processes (MATTHEWS; FUNG, 1987).

Junk and Welcomme (1990) defined floodplains as low land areas that are periodically inundated by lateral overflow from associated rivers or lakes subjected to intense water fluctuations known as flood pulse. According to Junk et al. (1989), the flood pulse connects the entire floodplain with river water, a process that controls the productivity, the existence, and the interactions between the environment and biota in floodplain ecosystems. Bonnet et al. (2008), studying the Lago Grande de Curuaí, identified that the Amazon river accounted for 77% of the total lake water input, followed by rainfall (9%), runoff (10%), and groundwater (4%). As a result, floodplains decrease the river peak due to water retention, minimizing the danger of flooding (KIEDRZYŃSKA et al., 2015; CHEN et al., 2014). Junk (1997) argued that floodplains can be classified according to the amplitude, frequency, predictability, and source of flooding. The Juruá River, for example, has a monomodal flood pulse with an early inundation peak, between March and June (SIPPEL et al., 1998). However, even with the water transfer between river and floodplain, the Juruá River experiences a water level amplitude that exceeds 10 m (HAWES; PERES, 2016).

Floodplains and water channels are the two most important suspended sediment storage systems, which operate in totally different time scales; seasonal and annual in river

channels and centennial to multimillennial along the floodplain area (MEADE, 1994). Bradley and Tucker (2013) informed that the constant deposition of sediments creates floodplains with a variety of depositional ages. The authors identified that newly sediment areas are more likely to suffer erosion than older sediment deposits. In a recent study, Fagundes et al. (2020), estimated that floodplains retain 12% of river sediment flows in South America. This number increases when Amazonian floodplains are considered, as in the Curuaí reach (between 41% and 53%) (BOURGOIN et al., 2007). This intense sediment retention promotes the river meandering process and thus the sinuosity of many Amazonian streams (AHMED et al., 2019; CONSTANTINE et al., 2014; RÍOS-VILLAMIZAR et al., 2014; JUNK et al. 2011; BOURGOIN et al., 2007; MARTINELLI et al., 1989; MARTINELLI et al., 1988).

However, for all these processes to occur, river channels must carry suspended sediments. In general, the concentration of sediments flowing in the Amazonian rivers is determined by the drainage basin extent and its geographical location. Rivers with large headwater fractions in the Andes have always high sediment and nutrient concentrations, as the Madeira river (MARTINELLI et al., 1988), while rivers with headwaters in the Sub-Andean region, as the Juruá river, have lower, but still high concentration values (MARTINELLI et al., 1989). These rivers are classified as white-water (JUNK et al. 2011) and have a higher sinuosity due to the intense meander migration (CONSTANTINE et al., 2014). On the other hand, rivers that drain the Amazon depression (black-water rivers) and the Central Brazilian archaic shield (clearwater rivers) have a low sediment concentration in its waters and thus a lower river meander migration process and sinuosity (CONSTANTINE et al., 2014; RÍOS-VILLAMIZAR et al., 2014; JUNK et al. 2011; MARTINELLI et al., 1988).

2.1.1 River meander migration

The river meander process constantly changes the environment, producing highly heterogeneous landscapes with a variety of channel morphologies, oxbow lakes, scroll bars, and meander scars (GÜNERALP; MARSTON, 2012). As the meander bends evolve, the shape of the curvature becomes round and asymmetric over time (concave on one side and convex on the other side) (PARKER et al., 1982). This shape is formed due

to three different processes, extension through lateral migration, rotation, and downstream or upstream migration (HOOKE, 1984). The lateral migration increases the meander length, while the translation and rotation increase the meander's asymmetry (GÜNERALP; MARSTON, 2012). These processes might be formed at the same time, creating complex and intricate meander bends (GÜNERALP; MARSTON, 2012). These intricate meander morphologies might result in compound loops, also known as multilobed meanders, which are characterized by long loops with multiple local maximum migration peaks (FROTHINGHAM; RHOADS, 2003). Simple bends are also present and are characterized by a single maximum migration peak in its curvature (FROTHINGHAM; RHOADS, 2003). Figure 2.1 shows different examples of intricate and simple loops along a reach of the Juruá River.

Figure 2.1 - A reach of the Juruá River showing a channel planform composed of simple and complex meander forms, such as compound loops. The plot on the left side shows the planform-curvature series in m/m (C) of simple bends (bends 1, 3-4, 7-9) and for compound loops (bends 2, 5-6). An image Landsat 7 (1999), Bands 7,4,2 as RGB are displayed.

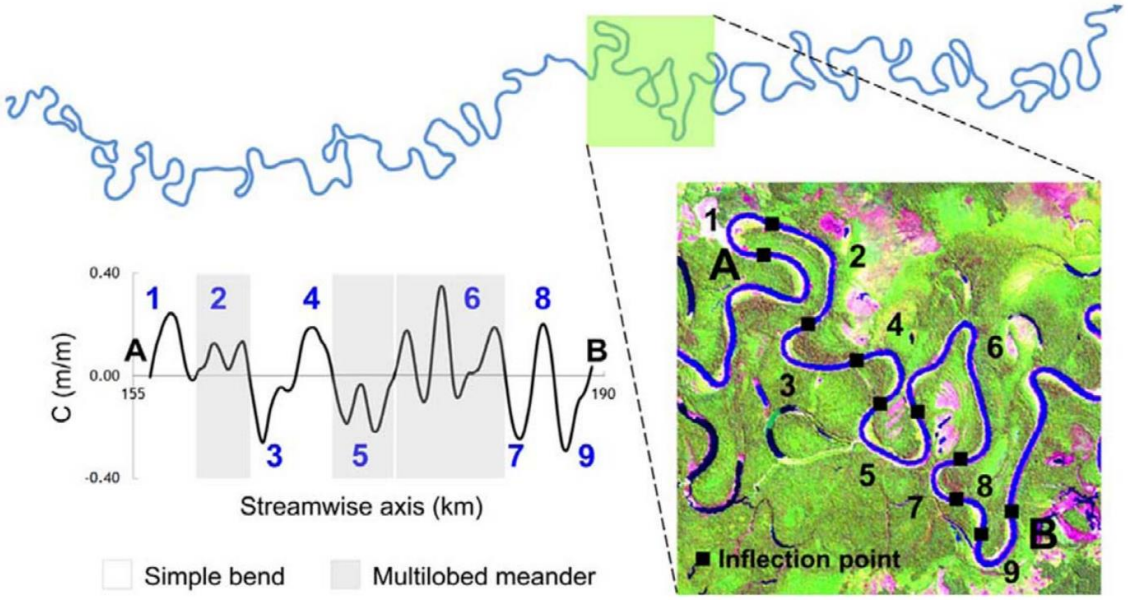

Source: Güneralp and Marston (2012).

The meander migration is controlled by two different mechanisms, sedimentation and point bar development (elevated region of sediment) in the inner bank (convex relative to

the channel centerline) due to the low-stress shear, and erosion in the outer bank (concave relative to the channel centerline) due to the high fluid momentum (LEGLEITER et al., 2011; DIETRICH, et al., 1979). Gautier et al. (2007), studying an Amazonian white-water river (Beni River), identified that flooding periods are a major force controlling the river morphology, while its duration is responsible for the massive exportation of sediment load. Confirming the sediment central role in river morphology, Constantine et al. (2014) found that rivers with high sediment concentration (white-rivers) in the Amazon experience higher rates of meander migration and more cutoff events when compared to rivers that drain the Central Amazon Trough and the Brazilian Shields.

In addition to sediment retention, variables such as vegetation cover, river curvature, catchment-basin size and relief, riverbed slope, bank material, and the river curvature also influence the rate of erosion and sedimentation and thus the formation of meanders (IELPI; aLAPÔTRE, 2020; SYLVESTER et al., 2019; HORTON et al., 2017). Perucca et al. (2007), for example, investigated the relationship between riparian vegetation and the formation of river meanders. The authors, assuming a linear relationship between the biomass and the bank erodibility, found that the variability of vegetation cover along the river creates a heterogeneous erosion capacity that influences the meander migration process and thus the river morphology. Ielpi and Lapôtre (2020), using remote sensing time series to study 483 rivers worldwide, found that vegetate meanders migrate slower than unvegetated ones when normalized by channel size, confirming the vegetation important role in slowing the river meander progress. As a result, deforestation has the potential to increase the rates of meander migration. Horton et al. (2017), for example, studying a river in Malaysia, found that a deforestation event that removed 50% of trees in the Sabah floodplain increased the rates of riverbank erosion by at least 23%. Those results bring concerns for Amazon, which experiences increasing rates of deforestation over the last years (BULLOCK et al., 2020).

The river morphology also highly influences the rates of meander migration. Nanson and Hickin (1983), for example, studying the relationship between the river curvature and the rates of meander migration, found that the migration rates reach their maximum value when the radius curvature is about two or three times higher than the river width. Furthermore, Sylvester et al. (2019), studying the Amazonian Juruá River, found that the maximum migration rate is not placed on the maximum local channel curvature, as

previously assumed. Instead, the maximum migration rate is positioned downstream the peak curvature, a process named phase lag (Figure 2.2) (SYLVESTER et al., 2019). An explanation for this condition is that the outer bank velocity is not just dependent on local curvature but on a weighted sum of upstream sinuosity (SYLVESTER et al., 2019). As a result, the integration of velocities results in a phase lag between curvature and migration rate (SYLVESTER et al., 2019; FURBISH, 1988; HOWARD; KNUTSON, 1984).

Figure 2.2 - A: Nominal (black arrows) and predicted (red arrows) migration rates showing downstream delay of predicted migration rate relative to bend curvature. The distance between locations of maximum curvature and maximum migration is named phase lag. B: River path along a short Juruá River section in 1987 (blue) and 2017 (red). C: Migration rate between 1987 (blue) and 2017 (red) along the same Juruá River segment. Bend numbers are the same as in B for identification.

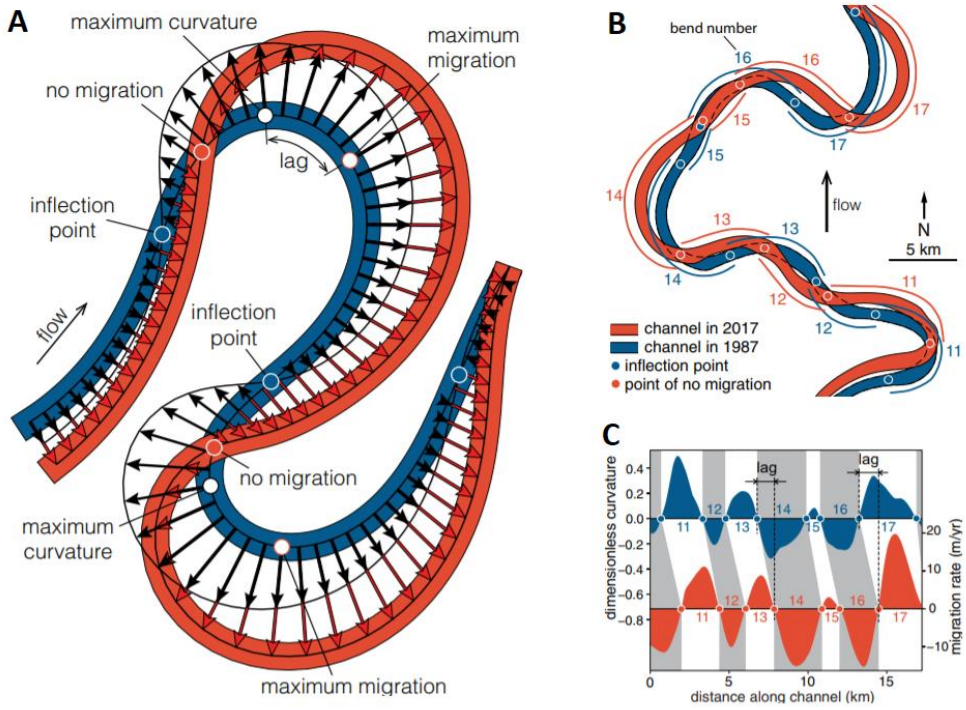

Source: Adapted from Sylvester et al. (2019).

However, the pattern of increasing the river sinuosity due to the erosion and sedimentation processes is not constant. The river forms curves in arc formats that grow until a cutoff happens, when the river favors a shorter path, reducing the river sinuosity (CAMPOREALE al., 2008). There are two different types of cutoff, the neck and chute cutoff. Chute cutoff occurs when a channel is formed and connects the upstream and

downstream limbs during flooding events, while the neck cutoff is formed when the continuous river meander migration intersects the upstream and downstream meander limbs (CONSTANTINE et al., 2010b; HOOKE, 2004). Soon after the cutoff is formed, the abandoned channel is filled with sediments, creating a barrier in its entrance (Figure 2.3) (KONDOLF; STILLWATER SCIENCES, 2007). The velocity of entrance deposition is determined by the angle between the main river and the abandoned channel (higher angles experience more rapid sediment deposition) (CONSTANTINE et al., 2010a). This condition occurs because the higher the diversion angle is, the lower the shear stress and the sediment transport capacity within the abandoned reach (CONSTANTINE et al., 2010a). As a result, chute cutoffs (Figure 2.3b), with usually lower angles, receive more water from the river and thus the entrance sediment barrier is formed later than that of neck cutoff channels (Figure 2.3a) (CONSTANTINE et al., 2010a).

Figure 2.3 - Flow dynamics and sediment deposits in neck (a) and chute cutoffs (b).

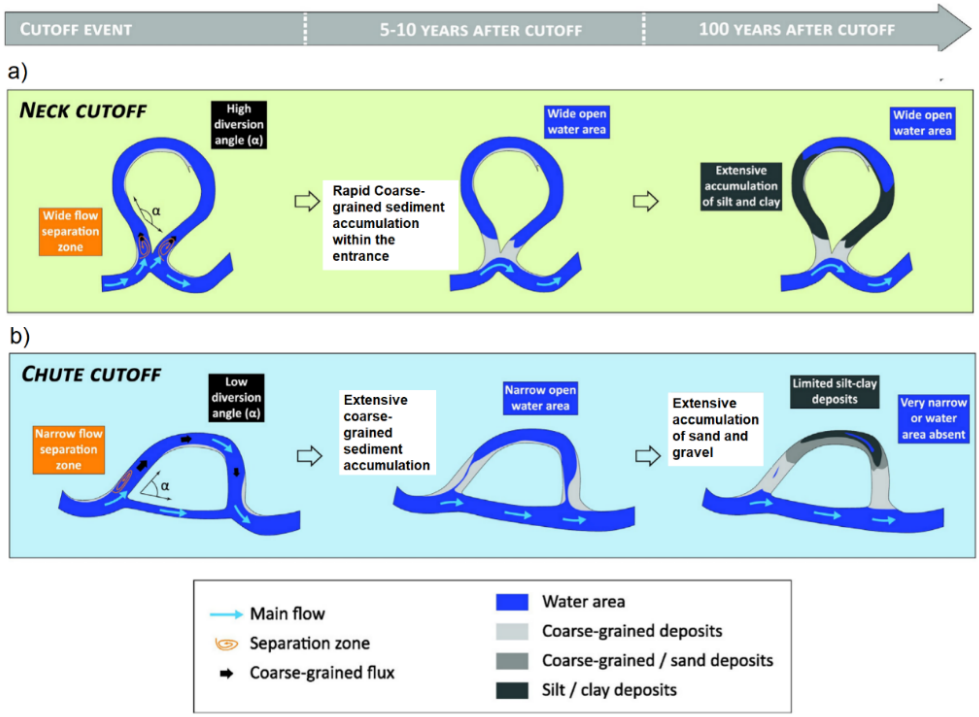

Source: Adapted from Dépret et al. (2017).

After the cutoff event, the abandoned river reach becomes an oxbow lake, a common feature in floodplain landscapes. Schmitt and Hornsby (1985), studying a floodplain in Savannah River Basin (USA), identified that oxbow lakes accounted for 24% of the freshwater area, a percentage that probably increases in Amazonian floodplains. In terms of size, studies have shown that the cumulative size-frequency of oxbow lakes could fit a power-scaling function (STØLUM, 1998), and a log-normal function in a non-cumulative distribution (CAMPOREALE; DUNNE, 2008), meaning that small lakes largely outnumber large ones. Furthermore, Howard and Knutson (1984) informed that neck cutoffs are more common in highly sinuous rivers when compared to chute cutoffs.

With the river meander migration and cutoff physical knowledge acquired in different studies several researchers have attempted to model the river meander migration to predict future erosion and sedimentation areas (ANNAYAT; SIL, 2020; GU et al., 2016; GUTIERREZ et al. 2014; ASAHI et al., 2013; SUN et al., 1996). Gu et al. (2016), for example, used the Bank Erosion and Retreat Model (BERM) (CHEN; DUAN, 2006) and a nonlinear hydrodynamic model of Blanckaert and de Vriend (2010) to simulate the river meander migration assuming a linear relationship between river longitudinal velocity and bank migration rate. Gutierrez et al. (2014), used a stochastic multivariate analysis to forecast the river meander migration in the Cahuacan River (Mexico) using explanatory variables such as river and meander width, basin surface area, curvature degree, dominant discharge (return period of 2 years), and so on. In a more direct approach, Annayat and Sil (2020) used an empirical model to predict the meander migration of the Barak river (India) using the Nanson and Hickin method (NANSON; HICKIN, 1983), which assumes the river bend curvature as the main influencing parameter. The authors obtained a moderate meander migration model with $R^2 = 0.50$, and migration rates between 0.54 to 85.69 m/year. However, from computational simulations to empirical models, the challenge to predict river meander migration is high and still not fully developed.

2.1.2 Floodplain biodiversity

The described high spatial and temporal variability promoted by the river meander migration creates a heterogeneous environment that supports high rates of biodiversity (MEITZEN, 2018). Oxbow lakes, for example, might keep interacting with the river

through small channels, promoting water, sediment, and biota exchanges (JUNK et al., 2012; CAMPOREALE et al., 2008). As a result, active oxbow lakes provide rich habitats for the aquatic ecosystem, since they are important places for fish spawning, nursery habitats and serve as fishery locations for local communities (STANFORD et al., 2020; PAUL; RASHID, 2016; PENCZAK et al., 2004; PETERMANN, 1997). Furthermore, the river meander migration forms water channels with a high hydraulic complexity that leads to the formation of pools, riffles, and a lateral diversity of depths, forming shallow and deep areas along the river (NAKANO; NAKAMURA, 2008; RHOADS; SCHWARTZ, 2003). This hydraulic complexity creates a habitat heterogeneity that supports higher biodiversity of aquatic species along the river (ZHOU; ENDRENY, 2020; GUALTIERI et al., 2020; GUALTIERI et al., 2017). Overall, the presence of rivers, wetlands, grassland, and forest in floodplains creates a habitat mosaic that is maintained by flooding events, conditions that provide unique habitat types for different terrestrial and aquatic species (OPPERMAN et al., 2013; SABO et al., 2005; TOCKNER; STANFOR, 2002; SALO et al., 1986).

The fast-annual hydrological variation induced by the flood pulse is essential to maintain aquatic ecosystems (FREITAS et al., 2014). During the flooding season, the floodplain lakes fill up and connect to the river, expanding the water area into the forest and creating more interconnected space and habitats for fish species (SIQUEIRA-SOUZA et al., 2016; THOMAZ et al.,2007). This water expansion also brings important food resources for fishery from the floodplain forest, such as seeds, fruits, terrestrial insects, and decaying forest vegetation (JUNK et al., 1989). During the receding season, the flooded area shrinks, decreasing habitat availability and promoting species isolation (SIQUEIRA-SOUZA et al., 2016). Fernandes et al. (2009), informs that the hydrological seasons change the interactions between the environment and aquatic biota, influencing the processes of predation and competition and thus the aquatic biodiversity.

However, fast annual variations promoted by the river meander migration and flood pulse are not the only variables that explain the high rates of biodiversity in Amazonian floodplains. Climatic variations in geological time scales in the region contributed to a succession of events that promoted speciation and thus diversification of species (THOM et al., 2020; SILVA et al., 2019; ALBERT et al., 2011). Thom et al. (2020), for example, studying birds, identified that the changes in Amazonian floodplains induced by climate

variation during the Mid - and Late Pleistocene induced specialization among species and thus diversification, with subsequent secondary contact. Those processes also drove the diversification of tree species in floodplain regions (FERREIRA et al., 2009), as supported by Luize et al. (2018), which discovered three times higher tree biodiversity in Amazonian wetlands than previously recorded. The intersection between long term climatic variations and fast variability driven by the flood pulse and meander migration might better explain the high rates of biodiversity in Amazonian floodplains.

2.1.3 Amazonian riverine communities

In a more general concept, Giddens (1991) informs that the community concept refers to places where culture, knowledge, and social structure are produced. Wenger (2011) and Vasconcellos and Sobrinho (2017), defined local Amazonian communities as places where the population lives according to their empirical knowledge developed throughout generations and where the population practices different socio-cultural activities. The social interactions between individuals over time results in stable social structures (PEARCE, 2000; CASTELLS, 1997). This social structure is important since it influences the community behavior and determines their social interactions, such as who becomes leaders and followers and the community interests (PEARCE, 2000; CHAMBERS, 1997). As a result, local communities are socio-dynamic places driven by cultural processes and knowledge production (SCHONHUTH, 2002).

Local communities are being recognized as important authors for the protection and sustainable management of ecosystems (CEBRIÁN-PIQUERAS et al., 2020; LEITHÄUSER; HOLZHACKER, 2020; EARLY-CAPISTRÁN et al., 2020; BERKSTRÖM et al., 2019; TOMASINI et al., 2019; KOTHARI et al., 2013). Coronel and Solórzano (2017), informed that local communities are applying their ancient empirical knowledge about the environment to manage different conservational programs, ensuring their success. In a recent study, McElwee et al (2020), identified that indigenous and local knowledge is important for applied ecology since they enrich our understanding of nature and its relationship with populations, support ecosystem change monitoring, and generate inclusive options for people. The authors informed that this knowledge might be used to achieve biodiversity global goals, such as Aichi Biodiversity

Targets and the Sustainable Development Goals. However, as pointed by Leithäuser and Holzhacker (2020), this knowledge must be applied beyond environmental aspects, including social and economic components to improve the local population's well-being.

The fish sustainable management promoted by locals on the Middle Juruá is a successful example of how local communities can support conservation practices. The fish management promoted on floodplain lakes ensures a fraction of the lakes for commercial and subsistence fisheries, while others are strictly fish protected lakes (CAMPOS-SILVA; PERES, 2016). Furthermore, the local communities guard the lake's entrance using a floating wooden guard post to guarantee the protection of the lakes (CAMPOS-SILVA; PERES, 2016). The fish management promoted on oxbow lakes remarkably increased the number of the giant arapaima (*Arapaima gigas*) on protected lakes (Campos-Silva; Peres, 2016). As a result, at the same time that sustainable management is securing the conservation of this important and threatened species, the local communities are ensuring economic gains and food stability (Campos-Silva; Peres, 2016). This successful example shows how local populations can support ecological conservation and at the same time improve their livelihood.

2.2 Landsat applications to water resources

The Landsat program started in 1972 and was supported by the National Aeronautics and Space Administration (NASA) and the U.S. Geological Survey (USGS). The availability of geo-radiometrically consistent and calibrated data lead to a new generation of algorithms and computational approaches (WULDER et al., 2019), innovations that came after the USGS adopted free and open data policy (WULDER et al., 2019; ZHU et al., 2019). The increase in computational power and cloud-shadow detection algorithms is enabling users to extract information from temporally-dense analysis over large areas (WULDER et al., 2019; ZHU et al., 2017). Landsat data and its huge historical database provide an ideal source of information to track surface changes, including water extension dynamics (WALKER et al., 2020; WANG et al., 2018; PEKEL et al., 2016), and wetlands monitoring (HIRD et al., 2017; HALABISKY et al., 2018; MEJIA ÁVILA et al., 2019). The Landsat 5 Thematic Mapper (TM) (1984 to 2013) and the Landsat 8 Operational Land Imager (OLI) (2013 to current dates) have 30m spatial resolution, are near-polar orbit with repeat cover every 16 days. The Landsat bands are described in Table 2.1.

Table 2.1 - Bands from Landsat 5 and 8.

Landsat 5 TM		Landsat 8 OLI	
Bands	Wavelength	Bands	Wavelength
Band 1 Visible	0.45 - 0.52 µm	Band 1 Coastal	0.43 - 0.45 µm
Band 2 Visible	0.52 - 0.60 µm	Band 2 Visible	0.45 - 0.51 µm
Band 3 Visible	0.63 - 0.69 µm	Band 3 Visible	0.53 - 0.59 µm
Band 4 Near-Infrared	0.76 - 0.90 µm	Band 4 Visible	0.64 - 0.67 µm
Band 5 SWIR	1.55 - 1.75 µm	Band 5 Near-Infrared	0.85 - 0.88 µm
Band 6 Thermal	10.4 -12.5 µm	Band 6 SWIR 1	1.57 - 1.65 µm
Band 7 SWIR	2.08-2.35 µm	Band 7 SWIR 2	2.11 - 2.29 µm
		Band 8 PAN	0.50 - 0.68 µm
		Band 9 Cirrus	1.36 - 1.38 µm
		Band 10 Thermal 1	10.6 - 11.19 µm
		Band 11 Thermal 2	11.5 - 12.51 µm

Landsat satellites have long been used to study water resource dynamics, such as the pioneer flood inundation mapping of the Mississippi river (DEUTSCH; RUGGLES, 1974; MCGINNIS; RANGO, 1975). Since then, improvements in sensor quality and longer historical image databases provided by Landsat 5 and Landsat 8 made water detection applications using Landsat very popular (NGUYEN et al., 2019; ACHARYA et al., 2016; LIU et al., 2016; KARAN; SAMADDER, 2016; XIE et al., 2016; DU et al., 2014; YANG et al., 2015; PARDO-PASCUAL et al., 2012). Water indexes, such as the Normalized Difference Water Index (NDWI – equation 1), which is a band ratio between the green (band 3 in Landsat 8) and NIR (band 5 in Landsat 8), and its modification (mNDWI – equation 2), band ratio between green and SWIR (band 6 in Landsat 8), are widely used to highlight and classify water surfaces (SIVANPILLAI et al., 2020; DU et al., 2014; FERRAL et al., 2019). Sivanpillai et al. (2020), for example, applied a normal difference of mNDWI to a pre and a post flooded events image to identify new flood areas. The authors applied different thresholds of ΔmNDWI (from 15% to 35%) to classify newly inundated areas, obtaining overall accuracies ranging from 78.0% to 93.2% among different areas of the United States.

$$NDWI = \frac{Green\ - NIR}{Green + NIR} \quad (1)$$

$$mNDWI = \frac{Green\ - SWIR}{Green + SWIR} \quad (2)$$

Generally, the mNDWI performs better than the NDWI (SIVANPILLAI et al., 2020) because it enhances water detection by suppressing vegetation and soil noise while overcoming the NDWI limitations on build-up areas (DU et al., 2014; XU 2006; MCFEETERS, 1996). Sarp and Ozcelik (2016), for example, applied different water indexes and classification algorithms to identity spatiotemporal changes in Lake Burdur (Turkish). The authors used a threshold of zero to separate water (higher than zero) and non-water (lower than zero) for all the water indexes. The results have shown that classifications based on Support Vector Machine (SVM) and mNDWI performed better than NDWI and the Automated Water Extraction Index (AWEI) for the study area (SARP; OZCELIK, 2016). Water indexes provide fast and easy methodologies to track water surface extensions using Landsat and other satellite images, a characteristic that might explain its use in river morphology dynamics studies (MUKHERJEE et al., 2017; SHAHROOD et al., 2020; MONEGAGLIA et al., 2018).

2.2.1 Landsat applications on river morphodynamics

Due to its huge historical database, Landsat images have long been used to study variations in river morphology over time (YOUSEFI et al., 2016; BAKI; GAN, 2012; PEIXOTO et al., 2009). Yousefi et al. (2016), for instance, used Landsat images from 1989-2008 to study 128km of the Karron River (Iran). The authors, using the SVM classifier to identify the river extension and its variations over time, found that the flow length (distance between two meander peaks) and the river sinuosity have decreased for the whole river, a result that might be related to deforestation in the region, sediment extraction, and a dam construction upstream (YOUSEFI et al., 2016). Landsat images were also used by Baki and Gan (2012) to identify erosion and accretion lands over 30 years in the Jamuna River (India). The authors identified rates of erosion ranging from 227 m/year to 271 m/year. In a different approach, Peixoto et al. (2009) used Landsat

images to analyzed areas of erosion and sedimentation along the Solimões, the Japurá, and the Aranapu River. The authors found that although the rates of erosion and sedimentation were similar, the erosion process destroyed the forest at a higher rate when compared to forest regeneration in the sedimentation areas.

Riverbank erosion is a natural and common problem that is promoting the loss of land and decreasing the livelihood of riparian communities in Bangladesh (BILLAH, 2018). As a result, different studies have been applying Landsat images to measure variations in river morphodynamics in this region (BILLAH, 2018; HASSAN; MAHMUD-UL-ISLAM, 2016; HOSSAIN et al., 2013). Billah (2018), for instance, used a long time series of Landsat images, from 1975 to 2015, to visually digitalize the river bank lines to identify areas of erosion and sedimentation along the Padma River. The authors found an increased rate of migration during the analyzed period, which in total produced a total of 49.951 hectares of eroded land and 83.333 hectares of sedimented land. In a similar paper, Hossain et al. (2013), manually delimitated the river bank lines using Landsat images to analyze the erosion and sedimentation patterns along the Ganges River. The authors discovered that the erosion magnitude along the river is highly related to the erodibility of riverbank materials. With a more automatic approach, Hassan and Mahmud-Ul-Islam (2016) delimitated the river extend using the Maximum Likelihood Classifier algorithm applied on Landsat images, producing classifications with overall accuracies between 97% and 98%. The results have shown that a total of 1340 hectares of land was eroded between 1989 and 2015 (MAHMUD-UL-ISLAM, 2016).

To automate the river meander migration, different studies have developed algorithms to identify spatial-temporal changes in river morphology (ANNAYAT et al., 2020; SHAHROOD et al., 2020; MONEGAGLIA et al., 2018; SCHWENK et al., 2017, ROWLAND et al., 2016; FISHER et al, 2013). Shahrood et al. (2020), for example, developed an algorithm in MATLAB (MATHWORKS, 2012) called River Morphodynamics Analysis based on Remote Sensing (RiMARS) to identify morphology variations and the river centerline migration using Landsat database and the water index mNDWI (Modified Normalized Difference Water Index). Schwenk et al. (2017), created the MATLAB algorithm River Morphodynamics from Analysis of Planforms (RivMAP) algorithm, which applies Support Vector Machine (SVM) to classify the water extend on Landsat time-series, and with this information measures the river meander migration over

time (Figure 2.4). Boothroyd et al. (2020) used the same algorithm to measure the Cagayan River (Philippines). To measure erosion and sedimentation areas, Rowland et al. (2016) developed the algorithm Spatially Continuous Riverbank Erosion and Accretion Measurements (SCREAM). The program measures the area of erosion and sedimentation based on water binary masks from two different images taken in different periods (ROWLAND et al., 2016). However, although the described automatic algorithms simplify the analysis of river meander migration, the download, storage, and manipulation of huge Landsat historical images are still required.

Figure 2.4 – River centerline obtained from the RivMAP using Landsat images from the Ucayali River (Peru) from 1985 to 2015. North arrows also show the direction of the flow, from R6 to R3.

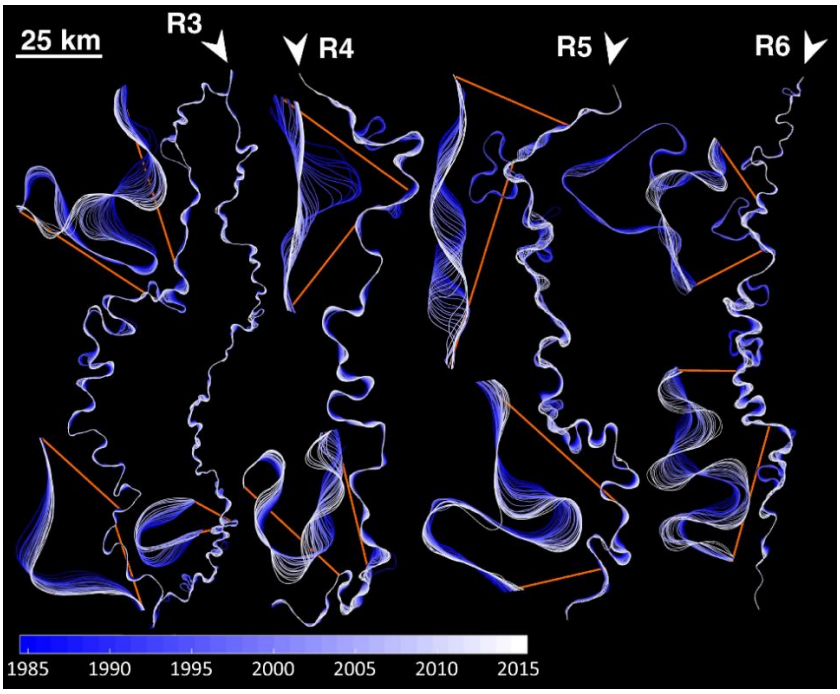

Source: Schwenk et al. (2017).

2.3 Cloud computing and time series analysis

Google Earth Engine (GEE) is a cloud-based that offers large amounts of geospatial datasets and high processing capabilities (GORELICK et al., 2017). The GEE offers a global-scale satellite imagery catalog working in parallel with thousands of computers for analysis (XIONG et al., 2017). The GEE Code Editor enables the users to perform

complex calculations using JavaScript API or Python algorithms for loading and visualizing large satellite imagery and to conduct geostatistical and geospatial operations (SIDHU et al., 2018). The processing of a full petabyte of Landsat data within a single day using GEE cloud-computing, for example, demonstrates the potential of this technology for large-scale geospatial analysis (HIRD et al., 2017). In GEE the temporal images produced by a single sensor are grouped and presented as "collections". These collections provide efficient ways for filtering and sorting to meet specific spatial and temporal criteria (GORELICK et al., 2017).

As a result, the use of satellite time-series and high processing capabilities available on GEE is becoming popular to monitor water extend and temporal dynamics (BOOTHROYD et al., 2020; HE et al., 2020; YANG et al, 2020; NGUYEN et al., 2019; WANG et al., 2018; PEKEL et al., 2016). In an example of GEE high processing capacity, Pekel et al. (2016) used millions of Landsat satellite images in GEE to globally quantify changes in global surface water from 1984 to 2016. The authors identified a permanent global surface water loss of 90,000 Km², in which 70% occurred in the Middle East and Central Asia, and an increase in water surface of 184.000 km² scattered in other parts of the word, mainly due to reservoir filling and climate change (by melting glaciers). Using a lower but still high number of Landsat images (2343 scenes), Wang et al. (2018) calculated the annual minimum and maximum water extend in 1990, 2000, 2010, and 2017 along the Yangtze River Basin (China). The authors used Random Forest classification to measure the water extend, obtaining overall accuracies ranging from 86% to 93%. The combination of Landsat long historical database and GEE high processing capabilities are transforming our knowledge about the dynamics of water resources on regional and global scales.

According to Boothroyd et al. (2020), the GEE characteristics are promising to detect meander migration and river morphology dynamics. However, despite the high GEE processing capabilities, a low number of papers have used this platform to study river planform variations. Li et al. (2020) analyzed the areas of accretion and erosion along the Yellow River (China) using GEE and Landsat images from 1976 to 2018. The authors identified that the annual land accretion rate of 28.60 km²/year decreased by 0.31Km²/year after the upstream construction of the Xiaolangdi reservoir in 2002. However, despite GEE capabilities, the authors used the platform only for Landsat pre-

processing, removal of clouds and shadows, and Random Forest image classification. The classified images were then transported for ArcGis software to identify the areas of accretion and erosion in the studied region (LI et al., 2020). In the same way, Schwenk et al. (2017) and Isikdogan et al. (2017) used GEE to pre-process and then download Landsat data, which were then used in other programming platforms to detect river width and meander migration. These examples show that GEE is so far being under-exploited to monitor and detect river meander migration and morphodynamics.

3. THE IMPACT OF MEANDER MIGRATION ON RIVERINE AMAZONIAN COMMUNITIES USING LANDSAT TIME SERIES AND CLOUD COMPUTING

3.1 Introduction

Amazonian white-water rivers are streams with high turbidity due to the sediment transportation coming from the Andean Mountains (RÍOS-VILLAMIZAR et al., 2014; JUNK et al. 2011; MARTINELLI et al., 1989; MARTINELLI et al., 1988). The high sediment concentration in those rivers plays an important role in promoting the meander migration and therefore influences the river sinuosity (AHMED et al., 2019; CONSTANTINE et al., 2014; JUNK et al. 2011). A curvature in a river channel produces high fluid momentum, increasing the shear stress and thus the erosion over the outer bank (DIETRICH, et al., 1979). The opposite happens in the inner bank, which has a low-stress shear, thus promoting sedimentation. The sediment attached to the meander inner banks (convex relative to the channel centerline) are called point bars, and they grow vertically and horizontally as the sediment accumulates in a process called migration (LEGLEITER et al., 2011). The presence of forest vegetation plays an important role in decreasing the rate of meander migration since it increases the resistance to erosion in outer banks (IELPI et al., 2020). As a result, deforestation along the river might increase the erosion process along the river (HORTON et al., 2017). Higher curvature is another important factor since it leads to higher erosion, increasing the river migration process (SYLVESTER et al., 2019). This migration, in turn, increases even further the river curvature, leading to higher erosion rates in a positive feedback cycle. This positive relationship increases the river curvature until a cutoff event happens, when the river favors a shorter path, leaving an oxbow lake as the abandoned river reach (CAMPOREALE al., 2008). These cutoff events reduce the river sinuosity (WEISSCHER et al., 2019), regulating the river meander formation.

The meander migration has been studied using different techniques, including hydrological and numerical models (LANGENDOEN et al., 2016; ZINGER et al., 2013), experimental laboratory studies (WEISSCHER et al., 2019; VAN DIJK et al., 2012), orbital remote sensing data (CONSTANTINE et al., 2014; SYLVESTER et al., 2019) and aerial photography (BERTALAN et al., 2018; PARSAPOUR-MOGHADDAM;

RENNIE, 2018; SCHOOK et al., 2017). Hydrological modeling approaches normally depend on precise topographic data and discharge information, requirements that limit their use in large and remote regions. Zinger et al. (2013), for example, measured the river velocity and bed elevation to study a single meander bend with two developing chute cutoffs on the lower Wabash River (USA). Other studies that require in-situ observation also limits the large-scale application. Parsapour-Moghaddam and Rennie (2018), for example, used aerial photography, light detection, LIDAR, bathymetric data, and field examination to study two reaches of a meandering creek in Canada. Bertalan et al. (2018), using a UAV (Unmanned Aerial Vehicle), studied a 2.2 Km reach of the Sajó River (Hungary) to assess the relationship between land cover and meander migration. Nevertheless, the combination of long-term time series of orbital Remote Sensing images and higher computer performance, allows researchers to study larger and remote floodplain dynamics with precision and accuracy (WANG et al., 2018; HIRD et al., 2017; Horton et al., 2017). Consequently, many different studies on river meander processes have been developed using those historical remote sensing information (MARTHA et al., 2015; SYLVESTER et al., 2019) and indexes that highlight water surfaces such as the mNDWI (Modified Normalized Difference Water Index) (SPADA et al., 2018; YANG et al., 2015; MOGHADDAM et al., 2015).

Some western Amazonian rivers give a great opportunity to study those processes without, so far, major engineering influences on the river meander mobility (AHMED et al., 2019), a condition that is rapidly changing due to the planning and construction of major dams over the Amazon (LATRUBESSE et al., 2017). The spatial and temporal variability of Amazonian rivers provide different habitats and thus speciation among species, partially explaining the high rates of biodiversity in Amazonian floodplains (FREITAS et al., 2014; ALBERT et al., 2011). The constant river meander migration promotes the formation of floodplain lakes (oxbow lakes and riparian lakes), which are rich in fishes such as Arapaima, and sandbanks used as nesting sites for turtles and birds (STANFORD et al., 2020; PEZZUTI et al., 2018; PETERMANN, 1997). These places give the local communities a reliable source of income and thus are essential to promote food security in the region (CAMPOS-SILVA; PERES, 2016). However, although the Amazonian riparian population highly depends on this process for economic stability, the constant meander migration might reduce the community's well-being. The constant river

migration might promote the loss of land and increase the inundation frequency due to erosion on the communities' shores. On the other hand, sedimentation can gradually increase the distance between their houses and the river. These processes have a profound impact on the local Amazonian river communities since they depend entirely on the river for transportation, agriculture, and fishery (NASCIMENTO; BECKER, 2010), conditions that might force them to leave to other regions. As a result, the identification of those communities is valuable information to promote public policies and improve the communities' well-being.

In Bangladesh, the erosion process is considered a natural disaster because it has huge impacts on the regional economy and riverine community well-being (BILLAH, 2018). In the same way, successful farmers lose their entire territories due to the intense erosion hazard (Bhuiyan et al. (2017). There are many studies on river morphology change impacts on Bangladesh riparian communities (MONIRUL et al., 2017, ISLAM et al., 2020; BHUIYAN et al., 2017; ISLAM et al., 2017). According to their estimates between 1973 and 2011, Bangladesh has lost a total of nearly 17 million dollars due to hazards caused by river erosion. However, due to the intense and common river morphology hazards, the local riparian communities have evolved different mechanisms to mitigate the flooding and erosion processes on their lands (ISLAM et al., 2017). The communities, for example, build thatch houses and bamboo fence houses that are easier to move away from areas affected by the flooding event (ISLAM et al., 2017). They also plant trees along their houses to decrease the wave impact during flooding and raise their poultry cages using bamboos to preserve their livestock (ISLAM et al., 2017).

In the Amazon, there are far fewer studies describing or analyzing the river meander migration impacts on local communities. Mello et al. (2012), for example, described a community living close to the Solimões River that created a technique to transport their houses to upper regions during flooding events without having to completely dismantle them (MELLO et al., 2012), a similar practice found in Bangladesh communities (ISLAM et al., 2017). Parintins city, along the Amazonian river, is facing erosion processes and suffering economic impacts related to land loss, property degradation, and harbor operational problems (MARQUES; CARVALHO, 2019). Considering that even cities with relatively good infrastructure suffer from channel migration in the Amazon, small villages and riparian communities with no direct access to basic public services are the

most vulnerable to these processes. Although river meander migration is driven by complex processes, river erosion and sedimentation areas are easily spotted using remote sensing time series. As a result, the orbital imagery might be used to track the relationship between local communities and floodplain natural processes and to identify the most vulnerable communities to meander migration impact on remote Amazonian regions.

Here we evaluated the number of communities vulnerable to the erosion and sedimentation process in the highly sinuous Juruá River. To identify the erosion and sedimentation areas, 36 years of Landsat images were used to reliably classify pixels under erosion or sedimentation processes along the period (1984-2020). The processing was performed in Google Earth Engine (GEE) using mNDWI temporal linear regressions to track the water surface change trend in all Juruá basin pixels. Then we systematically mapped riparian rural communities subject to the meander migration process along 3000 Km of the Juruá River (91% of the total river extend). A theoretical model was created to illustrate the main impacts of meandering processes on the local communities. We hypothesize that the communities' empirical knowledge about the floodplain dynamics mitigates the extend of the river meander impact on their populations. The results show the communities most affected by river meander migrations and aim to better guide public policies for Amazonian riparian communities. Integrating local human perspectives in the floodplain natural processes is promising to preserve both the local communities and ecosystem services (PEDERSEN et al., 2019).

3.2 Materials and methods

3.2.1 Study area

The Juruá watershed (Figure 3.1) has an extension of 224,000 km² with an altitude varying from ~453 m upstream to 40m downstream, in the confluence to Solimões River (SOUSA; OLIVEIRA 2016). The Juruá River has a length of 3,283 km and is considered one of the most sinuous rivers on Earth (SOUSA; OLIVEIRA 2016). Having the headwaters in Peru, the Juruá River crosses the Brazilian states of Acre and the southern Amazonas reaching the Solimões (COSTA et al. 2012; SOUSA; OLIVEIRA 2016). The BR 364 is the Juruá major road access, linking the Cruzeiro do Sul City to the Acre capital

Rio Branco. Although the Juruá basin is still highly preserved, close to the cities with road access (such as Cruzeiro do Sul) we identified deforestation along the river and a high presence of communities (Figure 3.1). Overall, the communities that live along the Juruá basin river banks are sparse and highly dependent on the water dynamics for agriculture, fishing, logging activities (DAVIDSON et al., 2012), and transportation.

The Jurua River basin, in this study, was divided into three different sections according to the width of the meander belt and basin geomorphology. The Upper Course encompasses from the headwater until the Juruá River confluence with the Tarauacá River. In this region, the basin is highly asymmetrical, with long rivers flowing from the eastern margin, and with a narrow and confined meander belt along the Juruá. In the Middle Course, the Juruá basin becomes narrow and symmetrical, and the meander belt width almost duplicates (from less than 10 km in the upper basin to more than 20 km. In the Lower Course, both the basin and the meander belt become wider toward the Solimões River confluence (Figure 3.1). The Juruá River has a monomodal flood pulse divided into four distinctive hydrological periods: the high-water period (March to May); the receding period (June to July), the low-water period (August to October), and the rising period (November to February). The season division was performed using Gavião fluviometric gauge mean discharge (Figure 3.1.a) and its first derivation (Figure 3.1.b) from 1972 to 2019.

Figure 3.1 - Study area and riparian community identification (a). Juruá mean discharge and its seasonal periods (a) and the discharge first derivation (b).

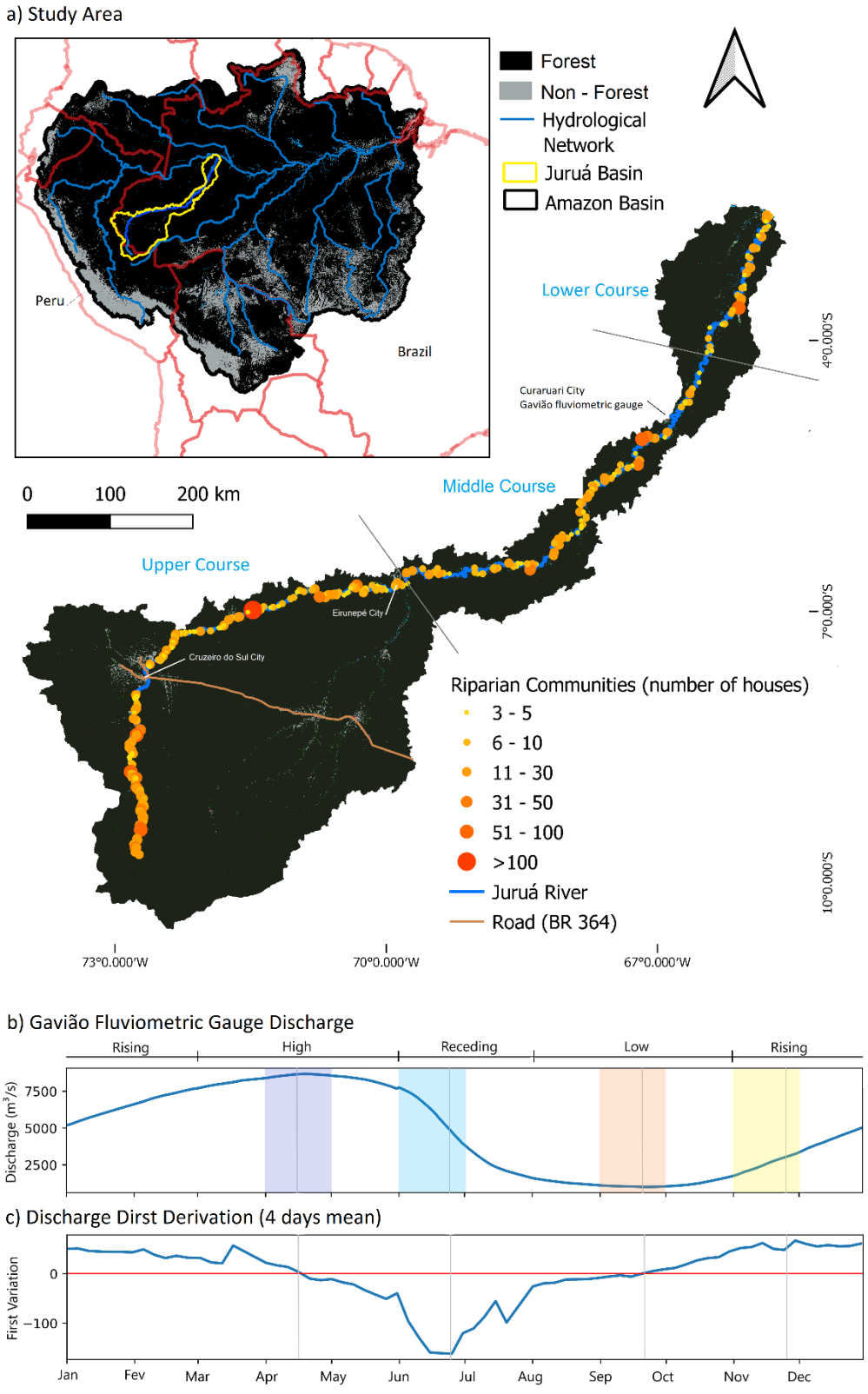

3.2.2 Water Surface Change Detection Algorithm (WSCDA)

The Water Surface Change Detection Algorithm (WSCDA) was developed in the GEE platform to identify the river meander migration based on regions of erosion and sedimentation. The algorithm computes a per-pixel analysis of temporal changes in water content along the river, identifying regions where the presence of water increased or decreased. For that, the water index mNDWI was used as a proxy of water presence, considering that high values of mNDWI are associated with a high proportion or entire coverage of surface water into the pixels, while low values of mNDWI suggest a low proportion or no surface water into the pixel. The processing was divided into three steps. Firstly, Landsat time-series data were selected in GEE, and pre-processing procedures were applied to construct a database with minimum cloud cover and representative of Juruá River channel dynamics. The mNDWI index was then applied in all pre-processed Landsat images. Secondly, a temporal linear regression was applied and the slope (θ) was obtained to identify pixels where the presence of water changed over time. Thirdly, the classification of pixel change was based on a slope threshold defined by using samples along the Juruá River. All three steps are discussed in the following sections. It is important to highlight that climate variables and their relationship with river meander migration were not analyzed in this study, since they are well covered in different papers in the region (CONSTANTINE et al., 2014; SYLVESTER et al., 2019).

3.2.2.1 Landsat time series selection and pre-processing

The Landsat availability of geo-radiometrically consistent and calibrated data has led to a new generation of algorithms and computational approaches (WULDER et al., 2019). Today, the Landsat program keeps in the lead of remote sensing development, thanks to its huge historical database and new imagery that allows the use of time series to study trends and spatial-temporal dynamics or Earth surface (WULDER et al., 2019). The Landsat 5 Thematic Mapper (TM) provides images from 1984 to 2013, while the Landsat 8 Operational Land Imager (OLI), launched in 2013, is still in orbit and thus provides images from 2013 to current dates. All Landsat satellites have 30m spatial resolution, are near-polar orbit with repeat cover every 16 days, and have bands that are suitable for water extraction, such as green, band 3 in Landsat 5 (0.52-0.60 µm) and band

4 in Landsat 8 (0.53-0.59 µm), and Short-wave infrared, band 7 in both Landsat 5 (2.08-2.35 µm) and Landsat 8 (2.11-2.29 µm).

The Landsat imagery and data processing was provided by the cloud-based platform Google Earth Engine (GEE). The GEE enables users to access high-performance computing resources to process huge geospatial datasets (GORELICK et al., 2017). The Landsat 5 and 8 datasets, with geometric and radiometric quality requirements and atmospherically corrected using LEDAPS software for Landsat 5 (SCHMIDT et al., 2013; GORELICK et al., 2017) and LaSRC for Landsat 8 are provided by the GEE. Additionally, the cloud platform provides images with cloud masks using the Landsat radiometric saturation (QA). The cloud mask is crucial to process large Landsat time series since it removes the undesirable cloud interference from the dataset. As a result, it provides an ideal source of information to track water surface changes and dynamics (WULDER et al., 2019; ZHU et al., 2017; WANG et al., 2018; PEKEL et al., 2016).

To perform the WSCDA, Landsat 5 and Landsat 8 surface reflectance from 1984 to 2020 were obtained from March to June in GEE platform. This period was chosen because it encompasses the highest erosion rates during the high-water season (March-May), and allows the identification of sand deposits provided by cloud-free images at the beginning of the falling water level (June). To cover the river spatially and temporally, 986 different Landsat 5 and 8 images were processed (paths 001 to 005 and rows 062 to 066). After the cloud mask application to the Landsat collection, the images with more than 50% cloud cover were excluded, leaving 637 scenes. The pre-processing techniques created a cloud-free database of Landsat 5 and 8, covering the Juruá River and its spatial-temporal hydrological dynamics.

3.2.2.2 Water surface change detection

After setting the Landsat time series, the Modified Normalized Difference Water Index (mNDWI), which is a band ratio between the green and the SWIR band, was applied in all available images to highlight the presence of open water. The mNDWI is a common index used in the literature to track open water dynamics (FERRAL et al., 2019; SIVANPILLAI et al., 2020), and has high accuracy when compared to other water indexes (SZABÓ et al., 2017). The mNDWI was developed to enhance water information

while suppressing the noise of vegetation and soil (XU, 2006), and thus has become an effective tool to monitor water resources surrounded by vegetation (SINGH et al., 2015), such as the Juruá floodplain lakes and river. Linear regressions, at pixel scale, were performed between historical mNDW and time (years) to identify erosion and sedimentation regions. This methodology allows identifying positive or negative temporal trends in the presence of open water in the pixels along the Juruá River channel. The classification methodology was based on the slope (angular coefficient of the mNDWI temporal linear regressions). The slope (θ) indicates the annual increase or decrease trend in mNDWI in all the scene pixels. The temporal linear regression is a way to identify consistently pixels that suffered erosion or sedimentation processes without major interference from spurious or cloudy pixels. Pixels with high positive θ, above a specified threshold, were classified as erosion areas since they move from a low mNDWI value (land pixel) to a high mNDWI (open water pixel) over the years. On the other hand, pixels with low negative θ, below a specified threshold, were classified as areas that suffered sedimentation over the years, since they move from a high mNDWI open (water pixel) to a low mNDWI (land pixel). Pixels with no significant change were not classified, as they represent stable areas. Although time series are normally based on binary thematic maps (water/no water) (FREY et al., 2015), in this study we used only mNDWI values to identify the temporal slopes to decrease the error associated with multiple classifications.

3.2.2.3 Threshold selection

To specify the slope thresholds used to classify erosion and sedimentation areas, 10000-pixel samples with temporal mNDWI slope information (1984 – 2020) were collected along the Juruá basin within areas of erosion and sedimentation with 100% and -100% normalized change in occurrence, respectively (PEKEL et al. (2016). The maximum normalized change in occurrence (100% and -100%) provided by Pekel et al. (2016) was selected to collect samples within reliable erosion and sedimentation areas. The slope values of the samples were then sorted and the 10% quantile representing sedimentation (-0.014 ΔmNDWI/year) and erosion (0.015 ΔmNDWI/year) were used as thresholds (**Figure 3.2**). Therefore, pixels that had a mean annual mNDWI increase higher than 0.015 over the analyzed period were classified as erosion areas, while pixels that had an

annual mNDWI decrease lower than -0.014 were classified as sedimentation areas. The 10% quantile allowed to exclude spurious pixels and classify only regions with substantial changes. Note that the areas of water change calculated from Pekel et al. (2016) were not directly used in this study because they result from a global generic algorithm for a shorter time series, and it does not allow the analysis of specific seasons to highlight river channel dynamics in different hydrological periods.

Figure 3.2 - mNDWI angular coefficient samples and the angular threshold used to classify erosion and sedimentation pixels (10% threshold). The slope samples were collected on erosion and sedimentation areas (100% and -100% normalized change in water occurrence) provided by Pekel et al. (2016) and organized in increasing order.

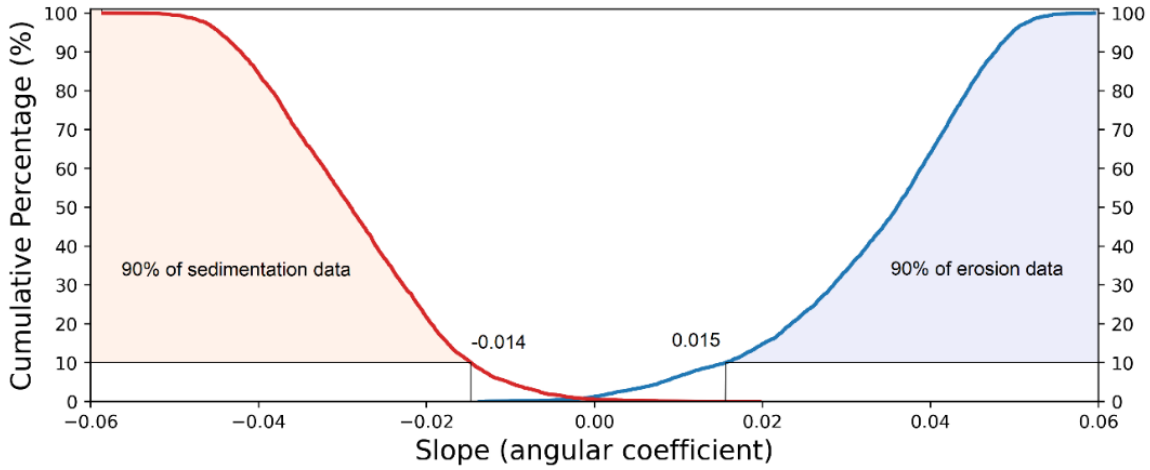

3.2.3 Accuracy assessment

The erosion and sedimentation maps generated by the WSCDA were evaluated in terms of omission and commission errors, as done by Pekel et al. (2016). To perform the validation, a set of 3000 points were randomly distributed within a 500m Juruá River centerline buffer. With this methodology, a wide range of river processes were covered, preventing the analysis from bias. The mean of the Landsat 5 and Landsat 8 bands from March to June of 1984 and 2020, respectively, were computed to create a true color composition of both years. Both images were used to identify whether the erosion and sedimentation maps generated were correctly classified according to the random samples. Specifically, for each random sample, we attributed a number whether the point suffered

erosion (1), sedimentation (2), or neither process (3) according to the Landsat Images and according to the erosion and sedimentation WSCDA classification. These values were then used to perform the confusion matrix. The number of correctly classified points of each category was divided by the total number of the reference points (identified using Landsat images) to perform the producer's accuracy (PA) and by the total number of points classified in each category (using WSCDA) to perform the user's accuracy (UA) (PATEL and KAUSHAL, 2010). The PA and UA were then subtracted from 100 (100 - PA and UA) to obtain the respective omission and commission errors. The accuracy evaluation was performed using a confusion matrix and the omission and commission errors were analyzed.

3.2.4 Community identification and impacts

According to Giddens (1991), the concept of community refers to a place where culture, knowledge, and social structure are produced. Vasconcellos and Sobrinho (2017) identified that in the Amazon, the concept of community has a fluid and dynamic meaning. The Amazonian communities are based on a place where the population is involved in a variety of socio-cultural practices, living according to the knowledge acquired from experiences developed throughout generations (Wenger, 2011; VASCONCELLOS and SOBRINHO, 2017). In this study, we defined communities based on their physical structure, assuming the existence of a certain number of houses. Regions with more than three houses clustered in a riverbank were mapped as communities

The community identification was performed using Esri base maps, which uses high-resolution SPOT imagery (2.5m), to visually track the communities in the Juruá using a 1:20000 fixed-scale to pinpoint the communities and the 1:5000 scale to count the number of houses. The Esri base map provides a single image mosaic of the Juruá River using SPOT images from different acquisition dates, ranging from 2005 to 2019 (Figure 3.3). As result, due to the lack of historical high spatial resolution imagery, the temporal variation of communities was not identified. We considered that the communities did not move during this period, a condition that although not properly correct, might be supported due to the higher number of recent images (after 2013 – Figure 3.3). The

Instituto Juruá (unpublished data) surveyed 94 communities along the Juruá in 2016, estimating that on average each house accommodates 4 people. As a result, we estimated the riverine population in the studied area by assuming this number of people per house. However, this methodology was only performed to have an overall estimation of the Juruá River population. To analyze the river meander migration impact on riverine communities, we used only the number of communities' estimation.

Figure 3.3 - Number of communities identified by SPOT images in different acquisition years.

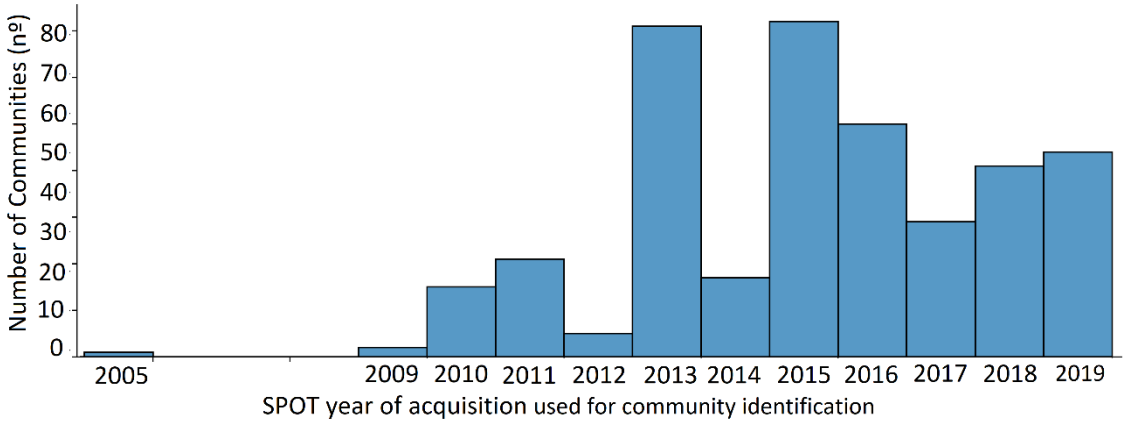

The sedimentation and erosion maps were used to identify and classify the communities according to three classes: riparian communities that live in locations threatened by erosion, sedimentation, and communities that live in stable locations along the Juruá River (Figure 3.4). Communities living in stable regions are not suffering erosion nor sedimentation along their shores. The criterium to classify a given community threatened by erosion (Figure 3.4.c) or sedimentation (Figure 3.4.d) is that the process must affect the entire community, from the first to the last house. Beyond erosion and sedimentation areas, the communities were assigned to stable areas when living close but between sedimentation and erosion areas (Figure 3.4.a) and living away from the migrating river meander (Figure 3.4.b).

Figure 3.4 - Visual scheme to show possible locations where local communities live along the Juruá River. The figure represents areas of erosion and sedimentation and communities living in stable, erosion, and sedimentation locations.

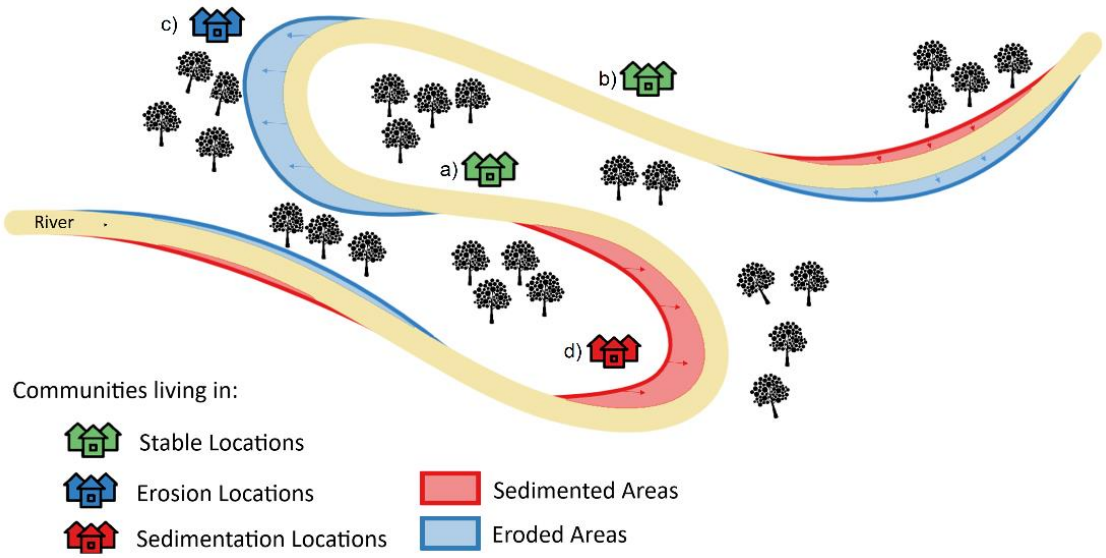

The river meander migration changes the floodplain landscape over time due to the processes of erosion and sedimentation. For communities that live along the river banks, those processes might impact directly their lands, leading to a territory expansion or reduction. The process of erosion, for example, might decrease the agricultural land available and ultimately threaten their houses. On the other hand, communities that live on river banks that are suffering sedimentation processes have the distance between the river and their houses increased over the years. Based on the literature and personal experience, the main erosion and sedimentation impacts on local riverine communities are discussed in our Theoretical Model. The model was divided into two different categories, direct impacts, which occur along the communities' shores, and indirect impacts, which happen on a regional scale and are related to food insecurity. Only direct impacts were mapped due to the simplicity of identifying erosion and sedimentation along the communities' shores. Indirect impacts, although not mapped, were included in our Theoretical Model.

3.3 Results

3.3.1 Water Surface Change Detection Algorithm (WSCDA)

The areas where the river sedimented or eroded from 1984 to 2020 were mapped using the WSCDA along the Juruá River (Figure 3.5). The results were visually accurate since the erosion pixels were placed on the outer bank river locations and the sedimentation on the inner bank locations, as defined by Legleiter et al. (2011). It is possible to observe a lower meander migration of the Jurua river channel in the Lower Juruá section (Figure 3.5.a) when compared to that of the Middle Juruá section (Figure 3.5.c). Furthermore, along the Upper Juruá section (Figure 3.5.b), the processes of sedimentation and erosion are not just changing the river contours, it is completely moving the river path through the landscape. In this region, the river path in 1984 completely sedimented, displayed in the sedimentation layer, and moved to a new location, represented in the erosion layer (Figure 3.5b). As a result, the processes of sedimentation and erosion are more intense concerning the river width in this section of the Juruá Upper Course.

Figure 3.5c also shows two examples of mNDWI variation over time for pixels classified as erosion (Figure 3.5.1A) and sedimentation areas (Figure 3.5.1B). From Figures 3.5.1A and 3.5.1B, both sedimentation and erosion rates at the two pixels indicate a change in erosion rates around 2005. Figure 3.5.1A, for example, allows us to assume that the pixel was occupied by land between 1985 and 2005 (negative values of mNDWI), and then, between 2005 and 2010 the erosion rate increased (mNDWI increase), causing the pixel to become open water after 2010 (positive values of mNDWI). The opposite has happened to the sedimentation pixel (Figure 3.5.1B), whose mNDWI value gradually decreased from 1985 to 2005, then stabilizing as a land pixel beyond 2005 (negative values of mNDWI). As a result, the erosion process over the Landsat pixel was more intense and happened during a shorter time interval (5 years), when compared to the sedimentation (20 or more years). The WSCDA only identifies the mNDWI linear regression slope (represented in Figures 3.5.1A and 3.5.1B) to classify the pixels as erosion or sedimentation. Additionally, upon all the three scene examples, communities living in stable, erosion, and sedimentation locations are represented. Overall, the figures show that most of the communities are placed in stable regions.

Figure 3.5 - Eroded and Sedimented areas for three regions (a, b, c) along the Juruá River. Zoom over the region 'c' allows comparing images from 1984 and 2020. On the right side, the mNDWI variation of two pixels classified as erosion (1.A) and sedimentation (1.B) are shown. Due to the low cloud coverage, Landsat SWIR maps during the dry season are presented. Over the maps, communities classified as living in stable, sedimentation or erosion locations are displayed.

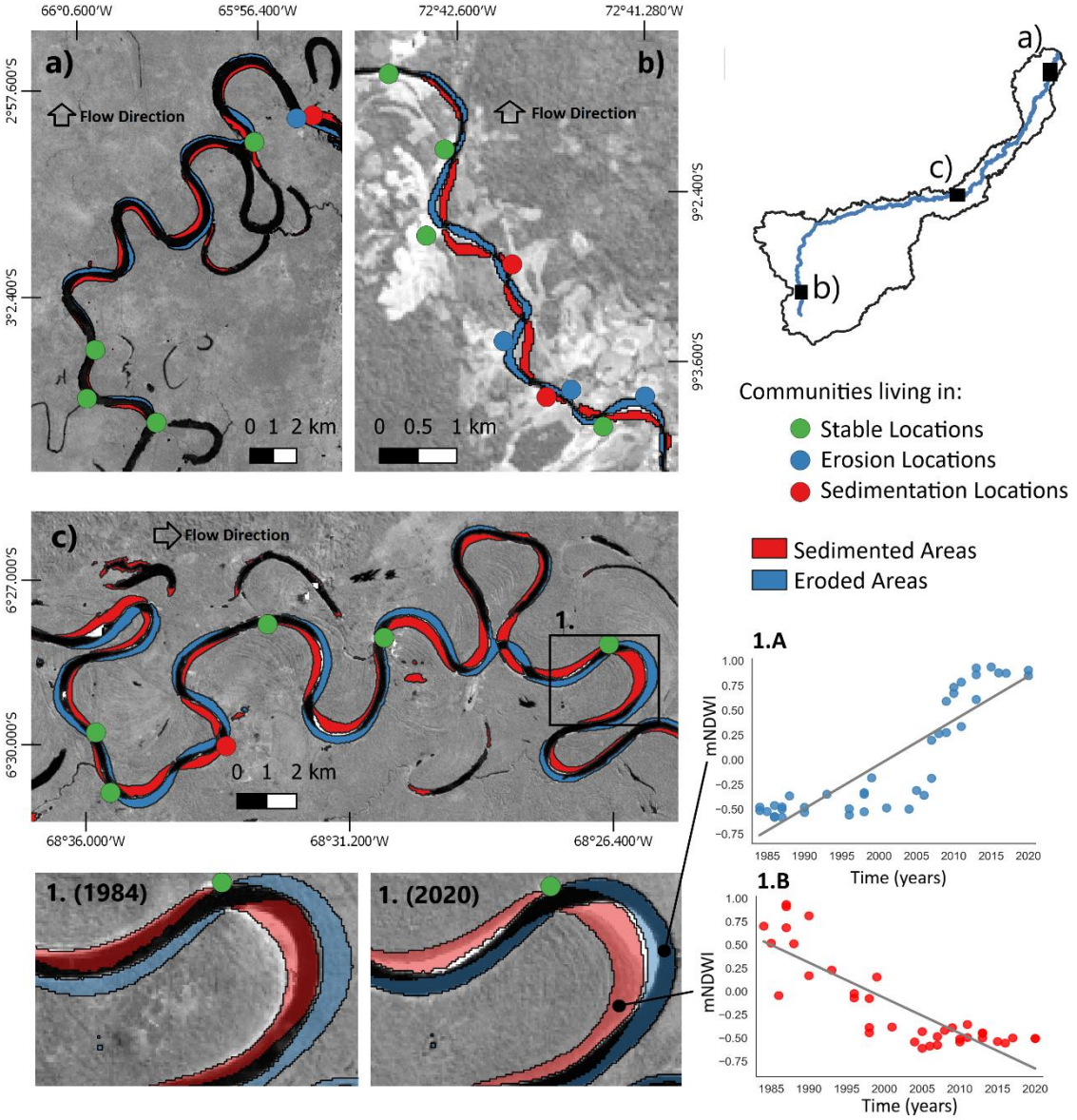

A zoom on a Juruá River region in 1984 and 2019 and the erosion and sedimentation areas are represented in Figure 3.6. The pattern of erosion on one bank side and sedimentation on the opposite bank was detected even in small areas, showing the great precision of the WSCDA. Although the cloudy pixels were not removed (Figure 3.6), the images displayed are the best pixels available in 1984 and in 2019 (March to June),

showing that the region is highly affected by cloud coverage. With this example, it is possible to assert that despite the huge cloud coverage of the region (Martins et al., 2018), erosion and sedimentation mapping is feasible. Furthermore, no pixels were detected on forest areas and on regions of no migration (considered stable by the algorithm), showing the algorithm good performance

Figure 3.6- Comparison between a 1984 and a 2019 Landsat SWIR map, showing areas classified as erosion and sedimentation regions aside Juruá River channel.

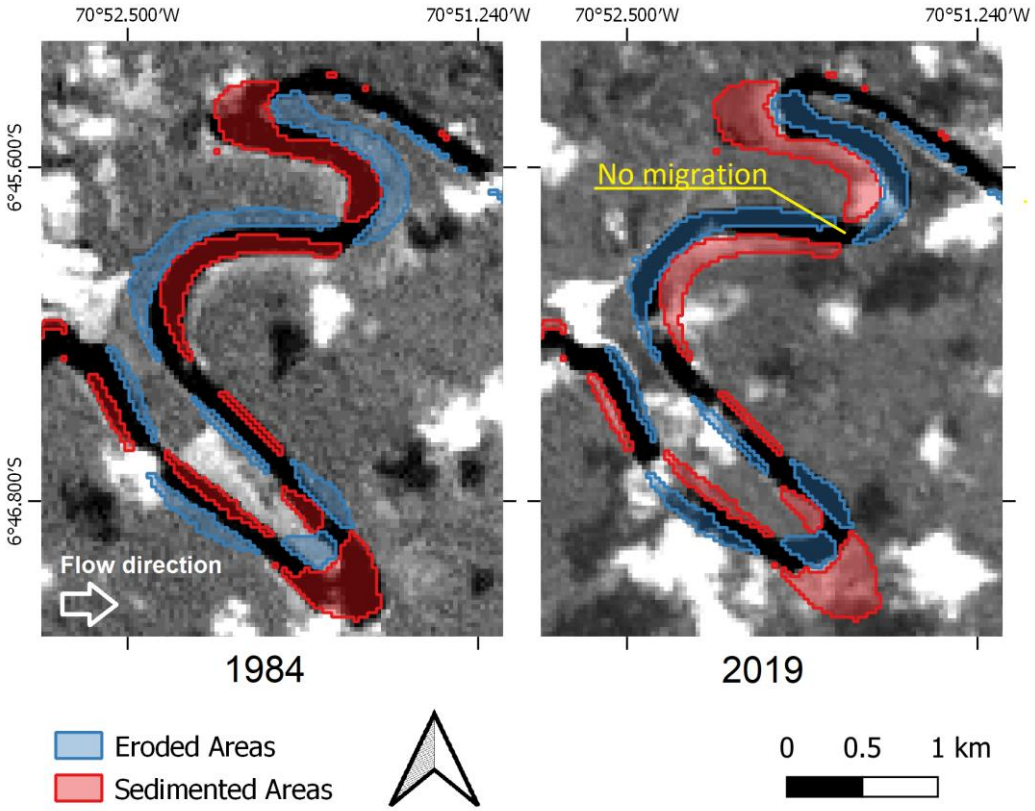

The confusion matrix (Table 2.1) indicates that the omission and commission errors were less than 14%, and 8%, respectively. Overall, commission errors were lower than the omission errors, showing the trend of underestimation of the areas subject to erosion. Most of the omission errors occurred in areas of recent erosion sedimentation since the recent changes in mNDWI are not powerful enough to change the linear regression slope value, limiting the meander detection of subtle channel migration by the algorithm. Furthermore, the 30m Landsat spatial resolution means that there is a high spectral mixture between forest/land and water in the river border pixels, which affects the

mNDWI variation and thus delays the detection of erosion and sedimentation. Since the erosion and sedimentation areas are well separated (Figure 3.6), there were no errors between both classes, but just between stable and meander migration areas. Nevertheless, the errors discussed do not affect the erosion and sedimentation identification along the river and thus do not impact the classification of communities living in unstable river locations.

Table 2.1 - Confusion Matrix for the WSCDA. The Omission and Commission errors are highlighted.

	Classified (nº of points)			
True (nº of points)	Stable	Erosion	Sedimentation	Omission error (%)
Stable	1730	5	17	1.26
Erosion	43	277	0	13.44
Sedimentation	24	0	223	9.72
Commission error (%)	3.73	1.77	7.08	
Overall Accuracy = 96% Kappa Index = 90%				

3.3.2 Meander migration community assessment

Overall, we identified 369 riparian communities living along the Juruá River. Considering that each house accommodates on average 4 people, we estimated that the riverine population along the Juruá River has a total population of 16636 people. Along the river, small communities are common, with only three houses (45 communities) (Figure 3.7A). We suppose that some of these small settlements are probably home to members of the same family. The number of communities steadily decreases for larger communities, reaching only one community with 19 houses. For even larger communities the number of settlements keeps low, with only 5 communities larger than 60 houses (Figure 3.7A). In terms of population, communities with 7 houses have the highest population combined, with 896 inhabitants (combined pop = 32 communities x 7 houses x 4 people per house) (Figure 3.7B). The combined total population decreases for communities larger than 7 and lower than 30 houses due to the lower number of settlements. For communities larger than 30 houses, the low number of communities is compensated by their higher number of houses, increasing the overall population. The largest identified community, for example, with identified 190 houses, was estimated to have alone approximately 760 inhabitants (combined pop = 190 houses x 4 inhabitants) (Figure 3.7B). Overall, the Juruá

River is home to small riparian communities, a condition that increases their vulnerability to natural processes such as the river meander migration.

Figure 3.7 - Number of communities according to their number of houses (A) and total combined population for each house group (B).

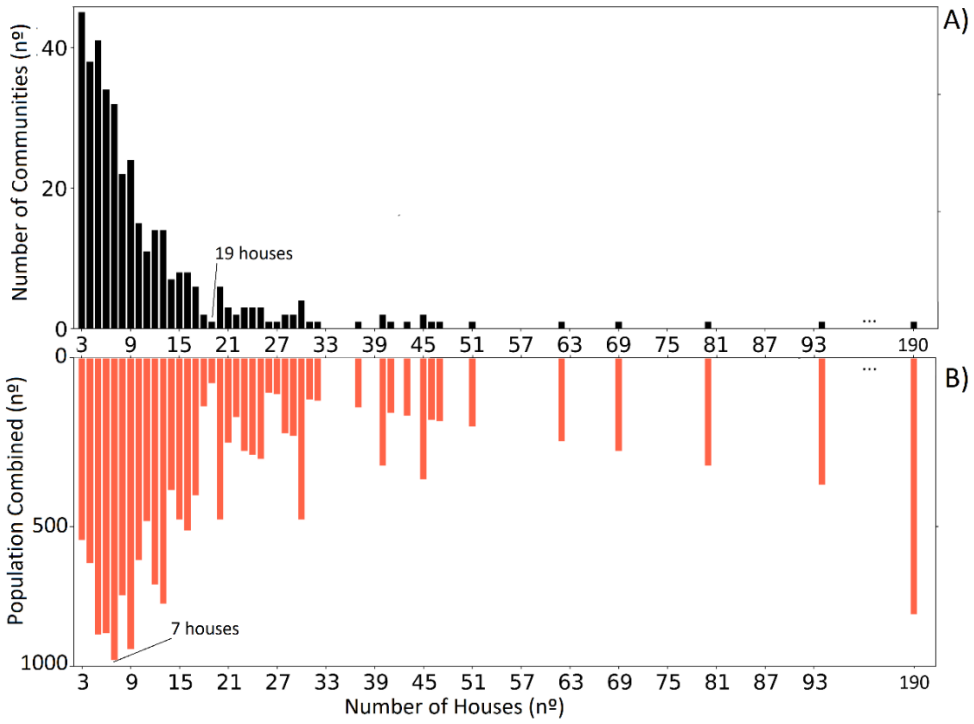

The accurate WSCDA allowed to classify the communities according to the following impact status: living in erosion, sedimentation, or in stable regions (not suffering any meander migration process). The meander migration impact on riverine communities can be observed in Figure 3.8, which shows a zoom on three different Juruá River locations. Within blue locations (eroded areas) it is possible to observe erosion marks on the land and communities nearby living closer to the Juruá River. In Figure 3.8.c, for example, the river moved 150m into community land, a fast process of erosion that might threaten the community in a near future. On the other hand, within red locations (sedimented areas) (Figure 3.8.a), higher sand deposits are presented and the communities nearby living at a higher distance from the river. In Figure 3.8.a, for example, there are two communities with opposite meander migration impacts, one living in a location threatened by erosion and the other by sedimentation. Furthermore, Figure 3.8.b shows a community living close but between sedimentation and erosion locations. This community and others in the

same condition, as explained, were classified as living in stable locations. Overall, Figure 3.8 highlights the differences between the 2.5m high spatial resolution, from Esri Basemap (used to identify the communities), and the meander migration areas classified using the 30m Landsat imagery.

Figure 3.8 - Erosion and sedimentation impact on communities in three different Juruá locations. An Esri basemap was used to show the communities and the river.

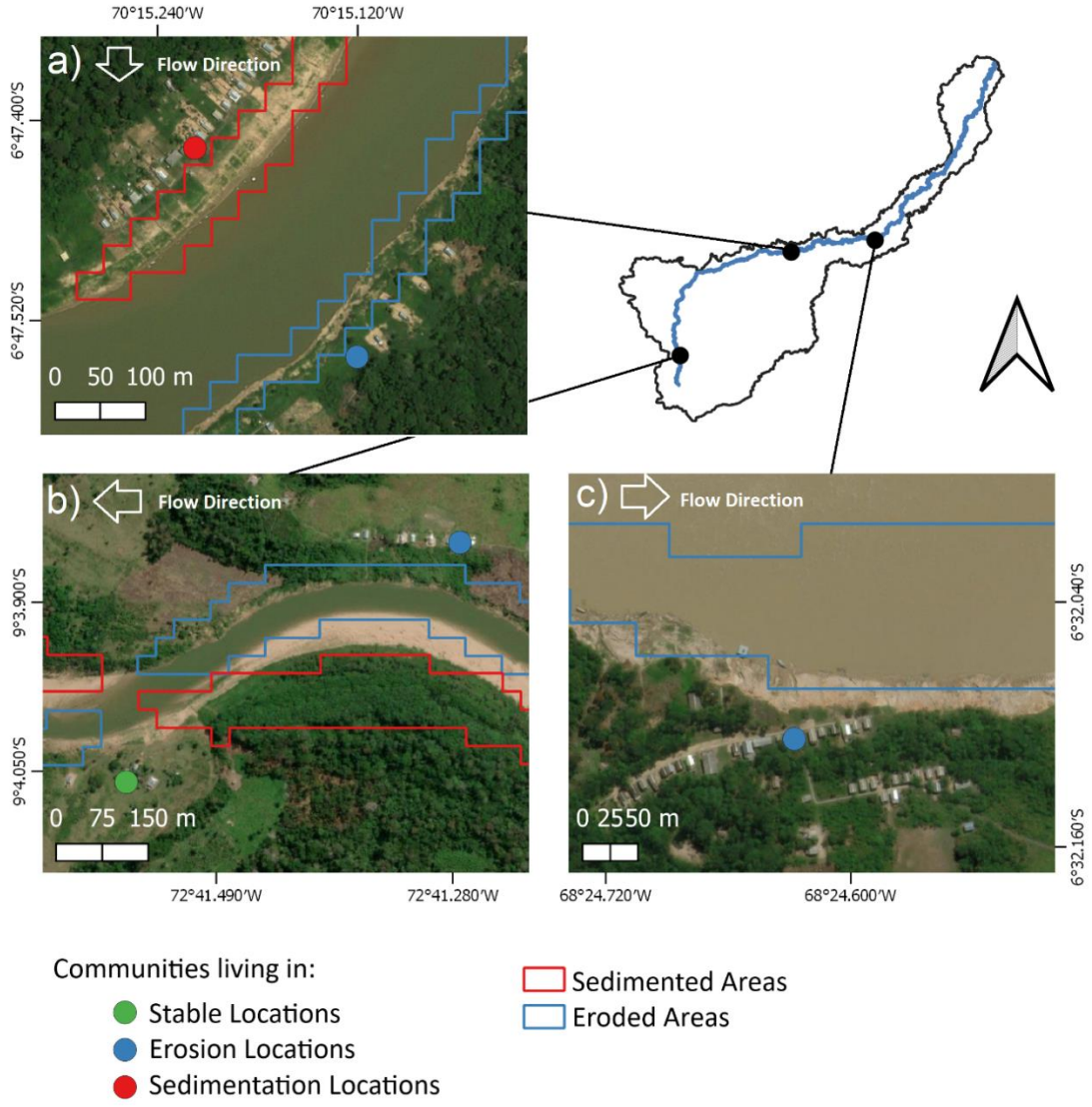

Overall, the majority of communities along the Juruá River live in stable regions (58.8% - 217 communities), followed by sedimented (26.02% - 96 communities) and eroded areas (15.18% - 56 communities). The classified communities over the entire Juruá River are

presented in Figure 3.9 which shows the Juruá River altitude variation (Figure 3.9.b), on top of the number of communities classified as living in stable, sedimentation or erosion locations (Figure 3.9.a) and at the bottom the proportion of classified communities living in the Upper, Middle and Lower Juruá course (Figure 3.9.c). The no-data presented around the Cruzeiro do Sul City and Carauari City (Figure 3.9.a) is caused by the fact that communities around these cities have road access to both cities and thus were excluded from the analysis. The river altitude profile shows that our analyzed river sections start at an altitude of 244m and end at an altitude of 40 (Juruá confluence into the Solimões River) (Figure 3.9.b). There is a higher number of communities living in the Upper Juruá Course, especially upstream the Cruzeiro do Sul City (Figure 3.9.a). In the Middle and Lower Juruá Course, the number of communities is smaller and more equally distributed. Overall, we observed that most of the communities live in stable locations, followed by sedimentation and erosion locations (Figure 3.9.c). In terms of regional differences, the Upper Course region has a lower proportion of stable communities (55.79%) when compared to the Middle (64.21%) and Lower River Courses (63.41%). Moreover, the Middle Course is where the communities are best adapted to erosion processes (9.47% of communities living in erosion areas) when compared to the Upper and Lower Course sections, with almost double the proportion.

Figure 3.9 - a) Number of communities living in stable, erosion, and sedimentation areas along the Juruá River (each bar represents 30Km of the river). b) Juruá River altitude and division between Upper, Middle, and Lower Course. c) Classified community proportion for the three different river sections.

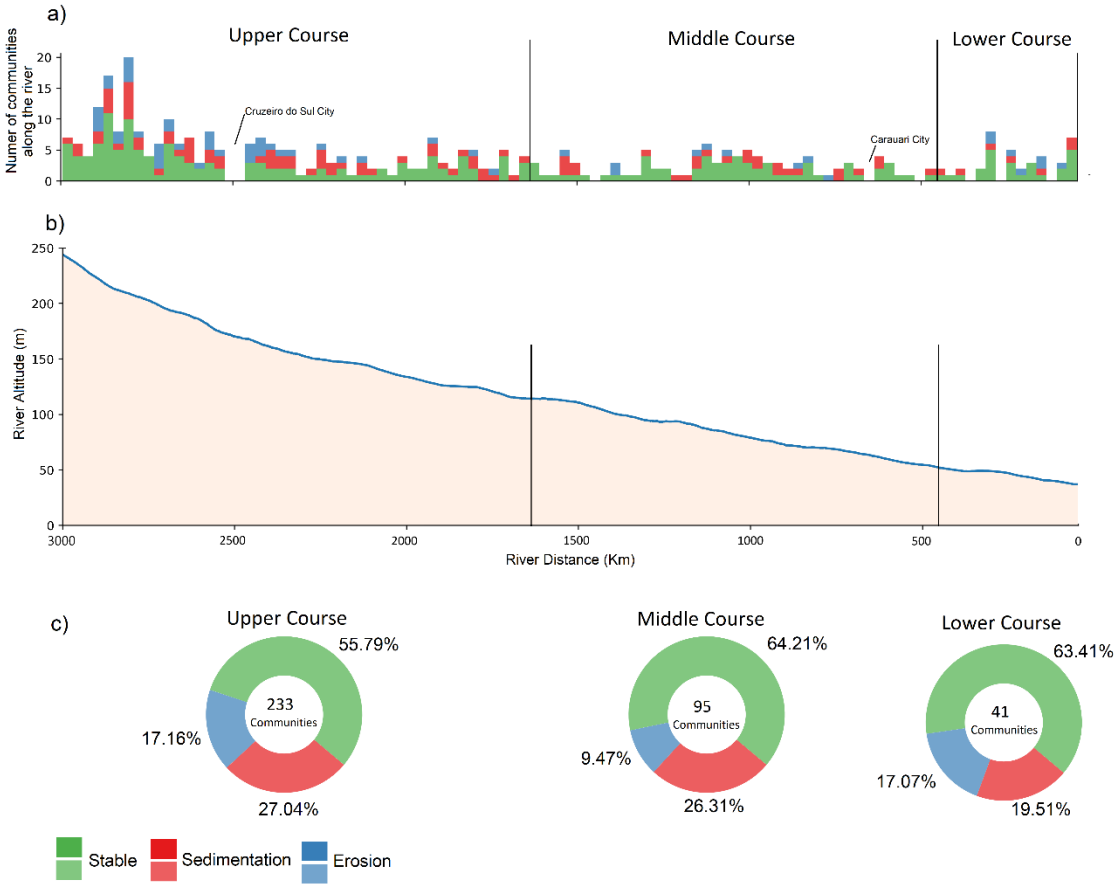

The spatial distribution of communities living in stable, erosion, and sedimentation areas is presented in Figure 3.10. Corroborating the results, Figure 3.10 shows a higher number of communities living in stable conditions, followed by sedimentation and erosion. On the same figure, a higher number of communities suffering erosion (Figure 3.10.b) and sedimentation processes (Figure 3.10.c) are observed upstream the Cruzeiro do Sul City. There is a region between the Lower Course and the Middle Course where no communities are living in erosion locations (Figure 3.10.b), probably due to the overall low number of communities in this specific region (Figure 3.10.a). This condition slightly changes along with the Middle Course, where there are few and sparse communities living in erosion locations.

Figure 3.10 - Spatial distribution of communities living in stable, erosion, and sedimentation locations.

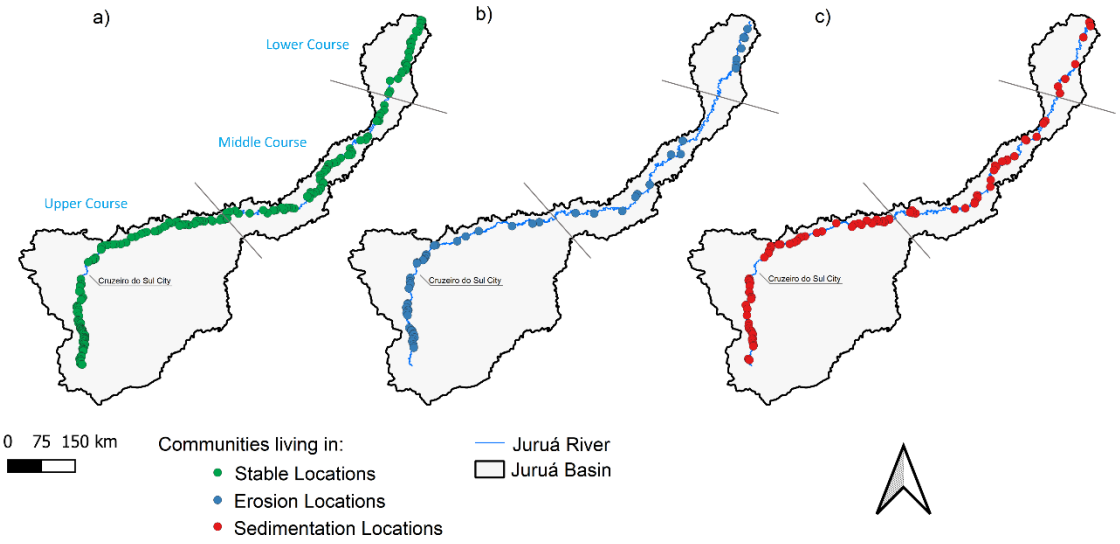

The proportion of classified communities related to their number of houses is presented in Figure 3.11. According to the results, there is a higher proportion of stable communities in settlements that have a higher number of houses (>20 houses – 70%), when compared to middle size communities (11 to 20 houses – 63.2%) and smaller communities (3 to 10 houses – 55.6%). Regarding the communities living in sedimentation and erosion locations, there is a higher proportion on smaller communities (erosion – 16.7%, sedimentation – 27.8%), followed by middle size (erosion – 14.5%, sedimentation – 22.4%) and larger communities (erosion – 10%, sedimentation – 20%). These results mean that stable regions offer ideal conditions for communities to grow, explaining the higher proportion of larger communities in stable regions. On top of Figure 3.11, the number of communities related to their number of houses is presented. Small communities are considerably more numerous (252 communities) when compared to middle size (76) and larger communities (40).

Figure 3.2 - Proportion of communities living in stable, erosion, and sedimentation areas according to their size (number of houses).

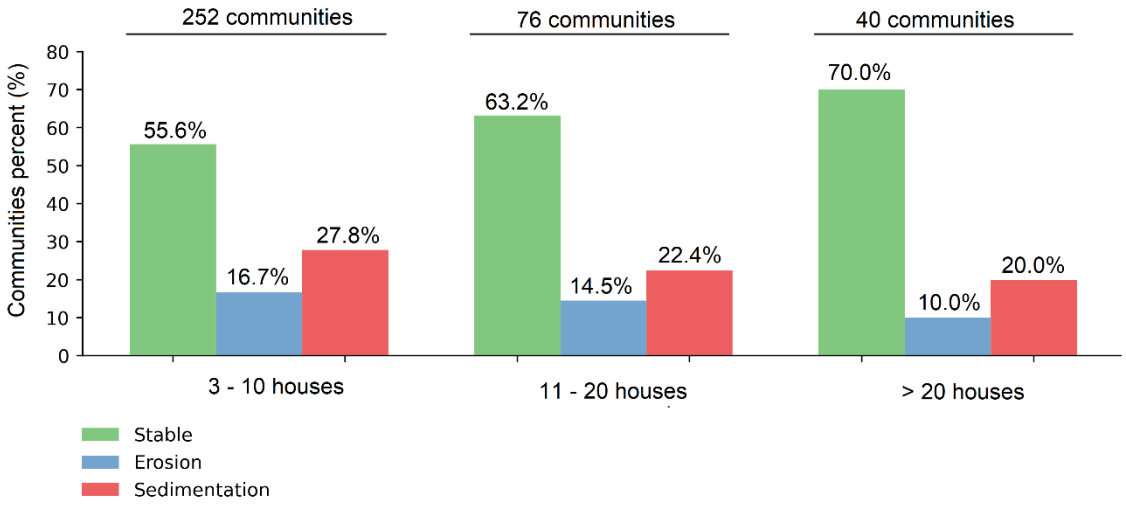

3.3.3 Theoretical model

The meander migration impacts on riverine communities are presented in our Theoretical Model (Figure 3.12). We identified four different impacts that the communities are likely to suffer from the meander migration, which includes changes in mobility, inundation, and food security (related to oxbow lakes and sand beaches). We also classified them as High, Medium, and Low impact risks (Figure 3.12). The combination of risks is higher in erosion areas (Figure 3.12.b - blue area), followed by sedimentation (Figure 3.12.c - red area) and stable areas (Figure 3.12.a - green area). The Inundation risk is high and more severe in communities that suffer erosion on their shores since they tend to live closer to the river and in outer bank locations (higher flow velocities) (FERGUSON et al., 2003). Changes in Mobility occurs when the meander migration happens directly on the community lands, impacting the mobility of local communities. In this context, the meander migration process can jeopardize access to the main river by sedimentation or threaten their shore navigation infrastructure due to erosion. Furthermore, when the river produces a cutoff, a process that occurs when the river favors a shorter path (leaving an oxbow lake), the community distance to nearby places might be reduced, improving the navigation access. The cutoff impact is not covered in our Theoretical Model because of the complexity of this event (this impact is discussed in section 4.0).

The food security of local communities can also be impacted due to the creation of new fishing grounds such as lakes and sand beaches near the local communities. When one of

the mentioned impacts or the combination of them becomes too high and thus unbearable, the communities might be forced to leave their original land and settle their houses in another river bank or move to the nearby cities. It is important to explain that due to the complexity of analyzing regional-scale impacts, this paper focused only on quantitatively investigating river meander migration's direct impact on community lands, covering exclusively the impacts of Inundation and Changes in Mobility. All the potential impacts are better discussed in the following paragraphs.

As informed, the processes of erosion and sedimentation impact directly communities that live along the Juruá banks. Communities that suffer sedimentation process (Figure 3.12.c), for example, tend to live away from the river and in regions where the river has a lower velocity (inner bank) (FERGUSON et al., 2003), reducing their susceptibility to inundation events (low Inundation impact). However, these communities tend to live away from the river, increasing their effort to reach the river shore and their boats (high Changes in Mobility). Communities that live in erosion locations (Figure 3.12.b) tend to live closer to the river and in places with higher river velocity (outer bank) (Ferguson et al., 2003), increasing their susceptibility to inundation (high Inundation impact). Those communities also have lower space to store their boats and any shore infrastructure is exposed to the water force and velocity, negatively impacting their navigability (Medium Changes in Mobility impact). Communities living in stable regions (Figure 3.12.a) were classified as living in Medium Inundation risk areas since they suffer periodic inundation events that are less frequent than erosion locations, but more intense than sedimentation areas. The higher advantage of stable communities relies on the fact that they can store their boats at an optimal distance to their houses and maintain a shore infrastructure, increasing their access to navigation (Low Changes in Mobility).

The processes of erosion and sedimentation might also naturally destroy places where the communities fish and collect turtles. The process of sedimentation, for example, might quickly sediment the channel that connects the floodplain lakes to the main river, emptying the lake over time, and thus extinguishing an important food source to local communities (High Food Insecurity - Fishing Grounds) (Figure 3.12.a). The process of erosion also impacts those floodplain lakes, since the river might advance into the lake, transforming the former lake into a river section over time. The erosion process was classified as Medium High Food Insecurity (Fishing Grounds) (Figure 3.12.b) since the

river might reclaim the oxbow lake, transforming it again on a river section. However, this process tends to be slower (the river needs to reach the lake border) when compared to sedimentation, which occurs directly on the river-lake connectivity channel. Stable regions are optimum places to preserve a floodplain lake (Low Food Insecurity - Fishing Grounds) since they tend to keep the lake at a constant distance to the river while maintaining the exchange of water promoted by the river-lake channel (Figure 3.12.a). As informed, sand beaches are also areas where the communities collect food. As a result, the sedimentation process might increase the area of those places, benefiting the activity (Low Food Insecurity - Sand Beaches), while the erosion process might destroy those areas (High Food Insecurity - Sand Beaches).

Figure 3.3 - Theoretical Model for communities living in stable (a), erosion (b), and sedimentation locations (c). The meander migration impacts were divided into High, Medium, and Low risk of Changes in Mobility, Inundation, Food Insecurity (fishing grounds), and Food Insecurity (sand beaches).

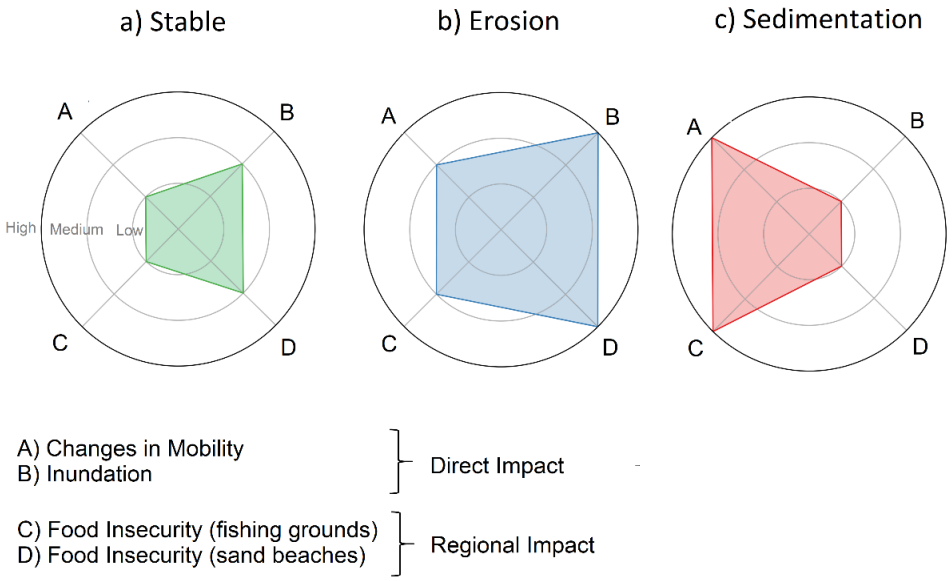

3.4 Discussion

Our results show a great number of communities being affected by erosion (56 communities) and sedimentation (96 communities) along the Juruá River. However, the majority of riparian communities are living in stable locations (217 communities - 58.8%), and thus are not directly affected by the Juruá meander migration processes. This

suggests that the communities have great local ecological knowledge (LEK) about the river, which was developed throughout generations, resulting in a successful adaptation to the environment. This result partially confirms our hypothesis that the communities' empirical knowledge decreases the extent of the meander migration impact on riverine communities. However, this hypothesis needs further studies to be confirmed. Although the riverine populations change their locations over time, our results show the current locations where the Juruá communities are living. Communities that are living in stable regions today may have been living in unstable regions in the past, and changed their locations in a constant trial and error process. Subsequently, many communities that are living in unstable locations today might move to other more stable regions in the future in a constant learning process. However, many communities that suffer from the river meander migration might decide to move to nearby cities, probably losing all the accumulated knowledge about the river and the surrounding environment over time. As a result, these riverine communities and their culture must be protected in order to combine environmental conservation with economic activities in the Juruá region.

LEK has been regarded as a social learning capacity, which leads to adaptive management and higher resilience (BERKES et al., 2000; PRICE et al., 2004). Many recent studies aimed to investigate this knowledge, showing the greater interest and importance that LEK has been obtaining in recent years (CEBRIÁN-PIQUERAS et al., 2020; LEITHÄUSER; HOLZHACKER, 2020; EARLY-CAPISTRÁN et al., 2020; BERKSTRÖM et al., 2019; TOMASINI et al., 2019). In developing countries, this practical knowledge might overcome the lack of data and resources to expand our ecological information and improve environmental management programs and approaches (BERKSTRÖM et al., 2019). Leithäuser and Holzhacker (2020), studying a local fishery village in Vietnam, identified that the LEK adapts to environmental changes and that this knowledge requires a high level of local participation to produce useful information for improved decision-making. Our paper results raised the hypothesis that the fact that most communities live in stable sections is due to their great local empirical knowledge (LEK) about the river dynamics, a hypothesis that still needs further studies to be confirmed.

We estimated a total population of 16636 riverine people distributed in 369 communities with no road access along the Juruá River. The majority of them are small, with only 3

houses. Larger communities, with more than 20 houses are a minority and represent only 11% of the communities. We identified that these larger communities tend to live in stabilized regions when compared to smaller communities. We hypothesized that stable regions allow communities to stay for longer periods and grow their population, without being disturbed by the process of erosion and sedimentation. On the contrary, we also hypothesized that smaller communities tend to be younger and with larger adaptation capacity, changing their locations according to river meander migration impacts. Spatial differences for the Upper, Medium, and Lower course are not discussed, since they might be affected by different social, economic, and environmental variables that were not considered in this study. The interaction between communities and their environment on a large scale is mostly unknown for both the government and the scientific community and should be addressed in future studies.

Our theoretical model hypothesized different impacts that might affect Juruá local communities due to the processes of erosion and sedimentation. Based on a survey, Islam et al. (2020), identified different impacts that the erosion process causes on Bangladesh riverine communities, including loss of homestead infrastructure, loss of land, income loss, scarcity of safe drinking water, disease, food scarcity, and crop and livestock loss. The authors informed that the low livelihood of riparian communities contributes to their low resilience to post-disaster problems. In the Amazon, we suppose that riverine communities face similar problems. Since they are highly dependent on the river for transportation, Mobility Change is an important variable affected by the meander migration processes along the Juruá River. Changes in mobility are high in sedimentation, medium in erosion, and low in stable communities. Inundation is another important variable that affects the communities during the high-water season. Communities living in erosion locations might experience more often and severe flooding than communities living in sedimentation areas. This condition happens because these erosion communities live along outer banks, regions that combine high inundation frequency and water velocities (FERGUSON et al., 2003), potentially threatening their houses and infrastructure. Indirect impacts were also covered in our theoretical model. Erosion and sedimentation processes, for example, might destroy oxbow lakes and sandbanks used by the locals for the fishery, threatening their economic stability and food security. However, our theoretical model is a simplification of complex processes and interactions between

the river meander migration and the local communities. As a result, the model aims to summarize the main erosion and sedimentation impacts based on personal experience and literature knowledge. It is important to mention that soon a comprehensive survey will be carried out within the communities to validate and improve the theoretical model.

Although the meander migration might destroy former environments where the communities used to collect food, the constant and dynamic river movement creates new oxbow lakes and sandbanks which the communities might use for the fishery. This dynamic environment is essential to keep biodiversity and must be managed wisely to guarantee economic stability for local communities. In the Middle Juruá Course (the region least affected by erosion process), for example, part of the floodplain lakes is subjected to sustainable fish exploitation to protect arapaima (Arapaima gigas) and other apex predators in the Médio Juruá Extractive Reserve (RESEX), giving the local communities a reliable source of fish income (CAMPOS-SILVA; PERES, 2016). Furthermore, the formation of sandbanks also created regions where is possible to fish on the river and collect turtles and their eggs.

The use of remote sensing time series is becoming popular to study the meander migration process (ANNAYAT et al., 2020; LI et al., 2020; SUIZU et al., 2018; ZEN et al., 2017). Some papers have attempted to develop automated algorithms to detect this process, such as RiMARS (SHAHROOD et al., 2020), PyRIS (MONEGAGLIA et al., 2018); RivMAP (SCHWENK et al., 2017), SCREAM (ROWLAND et al., 2016), and ChanGeom (FISHER et al, 2013). Shahrood et al. (2020), for example, applied the RiMARS on Landsat images acquired in 1993, 2003, 2011, and 2017 to study a 40-km stretch of the Kor River (Iran). In another paper, Monegaglia et al. (2018), used 28 Landsat images between 1984 and 2011 to study 240 km reach of the Xingu River. However, the described algorithms are performed within computing environments which require the download, storage, and manipulation of huge historical remote sensing images on processing servers. The Water Surface Change Detection Algorithm (WSCDA), by contrast, was developed entirely on Google Earth Engine (GEE), requiring only user's internet access to run the algorithm and extract the river meander migration information.

The WSCDA performed well to identify erosion and sedimentation locations along the Juruá River, with good accuracy and fast processing time on GEE (less than one minute

to compute and display the erosion and sedimentation areas over 3000 Km of the Juruá River). The algorithm does not classify the time series in water and non-water using water indexes specific threshold value (YANG et al., 2020; XIA et al., 2019; FREY et al., 2015; YANG et al., 2015), or time-consuming artificial intelligence (WANG et al., 2018). Instead, the WSCDA relies on the temporal variation of mNDWI to identify the time trend of increase or decrease of water within a given pixel. The mNDWI temporal linear regression provides a linear slope that is used to classify pixels in erosion (positive slope above a specific threshold) and sedimentation (negative slope below a specific threshold). This method, in addition to being fast, decreases the error of multiple classifications and reduces the negative impact of spurious and cloudy pixels, an important challenge when analyzing Amazonian floodplains. Furthermore, the algorithm allows the user to choose both, the best season and time interval under analyses.

The meander migration methodology biggest limitation relies on the Landsat 30m spatial resolution, which might be affected by spectral mixture on the river borders, delaying the detection of migration processes. We analyzed the river meander migration from the Juruá Upper Course, with a river width around 100m during the flooding season (with one Landsat pixel representing 33.33% of the river width) to the Lower Course, with a river width around 500m (Landsat pixel representing 6%). For smaller rivers, the method might produce lower accuracies due to the higher spectral mixture error concerning the river width and scale differences. Furthermore, the SPOT satellite high-resolution images provided by Esri Basemap have different dates of acquisition according to the location, which brings uncertainty to the actual number of communities and houses in a given date since they might be dynamic as well. Despite those limitations, remote sensing and cloud computing capabilities accurately identified erosion and sedimentation areas and were crucial to identify isolated communities.

So far, the majority of studies identified the river morphology's impact on vulnerable riparian communities in Bangladesh (ISLAM et al., 2020; FERDOUS et al., 2019; SARKER et al., 2019; MONIRUL et al., 2017; BHUIYAN et al., 2017; ISLAM et al., 2017; HAQUE; ZAMAN, 1989). However, although vulnerable riparian communities living in highly sinuous Amazonian rivers face the same problems, little effort has been made to study the impact of river meander migration on their livelihood. Furthermore, studies so far in the Amazon or Bangladesh are based on a small number of communities,

decreasing their representativeness. Our analysis, on the contrary, used remote sensing and cloud computing capabilities to monitor the meander migration impact on 369 communities along 3000 Km of the Juruá River, an unprecedented analysis scale that opens another important window for the application of remote sensing to study floodplains and remote communities. In this matter, this paper contributes to understanding how riparian communities adapt and are affected by erosion and sedimentation in one of the most sinuous and isolated rivers on Earth.

3.5 Conclusion

Most of the riparian communities along the Juruá River live in stable locations, showing their resilience and empirical knowledge about the river dynamics. We identified a higher proportion of larger communities living in stable regions than in smaller communities. The WSCDA performed well to identify erosion and sedimentation areas using Landsat long remote sensing time series. Furthermore, the WSCDA was developed on GEE, and thus might be accessed by a broader public to study any process that causes reduction of expansion of water, such as the studied river meander migration, dam filling, coastal infrastructure expansion, droughts, and so on. While the medium spatial resolution Landsat 5 and 8 were used to analyzed long-term meander migration, satellite high spatial resolution was essential to identify small riparian communities along the Juruá River. Our paper is one of the first attempts to systematically map communities and their interaction with the river using remote sensing and cloud computing. The results are intended to guide public policies for riparian communities, a vulnerable group that is highly exposed to climate change and environmental damage. This study aimed to improve our understanding of the interactions and adaptability between rural local communities and their surrounding environment, and with this knowledge support local and regional decision-making.

4. NECK CUTOFF PREDICTION USING LANDSAT TIME SERIES ALONG THE JURUÁ BASIN

4.1 Introduction

The river meander migration is a natural process that promotes erosion along the river outer bank (concave relative to the channel centerline) and sedimentation in the inner bank (convex relative to the channel centerline) (LEGLEITER et al., 2011). The development of meandering river channels is influenced by different variables such as flood pulse, sediment concentration, riparian vegetation, soil type, and river curvature (IELPI et al., 2020; SYLVESTER et al., 2019; HORTON et al., 2017). River curvature, for example, intensifies erosion in the outer bank, increasing the meander migration velocity over time (SYLVESTER et al., 2019). In contrast, vegetated banks act by decreasing the rate of meander migration due to the higher resistance to erosion (IELPI et al., 2020). In the Amazon, the process of meander migration is intense in rivers draining the Andes mountains, due to the powerful flood pulse and high sediment concentration (white-rivers) (AHMED et al., 2019; CONSTANTINE et al., 2014; RÍOS-VILLAMIZAR et al., 2014; JUNK et al. 2011; MARTINELLI et al., 1989; MARTINELLI et al., 1988). The river meander migration originates channel bends in arc formats that eventually causes the cutoff with the shorter path, leaving a new oxbow lake with no direct connection with the main river (CAMPOREALE al., 2008). As a result, while the river meander migration increases the river sinuosity over time, the cutoff events reduce the river curvature, maintaining the system in equilibrium (HOOKE et al., 2004).

There are two different types of cutoff, the neck and chute cutoff. Chute cutoff occurs when a channel is formed and connects the upstream and downstream limbs during flooding events, while the neck cutoff is formed when the continuous river meander migration intersects the upstream and downstream meander limbs (CONSTANTINE et al., 2010b; HOOKE, 2004).

Cutoff might result from two different processes: chute cutoffs and neck cutoffs (Figure 2.3) (EEKHOUT et al., 2015). A chute cutoff occurs when a new channel across an inner bend is formed and connects upstream and downstream limbs, leaving and abandoned

river reach which then becomes an oxbow lake (EEKHOUT et al., 2015; CONSTANTINE et al., 2010b). The neck cutoff is caused by a progressive self-intersection of a growing meander bend, which eventually intersects the upstream and downstream meander limbs by erosion (EEKHOUT et al., 2015; CAMPOREALE et al., 2008). In both events, the abandoned river reach becomes and oxbow lake. Rivers with high sinuosity experience frequent neck cutoff events (PEAKALL et al., 2007; KLEINHANS; VAN DEN BERG, 2011), while rivers with low sinuosity experience more frequent chute cutoffs. Stølum (1998) found that the cumulative size-frequency of oxbow lakes fits a power function, which means that in a floodplain there are far more small oxbow lakes than large ones. These lakes play an important role in aquatic ecosystems since they serve as fish spawning and nursery habitats (OBOLEWSKI, 2011, MIRANDA, 2005; PENCZAK et al., 2004). Furthermore, the process of river meander migration and channel cutoff creates a spatially and temporally dynamic environment, a condition that combined with past climatic changes has been contributing to the high biodiversity of trees, birds, and aquatic species in the floodplains (SILVA et al., 2019; FREITAS et al., 2014; ALBERT et al., 2011). While the cutoff processes are relevant to understand the formation of new lakes, the forecasting of these events is still complex and depends on detailed spatial data analysis.

There are several methods for studying cutoff events, such as laboratory simulation (LI et al., 2019; HAN et al., 2014; VAN DIJK et al., 2012; BRAUDRICK et al., 2009), numerical simulation (ASAHI et al., 2013), field observation (COOMES et al., 2005), and remote sensing (MARTHA et al., 2015; CONSTANTINE et al., 2014). Han et al (2014), for example, simulating the meandering process in a laboratory experiment, identified that the larger the slope of the meander neck, the larger the migration rates. According to them, high sediment fluxes contribute to the disconnection between the active channel and the oxbow lake. However, the authors acknowledge that the simplifications in the simulation limit the extrapolation to dynamic natural rivers. Remote sensing, by contrast, can be applied over large regions, covering a wide range of physiographic setups, in space and time, allowing to monitor the meander migration processes up to the cutoff event. The combination of remote sensing and cloud computing platforms, such as Google Earth Engine (GEE), are promising to study river meander

migration, since they provide high processing capabilities and long satellite historical databases (BOOTHROYD et al., 2020; HIRD et al., 2017).

Most of the rural communities in the Amazon live along the floodplain rivers due to their natural resources and economic importance (JUNK et al., 2012). These communities are highly dependent on the river for transportation, agriculture, and fishery in oxbow lakes (DAVIDSON et al., 2012). As a result, cutoff events are crucial for food and economic security in floodplain communities, since they provide oxbow lakes that are rich in fish. Along the Middle Juruá River, the successful fish sustainable management in those lakes is providing communities with a reliable income, ensuring access to education and health services and thus improving their socioeconomic welfare (CAMPOS-SILVA; PERES, 2016). However, despite the importance of the oxbow lakes, the riverine communities might be negatively impacted by cutoff events. A community living on the abandoned channel loses its connection to the river, and access to its only transportation system. Furthermore, the cutoff locally disturbs the river dynamics, increasing the channel width and the meander migration upstream and downstream of the cutoff section (LI et al., 2019; SCHWENK; GEORGIOU., 2016), potentially affecting nearby communities. Coomes et al. (2005) reported that a cutoff event in the Peruvian Amazon affected 20 communities and one city of 3500 inhabitants living in a river reach that was transformed into an oxbow lake. Furthermore, downstream the cutoff, at least one community was destroyed and others were affected by the intensification of the erosion process. This cutoff event, however, had a positive impact on the upstream communities due to the shorter path (reduction of 64 Km), which reduced transportation costs. These examples show that riverine communities are affected in different ways by cutoff events (COOMES et al., 2005). Therefore, the prediction of where and when these events will occur is key information for local planning, allowing the local population to mitigate cutoff negative impacts while intensifying their benefits.

This study proposes a methodology to predict future neck cutoff events using GEE cloud computing and Landsat-based time series over the Juruá River and its tributaries. Landsat database from 1984 to 2020 was used to identify past and calculate future neck cutoff regions along the Juruá Basin. The method uses a water surface detection algorithm to compute the rate of meander migration and then, uses this information, to predict the time-lapse till the next neck cutoff event (neck cutoff year of occurrence). To validate

the methodology, samples of past neck cutoffs (26 cutoffs) were identified and the methodology was applied to them. Then the difference between the predicted date and the actual date was computed. After methodology validation, the model was applied in river narrow necks to estimate the future cutoff year in regions with potential community impacts. The results intend to develop a fast and easy-to-use method to predict imminent neck cutoffs (cutoffs expected to occur in less than 20 years) in Amazonian floodplains. The methodology aims to support public policies and local planning for communities with potential cutoff impact.

4.2 Materials and methods

4.2.1 Study area

The study area is the Juruá River and its main tributaries, located on the Western Amazon. The Juruá river is one of the most sinuous rivers on Earth and thus is highly affected by cutoff events. Many communities live along the Juruá River and are highly dependent on the river for transportation and oxbow lakes for fishing. These communities also often live far away from cities (increased by the river sinuosity), a condition that decreases their access to public services. The Juruá Basin has an extension of 224.000 km², covering Peru and Brazil states (Acre and Amazonas) (Figure 4.1). The Juruá River has a length of 3283 km, starting in Peru and then crossing the Brazilian territory until reaching the Solimões river (COSTA et al. 2012; SOUSA; OLIVEIRA 2016).

The watershed is well preserved, with a high forest coverage, which means that the meander migration process is not highly affected by deforestation in most of the Juruá River and its tributaries. The Juruá River has a monomodal flood pulse divided into four distinctive hydrological periods according to the Gavião fluviometric gauge: the high-water period (March to May); the receding period (June to July), the low-water period (August to October), and the rising period (November to February). The cutoff analysis was performed on the rivers Juruá, Tarauacá (from the Tarauacá city to the Juruá confluence), and Envira (from Feijó city to the Tarauacá confluence) (Figure 4.1). Upstream sections were not considered because of the smaller river scale, making Landsat

imagery unable to precisely measure the river morphodynamics. We considered just river sections with widths larger than 100m during the flood season.

Figure 4. 1 - Juruá watershed and the rivers used in the study. The most important regional cities are presented.

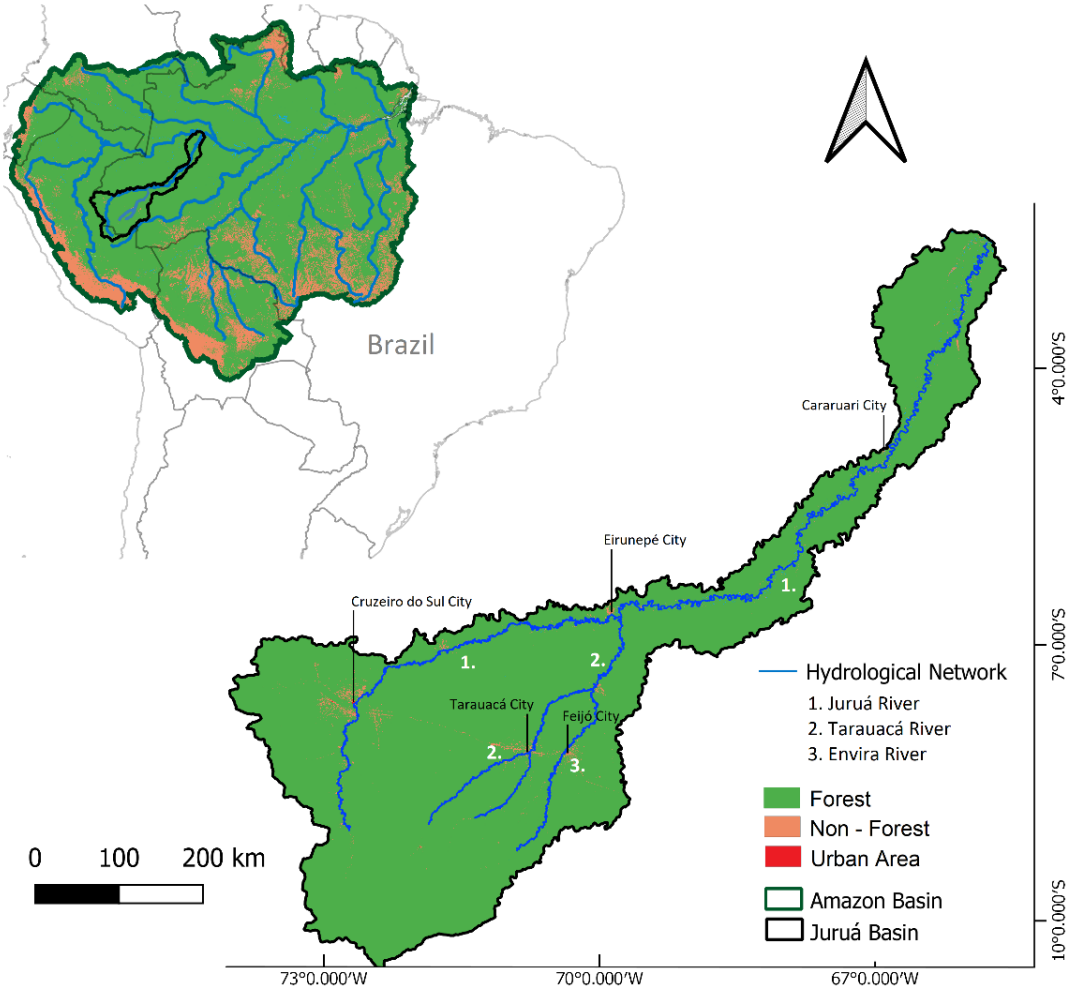

4.2.2 Water Surface Change Detection Algorithm (WSCDA) applied on Landsat imagery

The Landsat program long historical database (1984-2020) allows the use of time series to study spatial-temporal trends of changes in the Earth Surface (WULDER et al., 2019). In this sense, Landsat 5 Thematic Mapper (TM) and Landsat 8 Operational Land Imager (OLI) from March to June were used to identify the temporal and spatial changes of the Juruá River channel and its tributaries. This period was chosen since it includes the high-water and the beginning of the falling-water season, characterized by the highest erosion

rates (FLORSHEIM et al., 2008). From Landsat surface reflectance database, provided by GEE, the bands Green and SWIR were extracted to compute the water index mNDWI (Modified Normalized Difference Water Index). Preprocessing techniques to exclude noisy and cloudy pixels were applied over different Landsat time intervals to measure erosion and sedimentation in two different periods (explained in section 4.2.4).

The mNDWI database was then used by the Water Surface Change Detection Algorithm (WSCDA) to identify erosion and sedimentation areas. The WSCDA methodology is based on the Landsat time series of mNDWI (Modified Normalized Difference Water Index), which allows to identify pixels' subject to increased (erosion) or decreased (sedimentation) presence of water over time (Figure 4.2). The algorithm applies linear regressions between mNDWI and time (years) and classifies the pixels based on the mNDWI x time linear slope (θ). Pixels with positive θ (above the 0.015 ΔmNDWI/year threshold) indicate an increasing trend in the water surface over time and thus are classified as pixels subjected to erosion. Pixels with negative θ (below the -0.014 ΔmNDWI/year threshold) indicate a decrease of water surface over time and thus are classified as areas subject to sedimentation (Figure 4.2). Longer Landsat intervals improve the mNDWI temporal linear regression and thus the erosion and sedimentation classification. On the contrary, shorter time series tend to generate spurious misclassified pixels due to the lower data availability, a condition that increases the negative impact of cloudy pixels. More details about the WSCDA methodology and θ threshold identification are presented in the 3.2.2 Section.

Figure 4. 2 - Water Surface Change Detection Algorithm (WSCDA) flow chart.

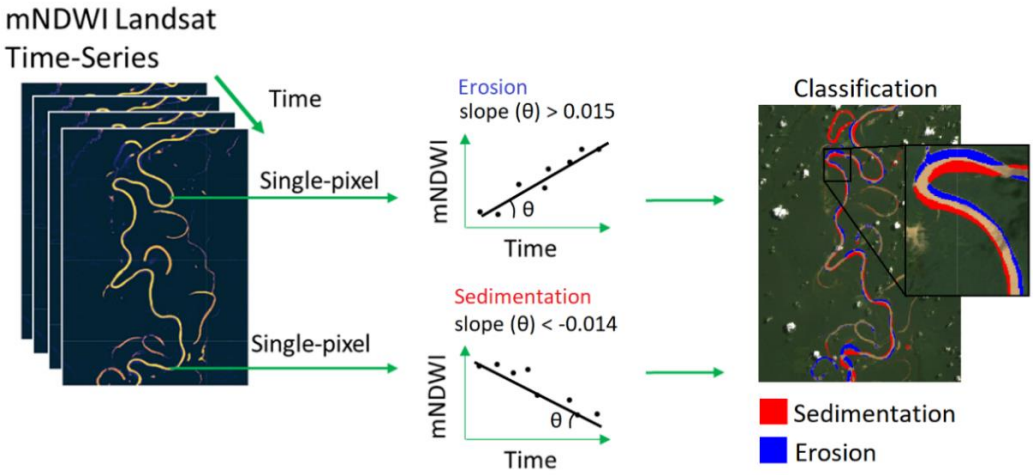

4.2.3 Cutoff year prediction methodology

To predict the neck cutoff year in a specific location, first, a satellite image must be displayed and the locally narrower neck distance measured (Figure 4.3i.1.2). Then, the WSCDA is applied to the river section to identify erosion and sedimentation areas that occurred in a given time interval (Figure 4.3i.2). With this information, the erosion and sedimentation distance vector (perpendicular to the river bend tangent) can be extracted on the locally narrower neck location (Figure 4.3i.2.1 and 4.3i.2.2). The Erosion Extend determined in WSCDA time-interval can be converted to migration rate (Erosion Extend / Time Interval) (Figure 4.3i.4.1). The migration rate (m/year) on the narrower neck location zone is valuable information to identify areas where the cutoff has a high probability of occurrence. With the local migration rate and the distance between two river sections (Neck Distance), it is possible to estimate the year that both river sections will connect, generating the cutoff (Cutoff Year = Neck Distance / Migration Rate) (Figure 4.3i.4.2). These described steps are common for all neck locations. However, corrections in the Neck Distance and the Meander Rate must be performed depending on the type of neck.

We classified the neck locations in three different classes: i) necks with erosion on one side and sedimentation on the other (Figure 4.3i), ii) necks with erosion on one side (Figure 4.3ii), and iii) necks with erosion on both sides (Figure 4.3iii). For necks with erosion occurring on one side, the cutoff prediction is performed using only the erosion

extend in one side of the neck (Figure 4.3ii). For cutoffs with both riversides suffering erosion, the erosion extend is summed, increasing the meander migration rate (Figure 4.3iii). And for cutoffs suffering erosion on one side and sedimentation on the other side of the neck, it is necessary to subtract the recent sediment extend from the neck distance (neck distance = neck distance – sediment extend) (Figure 4.3i.3). This neck distance correction is performed since the sedimented areas tend to have lower vegetation biomass (not deep roots) and have unconsolidated recent deposit sediments, offering little resistance to the erosion process (IELPI et al., 2020; SYLVESTER et al., 2019; HORTON et al., 2017). In summary, the neck distance and the erosion and sedimentation locations associated with their time interval are the only variables necessary to predict the cutoff year using the proposed methodology.

Figure 4.3 - Cutoff methodology prediction.

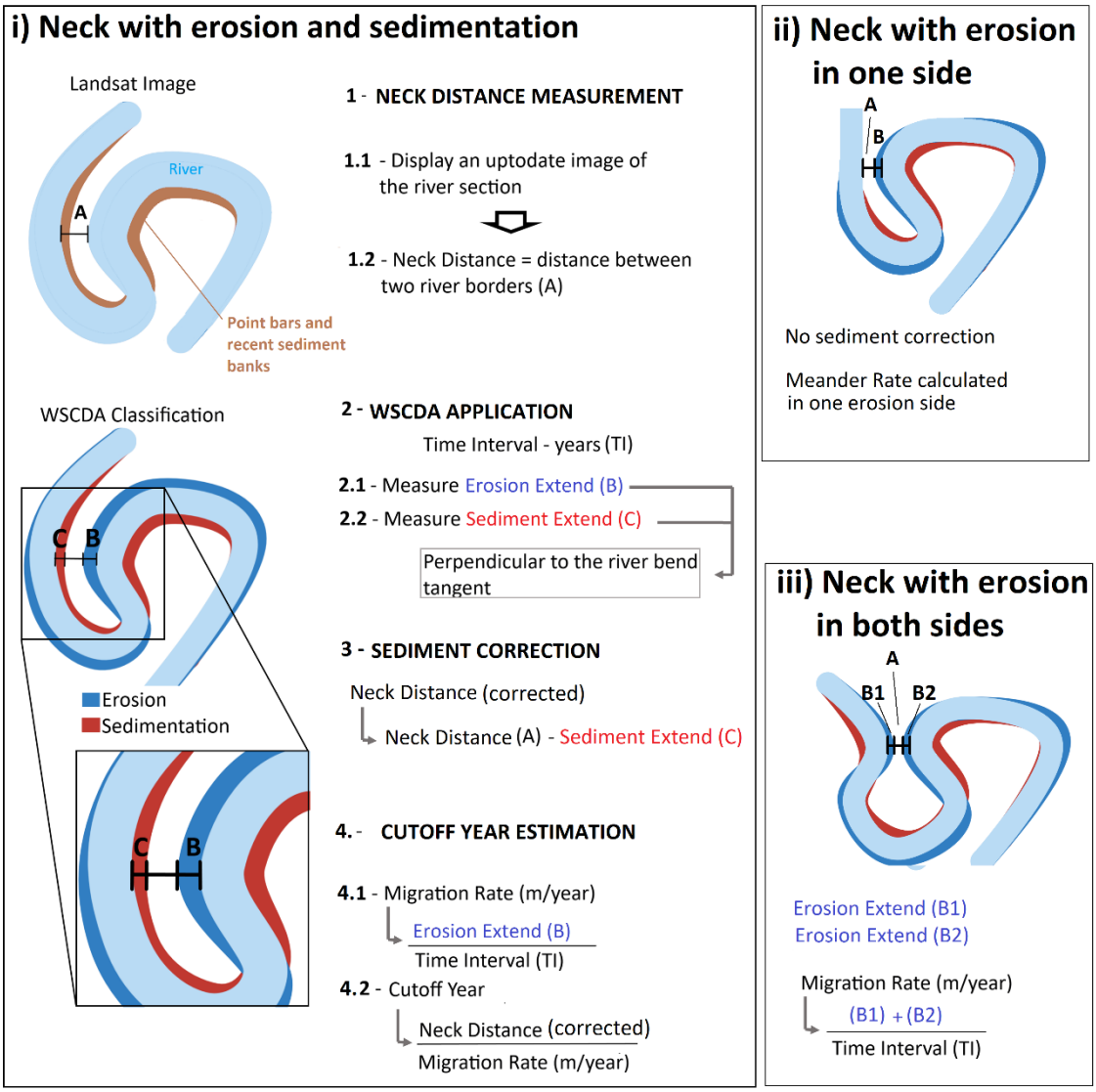

4.2.4 Cutoff prediction validation and application

Different neck cutoffs along the Juruá watershed were visually identified using the platform Google Earth Time-Lapse. The platform combines Landsat 5, Landsat 8, and Sentinel 2 for fast temporal identifications. We identified, but no applied the methodology on historical chute cutoff events since they are not properly formed by river movement but on channel formation between river sections. Furthermore, areas of erosion in narrow necks that, due to the water force, formed channels between the river sections and later a chute cutoff were also excluded from the methodology application. These events,

although not used to validate the model, were accounted to measure the proportion of Neck and Chute Cutoffs along the Juruá Basin.

To validate the methodology, 26 neck cutoffs that occurred between 1999 and 2020 were identified and the year of cutoff occurrence assigned to it (Figure 4.4.1a). We applied the cutoff prediction methodology for those 26 actual cutoffs and compared the predicted and the actual year of cutoff occurrence. To estimate cutoffs that occurred between 1999 and 2001, we used WSCDA erosion and sedimentation areas from 1984 to 1995 to identify the migration rate in the period, and a Landsat image in 1995 to measure the neck distance. To estimate cutoffs that occurred between 2001 and 2020 (Figure 4.4.1a), we used WSCDA erosion and sedimentation areas from 1984 to 2000 to measure the mean migration rate, and a Landsat image from 2000 to measure the neck distance (Figure 4.4.1b). Then, a comparison between the predicted and the real cutoff year was performed, and the Mean Absolute Percentage Error (MAPE) and the coefficient of determination (R^2) were analyzed (Figure 4.4.1c).

After the methodology validation, we estimated the cutoff year in necks near riverine communities (Figure 4.4.2). We used SPOT high-resolution satellite data, provided by Esri Basemaps, to identify communities that live close to local narrow necks or in river sections that will be abandoned by the river after a cutoff event. For this future cutoff determination, we used the 2000-2020 WSCDA mean migration rate (Figure 4.4.2). This erosion time-interval is similar to what we have used for validation. Since we validated cutoffs for a maximum prediction interval of 20 years, we recommend applying the methodology on local narrow necks and exclude estimations that pass 20 years (non-imminent cutoffs).

Figure 4.4 - Neck cutoff year of occurrence methodology flowchart.

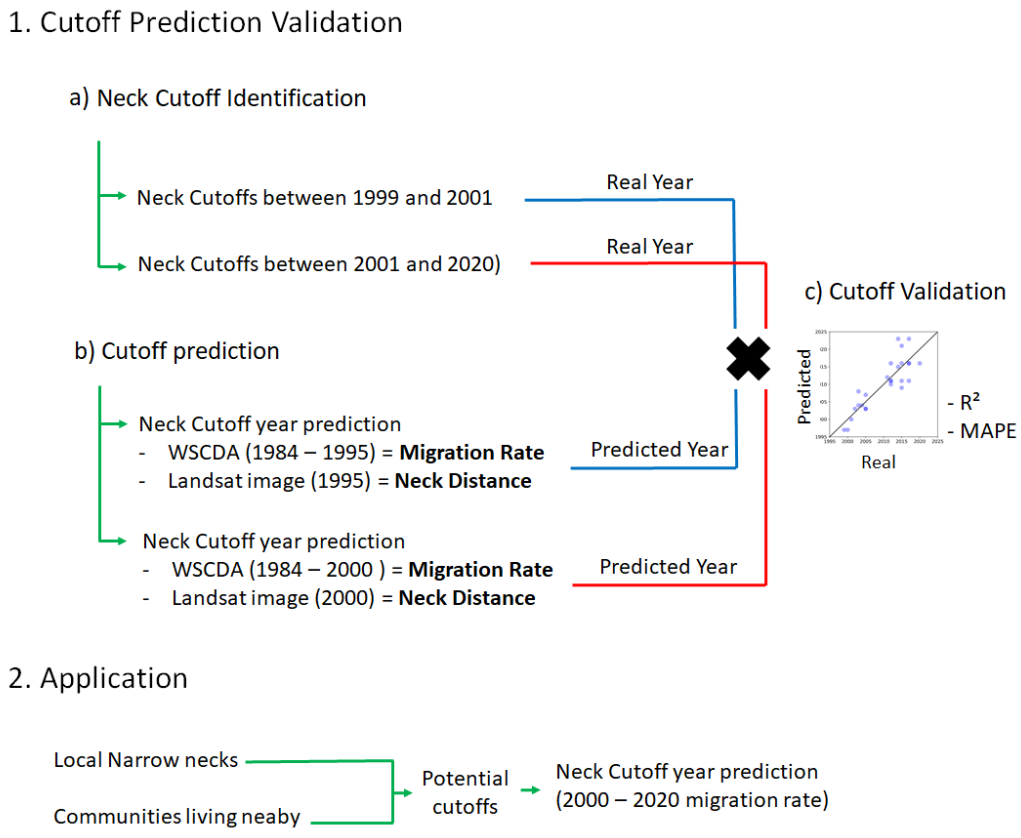

4.3 Results

4.3.1 Cutoff identification

The spatial distribution of neck and chute cutoffs, as well as oxbow formation examples, are presented in Figure 4.5. We identified a lower number of chute cutoffs (5) when compared to neck cutoffs (26) from 1999 to 2020. From the examples, it is possible to observe that the oxbow lake formation is fast, taking a couple of years to sediment the oxbow entrance after the cutoff event. Furthermore, the river section having very high suspended sediment concentration (bright blue color in the Landsat RGB composite SWIR2, SWIR1 and Red bands, becomes dark after the cutoff event and the disconnection of the oxbow lake (low concentration of suspended sediments). Figure 4.5.a also shows a point bar location that was eroded after the cutoff event. This happened because the cutoff

event changed the river morphology locally, so the point bar that used to be located on the inner bank (sedimentation area), became the outer bank (erosion area). These examples highlight the temporal and spatial Juruá dynamics and how the fast river migration process can be detected using satellite time series.

Figure 4.5 - Spatial distribution of neck selected for the methodology validation and examples of oxbow formation for three differnte sites. To highlight: water presence, Landsat 5 and 8 used with the RGB composite SWIR2, WIR1 and Red. The images were taken during the low-water season (August to October) in order to avoid cloud interference.

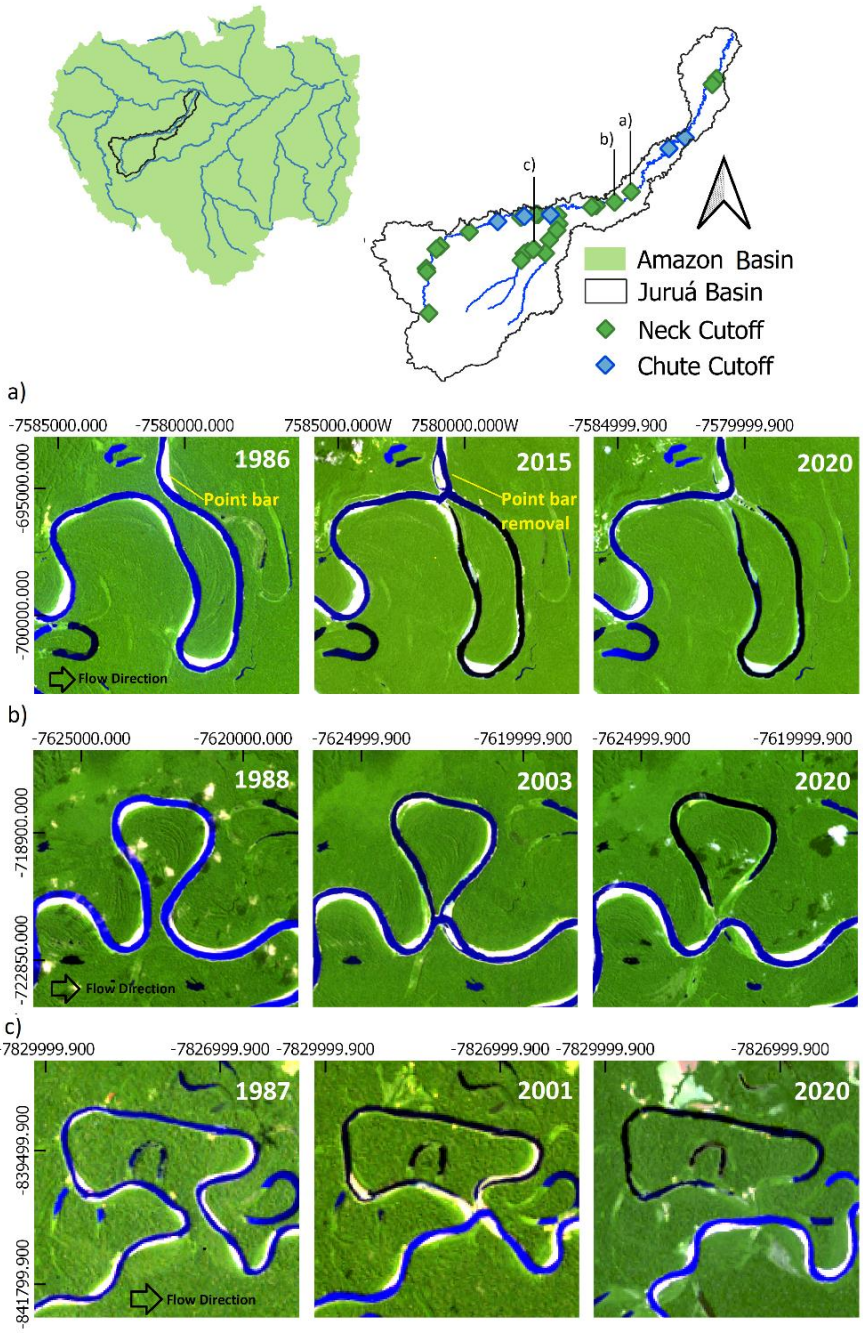

We identified rates of meander migration previous to neck cutoff events ranging from 3.5 m/year to 29 m/year for our selected region and time interval (1999 – 2020) (Figure 4.6). Most of the cutoffs were formed with meander rates between 9 to 14m/year (10 cutoffs),

followed by 3-9 m/year (6 cutoffs). High rates of meander migration (24-29m) were identified in two locations of the Tarauacá River and two distance locations of the Juruá River (one in the Juruá Lower Course and the other in the Upper Course). These values show that cutoff events might occur in a wide range of meander migration rates. The majority of cutoffs occurred in basin mid altitudes, with 12 cutoffs from 115 to 147m (Figure 4.6.b). The number decreases towards lower and higher altitudes, reaching 2 cutoffs between 48 and 81m, and between 181 and 213m (Figure 4.6.b). Visually it is possible to observe a higher concentration of neck cutoffs with higher rates of meander migration occurring along the Tarauacá River, followed by the Juruá and the Envira River (**Figure 4.6.a**). The examples show that remote sensing can be used to measure meander migration morphology parameters and their spatial distribution.

Figure 4.6 - Spatial distribution of mean migration rate computed from the Landsat time series previous to cutoff occurrence (a), the distribution of cutoffs according to the altitude (b), and the distribution of cutoffs according to the meander rate (c).

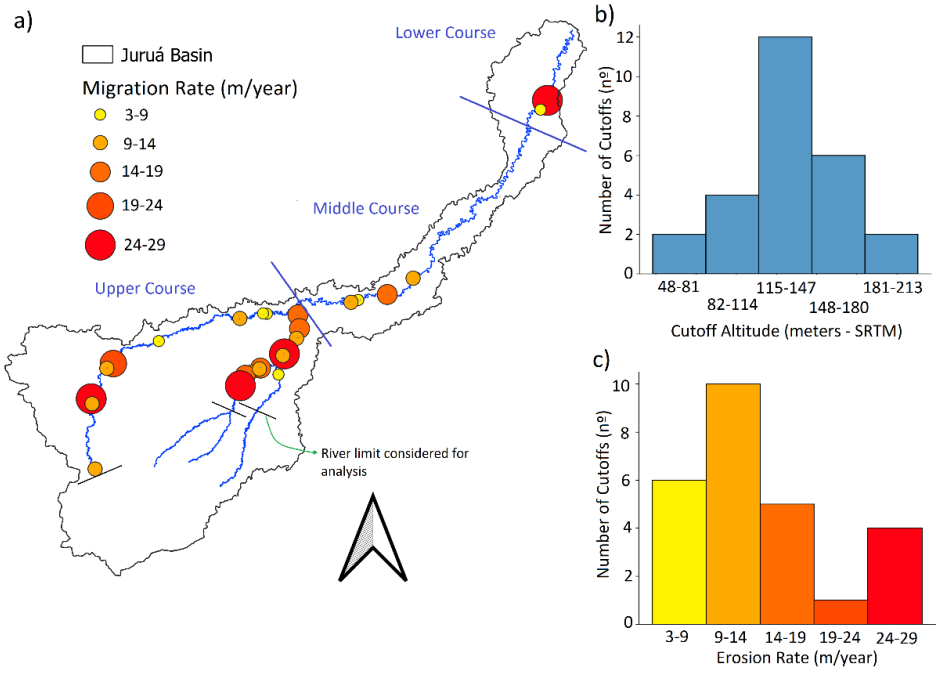

Using remote sensing high spatial resolution, we identified two communities that were affected by neck cutoff events. Figure 4.7A shows a community whose entire village was moved away from the abandoned river reach (Figure 4.7A.1) and resettled on the Juruá river shores (Figure 4.7A.2). The village relocation allowed the community to live near the previous location while maintaining easy access to the river. The apparent cutoff

beneficial in this case is that this community gained an oxbow lake, which might be used fishing. Figure 4.7B shows another community that used to live along the river (Figure 4.7B.1) when a cutoff event happened and left the community in an abandoned river reach (Figure 4.7B.2). The sedimentation process is advancing on its shores, replacing the water with sediments and vegetation and impacting their access to the river (Figure 4.7B). Although not captured by satellite images, this community may move and settle in another river bank. Both identified communities have no access by any other way with the nearest town, making the river essential for their survival. These high spatial images show direct impacts of the cutoff process on communities along the Juruá basin. When the community safety becomes unbearable due to the poor river access, the population moves and settles in other river banks.

Figure 4.7 - Cutoff impact on communities detected by high remote sensing resolution for two cutoff locations. The high-resolution imagery was provided by Esri basemaps.

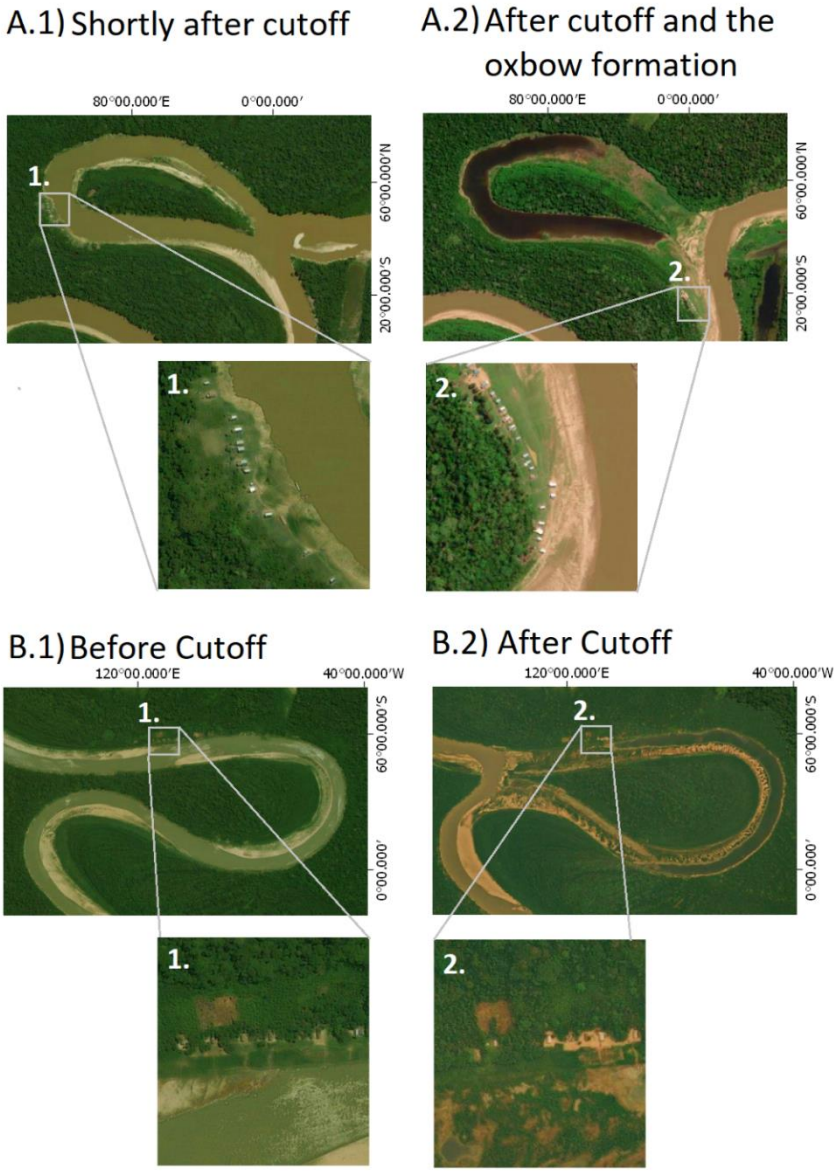

4.3.2 Cutoff validation and application

Figure 4.8.a shows an example of a neck cutoff whose occurrence was predicted for 2012. Overall, for this location, the WSCDA correctly classified the meander migration, since it classified erosion areas occurrence in the outer bank and sedimentation in the inner bank (LEGLEITER et al., 2011). Due to the smaller time interval (1984-2000), spurious misclassified pixels can be observed in the WSCDA product, such as sedimentation pixels in the outer bank (Figure 4.8.a). In this example, we estimated that the cutoff would occur

in 2011, showing great accuracy (1 year of error). It is important to highlight that 90m of sediment land was subtracted from the neck distance (decreasing the neck distance from 150m to 60m). If this sedimentation correction was not performed, the method would predict a cutoff in the year 2027 (15 years later). The comparison between the 26 total cutoff estimations is presented in Figure 4.8.b. The results show a great correlation (R^2 = 0.79) and a low error (MAPE = 13%) between the predicted and the real cutoff events. However, although accurate, the predictions tend to perform better in cutoffs that occurred around 2000, since they require fewer years to forecast, than cutoffs that occurred after 2010, with more years to predict (Figure 4.8.b). A possible explanation for this effect is that longer predictions give the river time to change variables that are not considered in the cutoff prediction methodology, such as the river sinuosity, discharge, vegetation cover, and so on.

Figure 4.8 - Cutoff prediction calculation for a cutoff event (a) and the relationship between predicted and real cutoffs (b).

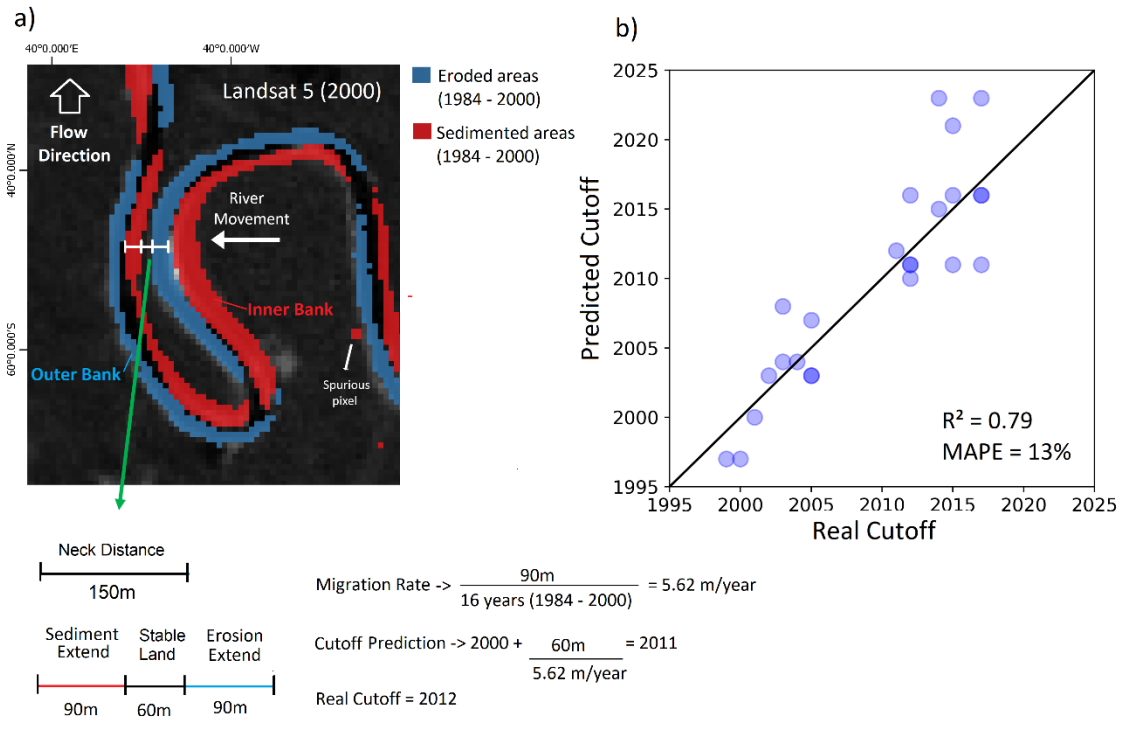

We applied the cutoff prediction methodology using WSCDA from 2000 to 2020 to identify three different future cutoffs that might impact local communities (Figure 4.9). It is possible to observe that in Figure 4.9.a and 4.9.b the erosion process is happening on

both sides of the meander neck, increasing the migration rate. Figure 4.9.a shows a community that is close to the location with a high possibility of cutoff occurrence. Since cutoffs increase the meander migration upstream and downstream, this community might be threatened by high rates of erosion or sedimentation when the cutoff event occurs. We predicted that the neck cutoff in this location will probably happen around the year 2030. Figure 4.9.b and Figure 4.9.c show two other communities that will be affected by a potential cutoff. These communities are living in a river section that will become an oxbow lake when the cutoff occurs, reducing their access to the river. However, as informed, the cutoff advantage is that these communities will gain an oxbow lake that might be used for fishing, increasing their economic stability. We predicted that the cutoff will probably happen around the year 2040 (Figure 4.9.b), and 2033 (Figure 4.9.c). According to the validation results, we expect a cutoff prediction error higher in Figure 4.9.b (20 years of prediction), followed by Figure 4.9.c (13 years of prediction) and Figure 4.9.a (10 years of prediction).

Figure 4.9 - Future neck cutoff prediction for three different locations with potential community effect.

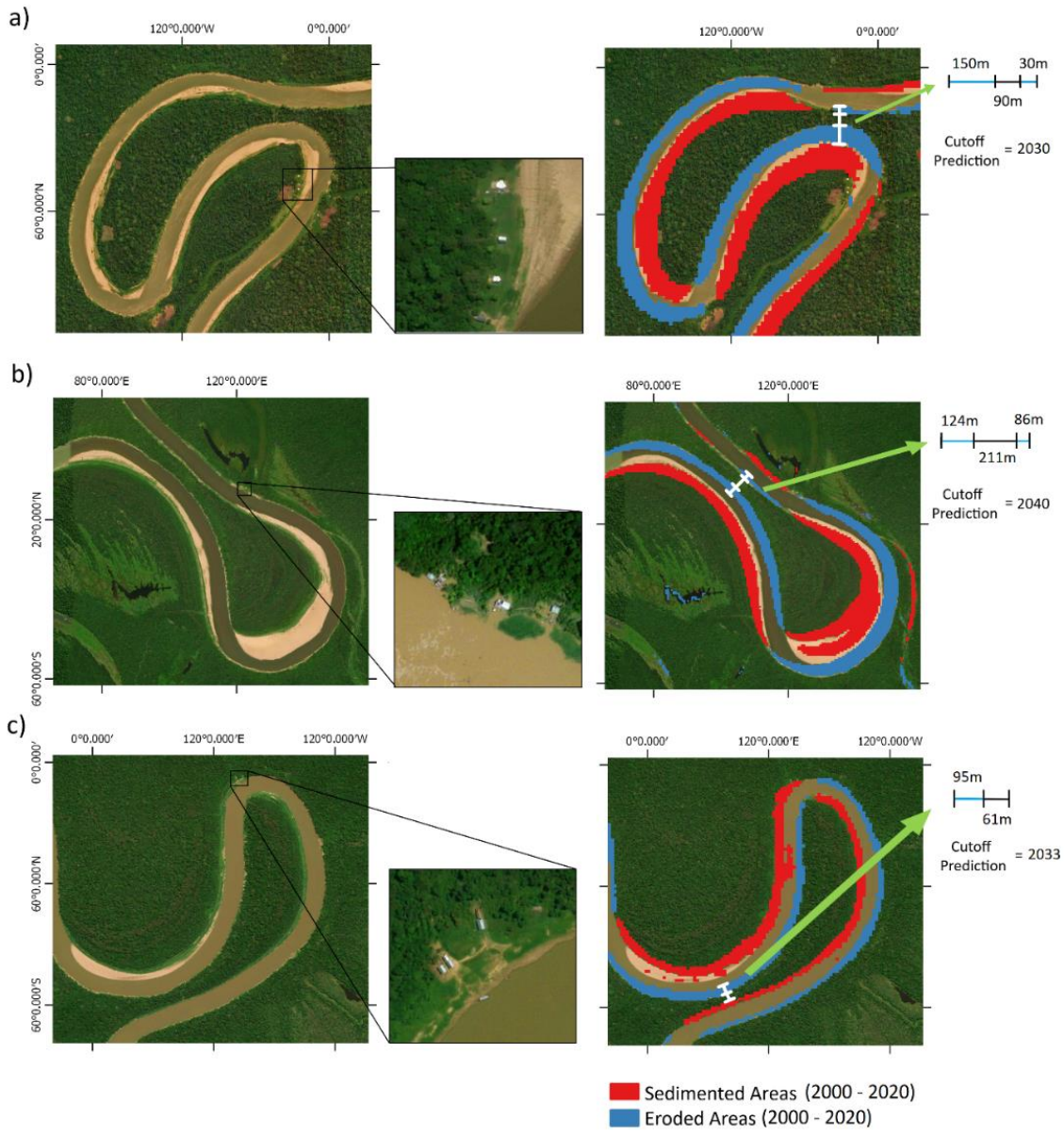

4.4 Discussion

The results have shown that remote sensing can be used to predict the neck cutoff year of occurrence using historical river meander migration dynamics. The Water Surface Change Detection Algorithm (WSCDA) correctly identified regions of erosion and sedimentation in different time intervals, information that was used to estimate the annual migration rate and the neck cutoff prediction year. Different studies have attempted to understand the river meander evolution based on different methodologies (LI et al., 2019;

HAN et al., 2014; VAN DIJK et al., 2012; BRAUDRICK et al., 2009; COOMES et al., 2005; MARTHA et al., 2015; CONSTANTINE et al., 2014), while others have attempted to predict the evolution of river meander migration and cutoff events (ASAHI et al., 2013; HEO et al., 2009). Sylvester et al., 2019, for example, studying the meander formation in the Juruá River, identified that the maximum migration rate is located downstream of the relative maximum curvature. Similarly, our study used Landsat historical data to identify the areas of maximum migration to estimate the neck cutoff year of occurrence along the Juruá basin. The proposed neck cutoff methodology relies entirely on remote sensing data and thus might be applied in any river with high rates of river meander migration.

Many studies (GU et al., 2016; ASAHI et al., 2013; SUN et al., 1996) aimed to model the river meander migration three-dimensionally, forecasting the river change in latitude, longitude, and time. Asahi et al. (2013), for example, numerically modeled the bank erosion and sedimentation, considering land accretion due to vegetation encroachment and the formation of neck cutoffs. Gu et al. (2016), used the Bank Erosion and Retreat Model (BERM) (CHEN; DUAN, 2006), which assumes a linear relationship between river longitudinal velocity and bank migration rate, and a nonlinear hydrodynamic model of Blanckaert and De Vriend (2010), to simulate the river meander migration. However, although the river meander migration patterns described by computational models are consistent, the model application on real rivers is limited due to the lack of data, such as topographic information, discharge, and flow velocities (LEGLEITER et al., 2011). Gutierrez et al. (2014), used a stochastic multivariate analysis to predict the meandering migration of Cahuacan River (Mexico), based on 15 different morphologic and fluvial variables, including river and meander width, basin surface area, curvature degree, dominant discharge (return period of 2 years), and so on (GUTIERREZ et al., 2014). The authors informed that the inclusion of more variables would improve the meander predictability, a condition not applicable for remote Amazonian rivers due to the low availability of data in the region. Instead, our paper simplifies the river meander process by creating one erosion vector that changes over time (two dimensions). This vector, when located on the locally narrower neck distance provides simple, but effective information to predict the moment (year) of neck cutoff occurrence.

We identified that recent sedimentation areas in neck regions do not prevent or delay the formation of neck cutoffs. This is because these areas have unconsolidated sediments and

are barely vegetated, reducing their resistance to the erosion process (IELPI et al., 2020; SYLVESTER et al., 2019; HORTON et al., 2017). The WSCDA was crucial to identify both the sedimentation areas, to avoid counting them as neck distance, and erosion areas used to estimate the meander migration rate. The WSCDA visually misclassified erosion and sedimentation in some regions. This is caused by the WSCDA temporal linear regression approach, which highly depends on the time interval and image availability (data for the regression) and the cloud filtering efficiency (spurious pixels on the regression), to identify erosion and sedimentation areas. These conditions are highly prominent in the cloudy Amazonian Juruá floodplain (MARTINS et al., 2018).

The Landsat spatial resolution (30m) limits the identification of recent erosion areas, negatively affecting the computation of the migration rate and thus the cutoff estimation. This scale problem is worse in smaller rivers and tributaries since the pixel size is large relative to the river width. However, despite the spatial scale limitation, the use of Landsat is essential since it offers satellite historical data, a requirement to track the meander migration evolution. This paper applied past mean migration rates to predict future neck cutoffs. As a result, the error associated with cutoff occurrence increases when using longer time series, since it tends to underestimate the actual rate of migration. This occurs because the river increases its meander velocity over time due to the curvature formation. Therefore, longer historical mean migration rates tend to be lower because they cover periods in which the meander was slower. In the same way, the prediction of cutoffs expected to occur in more distant futures might increase the error associated with variables that are not controlled and that might change in the future, such as migration rate (tend to increase over time), flooding patterns, deforestation, and so on. Subsequently, the neck cutoff estimation performs better in imminent cutoff locations (cutoffs expected to occur in less than 20 years) and using an optimum time series to measure the mean migration rate. As a result, we identified that a time series of 14 to 20 years is enough to correctly classify erosion areas using the WSCDA while maintaining an update migration rate estimation, both crucial conditions to predict imminent neck cutoffs.

Furthermore, although less frequent in the Juruá floodplain, chute cutoffs might occur before neck cutoffs in many locations. However, in the same way that chute cutoffs might take a longer time to form oxbow lakes (DÉPRET et al., 2017), these events disturb the

environment at a slower pace when compared to neck cutoffs. The channel that connects both riversides might take years and different flooding events to fully grow and become a new river path. As a result, we suppose that this slower chute cutoff development time might give local communities a better chance to adapt. On the contrary, neck cutoffs are fast and locally increase the rates of erosion (LI et al., 2019), potentially affecting entire nearby villages. Chute cutoffs are not detectable by our neck cutoff prediction methodology and thus have the potential to greatly increase the prediction error. Nevertheless, although not covered in our methodology, the channel formation between two river sections is easily identified using high spatial resolution such as PlanetScope, and thus these images have the potential to be used to monitor chute cutoffs. Therefore, a cutoff monitoring program might use both types of information, high spatial resolution imagery to identify the formation of chute cutoffs, and the WSCDA using Landsat time series to predict the neck cutoffs.

Cutoff events might positively or negatively impact local communities. These events, for example, might produce new oxbow lakes that can be used by locals for fishing, improving their food security and economic gains. Furthermore, the decrease of river sinuosity caused by cutoff events might also improve community access to other regions due to the distance reduction (COOMES et al., 2005). However, there are also negative impacts on communities caused by the meander migration intensification and oxbow lake formation after cutoff events. Unfortunately, many of these impacts have not been properly studied or analyzed (Coomes et al., 2005), a condition that contrasts with the high number of papers describing physically the meander migration and cutoff process (IELPI et al., 2020; SYLVESTER et al., 2019; LI et al., 2019; HORTON et al., 2017, GU et al., 2016; MARTHA et al., 2015; CONSTANTINE et al., 2014; HAN et al., 2014; ASAHI et al., 2013; VAN DIJK et al., 2012; LEGLEITER et al., 2011; SUN et al., 1996). As a result, our paper aims to predict neck cutoffs to reduce the negative impacts and intensify the benefits on local communities. We developed a direct methodology to predict cutoffs based entirely on remote sensing, without the requirement of topographic data, river discharge, etc. Since oxbow lakes are rich in fish, the cutoff prediction might be used to plan future spatial zoning of fishing along the Juruá and other regions. In the same way, the cutoff information might be applied to identify and guide spatial conservation prioritization along floodplains. Furthermore, the information provided by

this method can be used to measure where the risk of cutoff is higher and thus support local planning and reduce the communities' social and economic vulnerability.

4.5 Conclusion

The neck cutoff prediction successfully estimated cutoffs along the Juruá basin. The methodology was validated on 26 past cutoffs that occurred between 1999 to 2020. The simple, but effective method relies on Landsat time series and cloud computing to identify erosion areas and the meander migration rate along the floodplain. The Juruá basin is home to many communities that live along the river, a condition that decreases their access to public policies and services. As a result, we applied the methodology in three different imminent cutoffs that have the potential to affect local communities. The prediction of where cutoff has a higher risk of occurrence is valuable information to support local and government planning. This information might be used by local communities and community associations to prepare and mitigate negative cutoff effects.

5. FINAL CONSIDERATIONS

The meander river migration is a common and well well-known process for local riparian communities of the Amazon white-water rivers. Despite their socioeconomic vulnerability and high dependence on the river, little attention has been paid to the impacts of river migration in the process of erosion, sedimentation, and cutoff in their lives. These populations and their culture must be protected to save their great empirical knowledge about the environment and biodiversity, essential information to achieve a sustainable economy in the region. This dissertation aimed to contribute to the resilience of these local communities providing an overview of information about the interactions between their communities and the river along the Juruá Basin. This information intends to improve local and government planning and thus their resilience to natural and anthropogenic environmental changes in the region, conditions that are expected to increase due to climate change.

Remote Sensing has long been used to study natural processes that impact our society, improving our understanding of the world. With the advent of cloud high processing capabilities, temporal studies that once were restricted to laboratories that could afford supercomputers, now are available to a wide public of researchers. In the Amazon, there is a long history of papers describing the physical interactions between water, land, forest, and biodiversity (FAGUNDES et al. 2020; AHMED et al., 2019; CAMPOS-SILVA; PERES, 2016; RÍOS-VILLAMIZAR et al., 2014; JUNK et al., 2012; JUNK et al. 2011; CAMPOREALE et al., 2008; BOURGOIN et al., 2007; HECKENBERGER et al., 2007; OKI; KANAE, 2006; DAI; TRENBERTH, 2002; MARTINELLI et al., 1989; MARTINELLI et al., 1988). This dissertation aimed to include the people that live in these environments to study the interactions between hydrology and their communities using modern techniques of remote sensing and cloud computing. To better discuss the main achievements, the research questions (italic) listed in section 1.2 are addressed below.

1. Is cloud computing effective to automatically detect erosion and sedimentation processes using remote sensing image time series? What are the main advantages and restraints when compared to traditional algorithms?

The results show that the Water Surface Change Detection Algorithm (WSCDA) is accurate to identify areas of erosion and sedimentation from 1984 to 2020 along the Juruá River, with omission and commission errors lower than 13.44% and 7.08%, respectively. The WSCDA results show that the algorithm tends to underestimate the areas of erosion and sedimentation, mainly in recent meander migration areas. This is caused by the WSCDA methodology, which uses mNDWI temporal linear regressions and its slope to identify areas of erosion and sedimentation. As a result, recent eroded or sedimented areas are not powerful enough to change the linear regression slope value. This is exacerbated by the 30m Landsat resolution that promotes spectral mixture on the river borders, a condition that delays the mNDWI water response and thus the meander migration detection. However, although these specific limitations, the algorithm is accurate and detected even small areas of erosion and sedimentation along the Juruá River. The WSCDA good accuracy is even more impressive considering that we applied the algorithm to analyze the Juruá River during the Amazonian cloudy and atmospheric complex flooding season.

Cloud computing offers many advantages when compared to traditional algorithms. The cloud platform Google Earth Engine (GEE), for example, allows the WSCDA algorithm to process hundreds or even thousands of Landsat images at unprecedented speed. This high number of images prevents the algorithm analysis from bias since it includes all river spatial-temporal dynamics. Furthermore, the WSCDA algorithm can be applied in any river, lake, or coastal environment to identify conditions where the surface water increased or decreased over the years (examples provided in the link below). This analysis can be performed by anyone with internet access and with the WSCDA code link, conditions that might improve remote sensing accessibility. The Google Earth Engine restrains are related to the lower number of spatial analysis that the platform offers. As a result, although river meander migration algorithms such as RiMARS, build on MATLAB (SHAHROOD et al., 2020), and PyRIS, build on Python (MONEGAGLIA et al., 2018), require the storage, manipulation, and processing of Landsat images, these

algorithms perform better to identify and quantify changes in sinuosity, river centerline migration, and others river morphology variations. However, future studies are expected to address these limitations and include automatic spatial analysis in the GEE platform.

Examples of different WSCDA uses are provided in the Google App: https://gustavoonagel.users.earthengine.app/view/water-surface-change-detection-algorithm-wscda

6. What is the proportion of riverine communities living in areas subject to the meandering of the Juruá River? How are these communities affected by erosion and sedimentation processes along their shores?

We identified 369 rural riparian communities living along the Juruá banks, from which 56 are suffering erosion (15.18%) and 96 sedimentation (26.02%) on their shores. However, surprisingly, the majority of communities are living in regions not affected by the river meander migration (217 communities = 58.8%), a condition that suggests their great empirical knowledge about the river dynamics. Furthermore, we identified that larger communities, with more than 20 houses, tend to live in more stable locations (70%), when compared to middle size communities, with 10 to 20 houses (63.2%), and small communities, with less than 10 houses (55.6%). This result suggests that stable locations offer better conditions for communities to grow their population, while smaller communities are more dynamic and adapt to changes in the river morphology. Spatial changes were also identified, with a lower proportion of communities living in stable locations in the Upper Course (55.79), when compared to the Middle (64.21) and Lower Course (63.41%). However, the differences between regions were not discussed due to the high variability of economic, social, and environmental factors that might influence this result.

A theoretical model was created to discuss the main impacts caused by the river meander migration. Impacts on community mobility, inundation, and food security were classified as high, medium, and low for communities suffering erosion, sedimentation, and for communities living in stable locations. Communities that suffer erosion, for example, might suffer more frequent and severe inundation than communities living in sedimentation locations. Furthermore, communities suffering sedimentation along their

shores will gradually increase the distance between the river and their houses, impacting their access to their boats and thus to navigation. Impacts that are regional and thus more complex to assess were discussed but not monitored. An oxbow lake that suffers sedimentation in its river-lake channel will dry out and thus impact an important source of fishing, impacting their food security. In the same way, the erosion process along sandbanks, where communities use for fishing and collect turtles, might locally destroy this environment and thus also impact their food security. Cutoff events, when the river favors a shorter path, might decrease the river access for communities that live in the abandoned river reach (transformed in an oxbow lake), while increasing the navigation access for upstream communities due to the river's shorter path (reduction of river length).

7. Can satellite river meander monitoring be applied to predict neck cutoffs? How can this forecast be used to improve inundation hazard mitigation actions and community safety?

The remote sensing time series allowed us to identify the past river meander erosion rate to predict future neck cutoffs along the Juruá Basin. The methodology showed good accuracy to predict imminent cutoffs (expected to occur in less than 20 years), with R^2 = 0.79 and MAPE = 13%. The methodology is based on two variables, the neck distance from one river border to the other, and the rate of meander migration, calculated using the erosion areas and the associated time interval (provided by WSCDA). Applying simple uniform movement equations of velocity, we can detect the year that both river sections will connect, producing the neck cutoff. This simple, but effective methodology, can be used to predict the risk of cutoff in locations with potential impact on local communities. Chute cutoffs can occur before neck cutoffs, increasing the methodology error. However, chute cutoffs can easily be identified using satellite high spatial resolution, and thus might be used to monitor these events along inhabited floodplains.
As informed, cutoffs have positive and negative impacts on riverine communities. Cutoffs, for example, produce oxbow lakes that might be used for local communities for fishing, increasing their economic stability and food security. Furthermore, cutoffs reduce the river sinuosity, decreasing the distance between riverine communities and cities and thus improving navigation. However, cutoffs can locally increase the river meander

migration, impacting nearby communities, or decrease the river access to communities living in the river abandoned reach. As a result, the information that a cutoff might happen in the following years is valuable for local and government planning, improving the community resilience for cutoff negative effects while intensifying their benefits.

REFERENCES

ABEL, E. L. S. et al. Environmental dynamics of the Juruá watershed in the Amazon. **Environment, Development and Sustainability**, 2020. doi:10.1007/s10668-020-00890.

ACHARYA, T. D.; LEE, D. H.; YANG, I. T.; LEE, J. K. Identification of water bodies in a Landsat 8 OLI image using a J48 Decision Tree. **Sensors**, v. 16, n.7, 2016.

AHMED, J.; CONSTANTINE, J. A; DUNNE, T. The role of sediment supply in the adjustment of channel sinuosity across the Amazon Basin. **Geology**, v. 47, p. 807–810, 2019.

ALBERT, J. S. et al. Aquatic biodiversity in the Amazon: habitat specialization and geographic isolation sromote species Richnness. **Animals**, v. 1, p. 205-241, 2011.

ANNAYAT, W.; SIL, B. S. Changes in morphometric meander parameters and prediction of meander channel migration for the alluvial part of the Barak River. **Journal of the Geological Society of India**, v. 96, n. 3, p. 279–291, 2020. Available from: https://doi.org/10.1007/s12594-020-1548-3.

ASAHI, K.; SHIMIZU, Y.; NELSON, J.; PARKER, G. Numerical simulation of river meandering with self-evolving banks. **Journal of Geophysical Research: Earth Surface**, v. 118, p. 2208–2229, 2013.

BAKI, A. B. M., GAN, T. Y. Riverbank migration and island dynamics of the braided Jamuna River of the Ganges e Brahmaputra basin using multi-temporal Landsat images. **Quaternary International**, v. 263, p. 148-161, 2012.

BERKES, F.; COLDING, J.; FOLKE, C. Rediscovery of traditional ecological knowledge as adaptive management. **Ecological Applications**, v. 10, p. 1251–1262, 2000.

BERKSTRÖM, C.; PAPADOPOULOS, M.; JIDDAWI, N. S.; NORDLUND, L. M. Fishers' Local Ecological Knowledge (LEK) on connectivity and seascape management. **Frontiers in Marine Science**, v. 6, 2019.

BERTALAN, L. et al. Issues of meander development: land degradation or ecological value? the example of the Sajó River, Hungary. **Water (Switzerland)**, v. 10, n. 11, 2018.

BHUIYAN, M. A. H.; ISLAM, S. M. D.-U.; AZAM, G. Exploring impacts and livelihood vulnerability of riverbank erosion hazard among rural household along the river Padma of Bangladesh. **Environmental Systems Research**, v. 6, n. 1, 2017. Available from: https://doi.org/10.1186/s40068-017-0102-9.

BILLAH, M. M. Mapping and monitoring erosion-accretion in an alluvial river using satellite imagery - the river bank changes of the Padma river in Bangladesh**. Quaestiones Geographicae**, v. 37, n. 3, p. 87–95, 2018. Available from: https://doi.org/10.2478/quageo-2018-0027.

BLANCKAERT, K.; DE VRIEND, H. J. Meander dynamics: a nonlinear model without curvature restrictions for flow in open-channel bends. **Journal of Geophysical Research**, v. 115, p. 79–93, 2010.

BONNET, M. P. et al. Floodplain hydrology in an Amazon floodplain lake (Lago Grande de Curuaí). **Journal of Hydrology**, v. 349, p. 18-30, 2008.

BOOTHROYD, R. J.; WILLIAMS, R. D.; HOEY, T. B; BARRETT, B.; PRASOJO, O. A. Applications of Google Earth engine in fluvial geomorphology for detecting river channel change. **WIREs Water**, 2020. Available from: https://doi.org/10.1002/wat2.1496.

BOURGOIN, L. M. et al. Temporal dynamics of water and sediment exchanges between the Curuaı´ floodplain and the Amazon River, Brazil. **Journal of Hydrology**, v. 335, p. 140– 156, 2007.

BRADLEY, D. N.; TUCKER, G. E. The storage time, age, and erosion hazard of laterally accreted sediment on the floodplain of a simulated meandering river. **Journal of Geophysical Research: Earth Surface**, v. 118, n. 3, p. 1308–1319, 2013. Available from: https://doi.org/10.1002/jgrf.20083.

BRAUDRICK, C. A.; DIETRICH, W. E.; LEVERICH, G. T.; SKLAR, L. S. Experimental evidence for the conditions necessary to sustain meandering in coarse-bedded rivers. **Proceedings of the National Academy of Sciences of the United States of America**, v. 106, p. 16936–16941, 2009.

BULLOCK, E. L.; WOODCOCK, C. E.; SOUZA, C.; OLOFSSON, P. Satellite-based estimates reveal widespread forest degradation in the Amazon. **Global Change Biology**, v. 26, n. 5, p. 2956–2969, 2020. Available from: https://doi.org/10.1111/gcb.15029.

CAMPOREALE, C.; PERUCCA, E.; RIDOLFI, L. Significance of cutoff in meandering river dynamics. **Journal of Geophysical Research**, v. 113, n. 1, 2008.

CAMPOS-SILVA, J. V.; PERES, C. A. Community-based management induces rapid recovery of a high-value tropical freshwater fishery. **Scientific Reports,** v. 6, 2016.

CASTELLS, M. **The power of identity**: the information age: economy, society, and culture. [S.l.]: Wiley-Blackwell, 2010. 537p.

CEBRIÁN-PIQUERAS, M. A. et al. Scientific and local ecological knowledge, shaping perceptions towards protected areas and related ecosystem services. **Landscape Ecology**, v. 35, n. 11, p. 2549–2567, 2020.

CHAMBERS, R. **Whose reality counts?** putting the first last. London: Intermediate Technology Publications, 1997.

CHEN, D.; DUAN, J. D. Simulating sine-generated meandering channel evolution with an analytical model. **Journal of Hydraulic Research**, v. 44, p. 363–373, 2006.

CHEN, Y.; WANG, B.; POLLINO, C. A.; CUDDY, S. M.; MERRIN, L. E.; HUANG, C. Estimate of flood inundation and retention on wetlands using remote sensing and GIS. **Ecohydrology**, v. 7, p. 1412–1420, 2014. Available from: https://doi.org/10.1002/eco.1467.

CORONEL M.; SOLÓRZANO J. **Comunidades locales y pueblos indígenas:** su rol en la conservación, mantenimiento y creación de áreas protegidas: iniciativa visión Amazónica. [S.l.]: REDPARQUES, WWF, FAO, UICN, ONU Medio Ambiente. 2017. 192p.

CONSTANTINE, J. A.; DUNNE, T.; AHMED, J.; LEGLEITER, C.; LAZARUS, E. D. Sediment supply as a driver of river meandering and floodplain evolution in the Amazon Basin. **Nature Geoscience**, v. 7, n. 12, p. 899–903, 2014.

CONSTANTINE, J.A.; DUNNE, T.; PIÉGAY, H.; KONDOLF, G.M. Controls on the alluviation of oxbow lakes by bed-material load along the Sacramento River, California. **Sedimentology**, v. 57, n. 2, p. 389–407, 2010a.

CONSTANTINE, J. A.; MCLEAN, S. R.; DUNNE, T. A mechanism of chute cutoff along large meandering rivers with uniform floodplain topography. **Bulletin of the Geological Society of America**, v, 122, n. 5/6, p. 855–869, 2010b. Available from: https://doi.org/10.1130/B26560.1.

CONSTANTINE, J. A.; DUNNE, T. Meander cutoff and the controls on the production of oxbow lakes. **Geology**, v. 36, n. 1, p. 23–26, 2008. Available from: https://doi.org/10.1130/G24130A.1.

COOMES, O. T.; ABIZAID, C.; LAPOINTE, M. Human modification of a large meandering Amazonian River: genesis, ecological and economic consequences of the Masisea Cutoff on the Central Ucayali, Peru. **Ambio**, v. 38, n. 3, p. 130–134, 2009.

COSTA, A. C. S.; SOUZA, L. P.; DELGADO, R. C.; GOMES, F. A. Períodos de cheia e vazante do rio Juruá na região de Cruzeiro do Sul, Acre. **Enciclopédia Biosfera**, v. 8, n. 14, p. 1343–1349, 2012.

DAI, A.; TRENBERTH, K. E. Estimates of freshwater discharge from continents: latitudinal and seasonal variations. **Journal of Hydrometeorology**, v. 3, n. 6, p. 660-687, 2002.

DAVIDSON, E. A. et al. The Amazon basin in transition. **Nature**, v. 481, p. 321–328 2012.

DAVIS, W. **The wayfinders**: why ancient wisdom matters in the modern world. [S.l.]: House of Anansi Press, 2009.

DÉPRET, T.; RIQUIER, J.; AND PIÉGAY, H. Evolution of abandoned channels: insights on controlling factors in a multi-pressure river system. **Geomorphology**, v. 294, p. 99–118, 2017.

DEUTSCH, M.; RUGGLES, F. Optical data processing and projected applications of the ERTS-1 imagery covering the 1973 Mississippi River Valley floods. **Water Resources Bulletin**, v. 10, n. 5, p. 1023–1039, 1974.

DIETRICH, W. E.; SMITH, J. D.; DUNNE, T. Flow and sediment transport in a sand bedded meander. **Journal of Geology**, v. 87, p. 305–315, 1979.

DU, Z. et al. Analysis of Landsat-8 OLI imagery for land surface water mapping. **Remote Sensing Letters**, v. 5, n. 7, p. 672–681, 2014. Available from: https://doi.org/10.1080/2150704X.2014.960606.

EARLY-CAPISTRÁN, M. M. et al. Quantifying local ecological knowledge to model historical abundance of long-lived, heavily-exploited fauna. **PeerJ**, v. 8, 2020.

EEKHOUT, J. P. C.; HOITINK, A. J. F. Chute cutoff as a morphological response to stream reconstruction: the possible role of backwater. **Water Resources Research**, v. 51, p. 3339-3352, 2015.

ENCYCLOPEDIA BRITANNICA. **The Juruá River**. 2019. Available from: https://www.britannica.com/place/Jurua-River.

FAGUNDES, H. O.; FAN, F. M.; PAIVA, R. C. D.; SIQUEIRA, V. A.; BUARQUE, D. C.; KORNOWSKY, L. W.; SANTOS, L. L; COLLISCHONN, W. Sediment flows in South America supported by daily hydrologic-hydrodynamic modeling. **Water Resources Research**, 2020.

FASSONI-ANDRADE, A. C.; PAIVA, R. C. D. Mapping spatial-temporal sediment dynamics of river-floodplains in the Amazon. **Remote Sensing of Environment**, v. 221, p. 94-107, 2019.

FERDOUS, M. R.; WESSELINK, A.; BRANDIMARTE, L.; SLAGER, K.; ZWARTEVEEN, M.; DI BALDASSARRE, G. The costs of living with floods in the Jamuna floodplain in Bangladesh. **Water (Switzerland)**, v. 11, n. 6, 2019. Available from: https://doi.org/10.3390/w11061238.

FERGUSON, R. I.; PARSONS, D. R.; LANE, S. N.; HARDY, R. J. Flow in meander bends with recirculation at the inner bank. **Water Resources Research**, v. 39, n. 11, 2003. Available from: https://doi.org/10.1029/2003WR001965.

FERNANDES, R.; GOMES, L. C.; PELICICE, F.; AGOSTINHO, A. A. Temporal organization of fish assemblages in floodplain lagoons: the role of hydrological connectivity. **Environmental Biology of Fishes**, v. 85, n. 2, p. 99-108, 2009. Doi: 10.1007/s10641-009-9466-7.

FERRAL, A.; LUCCINI, E.; ALEKSINKÓ, A.; SCAVUZZO, C. M. Flooded-area satellite monitoring within a Ramsar wetland Nature Reserve in Argentina. **Remote Sensing Applications: Society and Environment**, v. 15, 2019.

FERREIRA, C. D. S.; PIEDADE, M. T. F.; TINÉ, M. A. S.; ROSSATTO, D. R.; PAROLIN, P.; BUCKERIDGE, M. S. The role of carbohydrates in seed germination and seedling establishment of Himatanthus sucuuba, an Amazonian tree with populations adapted to flooded and non-flooded conditions. **Annals of Botany**, v. 104, n. 6, p. 1111–1119, 2009. Available from: https://doi.org/10.1093/aob/mcp212.

FISHER, G. B.; BOOKHAGEN, B.; AMOS, C. B. Channel planform geometry and slopes from freely available high-spatial resolution imagery and DEM fusion: implications for channel width scalings, erosion proxies, and fluvial signatures in tectonically active landscapes. **Geomorphology**, v. 194, p. 46–56, 2013.

FLORSHEIM, J. L.; MOUNT, J. F.; CHIN, A. Bank erosion as a desirable attribute of rivers. **BioScience**, 2008. Available from: https://doi.org/10.1641/B580608.

FRAINER, A.; et al. Cultural and linguistic diversities are underappreciated pillars of biodiversity. **Proceedings of the National Academy of Sciences of the United States of America**, v. 117, n. 43, p. 26539–26543, 2020. Available from: https://doi.org/10.1073/pnas.2019469117.

FRANZOLIN, F.; GARCIA, P. S.; BIZZO, N. Amazon conservation and students' interests for biodiversity: the need to boost science education in Brazil. **Science Advances,** v. 6, n. 35, 2020. Available from: https://doi.org/10.1126/sciadv.abb0110.

FRAXE, T. J. P.; PEREIRA, H. S.; WITKOSKI, A. C. **Comunidades ribeirinhas amazônicas**: modos de vida e uso dos recursos naturais. Manaus: Universidade Federal do Amazonas, 2007. 224p. Projeto Piatam.

FREITAS, C. E. C.; SIQUEIRA-SOUZA, F. K.; FLORENTINO, A. C.; HURD, L. E. The importance of spatial scales to analysis of fish diversity in Amazonian floodplain lakes and implications for conservation. **Ecology of Freshwater Fish**, v. 23, n. 3, p. 470–477, 2014. Available from: https://doi.org/10.1111/eff.12099.

FREY, C. M.; KUENZER, C. Remote sensing time series - revealing land surface dynamics. **Remote Sensing and Digital Image Processing**, v. 22, p. 119–140, 2015.

FROTHINGHA, K. M; RHOADS, B. L. Threedimensional flow structure and channel change in an asymmetrical compound meander loop, Embarras River, Illinois. **Earth Surface Processes and Landforms**, v. 28, p. 625–644, 2003.

FURBISH, D. J. River-bend curvature and migration: how are they related? **Geology**, v. 16, p. 752–755, 1988. Available from: https://doi.org/10.1130/0091-7613(1988)0162.3.CO;2.

GAUTIER, E.; BRUNSTEIN, D.; VAUCHEL, P.; ROULET, M.; FUERTES, O.; GUYOT, J.L.; DAROZZES, J.; BOURREL, L. Temporal relations between meander deformation, water discharge and sediment fl uxes in the fl oodplain of the Rio Beni (Bolivian Amazonia). **Earth Surface Processes and Landforms**, v. 32, n. 2, p. 230-248, 2007.

GIDDENS, A. **Modernity and self-identity**: self and society in the late modern age. [S.l.]: Stanford University Press, 1991. 264p.

GORELICK, N. et al. Google Earth Engine: planetary-scale geospatial analysis for everyone. **Remote Sensing of Environment**, v. 202, p. 18–27, 2017.

GU, L.; ZHANG, S.; HE, L.; CHEN, D.; BLANCKAERT, K.; OTTEVANGER, W.; ZHANG, Y. Modeling flow pattern and evolution of meandering channels with a nonlinear model. **Water (Switzerland)**, v. 8, n. 10, 2016. Available from: https://doi.org/10.3390/w8100418.

GUALTIERI, C.; ABDI, R.; IANNIRUBERTO, M.; FILIZOLA, N.; SANTOS, R.; ENDRENY, T. A 3D analysis of spatial habitat metrics about the confluence of Negro and Solimões rivers, Brazil. **Ecohydrology**, v. 13, n. 1, 2020.

GUALTIERI, C.; IANNIRUBERTO, M.; FILIZOLA, N.; SANTOS, R.; ENDRENY, T. Hydraulic complexity at a large river confluence in the Amazon basin. **Ecohydrology**, v. 10, n. 7, 2017. Available from: https://doi.org/10.1002/eco.186.3.

GÜNERALP, I.; MARSTON, R.A. Process-form linkages in meander morphodynamics: bridging theoretical modeling and real world complexity. **Progress in Physical Geography**, v. 36, n. 6, p. 718–746, 2012.

GUTIERREZ, A.; CONTRERAS, V.; RAMIREZ, A. I.; MEJIA, R. Risk zone prediction in meandering rivers by using a multivariate approach. **Journal of Hydrologic Engineering,** v. 19, n. 9, 2014. Available from: https://doi.org/10.1061/(asce)he.1943-5584.0000631.

HALABISKY, M.; BABCOCK, C.; MOSKAI, L. M. Harnessing the temporal dimension to improve object-based image analysis classification of wetlands. **Remote Sensing**, v. 10, n. 9, 2018.

HAQUE, C. E.; ZAMAN, M. Q. Coping with riverbank erosion hazard and displacement in Bangladesh: survival strategies and adjustments. **Disasters**, v. 13, n. 4, p. 300–314, 1989. Available from: https://doi.org/10.1111/j.1467-7717.1989.tb00724.x.

HAN, B.; ENDRENY, T. A. Detailed river stage mapping and head gradient analysis during meander cutoff in a laboratory river. **Water Resources Research**, v. 50, n. 2, p. 1689–1703, 2014.

HASSAN, M. D. S.; MAHMUD-UL-ISLAM, S. Quantification of river bank erosion and bar deposition in Chowhali Upazila, Sirajganj District of Bangladesh: a remote sensing study. **Journal of Geoscience and Environment Protection**, v. 4, n. 1, p. 50–57, 2016. Available from: https://doi.org/10.4236/gep.2016.41006.

HAWES, J. E.; PERES, C. A. Patterns of plant phenology in Amazonian seasonally flooded and unflooded forests. **Biotropica**, v. 48, n. 4, p. 465-475, 2016.

HE, T.; XIAO, W.; ZHAO, Y.L.; DENG, X.; HU, Z. Identification of waterlogging in Eastern China induced by mining subsidence: a case study of Google Earth Engine time-series analysis applied to the Huainan coal field. **Remote Sensing of Environment**, v. 242, 2020. doi:10.1016/j.rse.2020.111742.

HECKENBERGER, M. J.; RUSSELL, J. C.; TONEY, J. R.; SCHMIDT, M. J. The legacy of cultural landscapes in the Brazilian Amazon: implications for biodiversity. **Philosophical Transactions of the Royal Society B: Biological Sciences**, v. 362, p. 197–208, 2007. Available from: https://doi.org/10.1098/rstb.2006.1979.

HEO, J.; DUC, T. A.; CHO, H. S.; CHOI, S. U. Characterization and prediction of meandering channel migration in the GIS environment: a case study of the Sabine River in the USA. **Environmental Monitoring and Assessment**, v. 152, n. 1-4, p. 155–165, 2009.

HESS, L. L.; MELACK, J. M.; AFFONSO, A. G.; BARBOSA, C.; GASTIL-BUHL, M.; NOVO, E. M. L. M. Wetlands of the lowland Amazon Basin: extent, vegetative cover, and dual-season inundated area as mapped with JERS-1 Synthetic Aperture Radar. **Wetlands**, v. 35, n. 4, p. 745–756, 2015. Available from: https://doi.org/10.1007/s13157-015-0666-y.

HIRD, J. N.; DELANCEY, E. R.; MCDERMID, G. J.; KARIYEVA, J. Google Earth Engine, open-access satellite data, and machine learning in support of large-area probabilistic wetland mapping. **Remote Sensing**, v. 9, n. 12, 2017.

HOOKE, J. M. Changes in river meanders: a review of techniques and results of analyses. **Progress in Physical Geography**, v. 8, p. 473–508, 1984.

HOOKE, J. M. Cutoffs galore! occurrence and causes of multiple cutoffs on a meandering river. **Geomorphology**, v. 61, p. 225-238, 2004.

HORTON, A. J. et al. Modification of river meandering by tropical deforestation. **Geology**, v. 45, n. 6, p. 511–514, 2017.

HOSSAIN, M. A.; GAN, T. Y.; BAKI, A. B. M. Assessing morphological changes of the Ganges River using satellite images. **Quaternary International**, v. 304, p. 142–155, 2013. Available from: https://doi.org/10.1016/j.quaint.2013.03.028.

HOWARD, A.D.; KNUTSON, T.R. Sufficient conditions for river meandering: a simulation approach. **Water Resources Research**, v. 20, p. 1659– 1667, 1984. Available from: https://doi.org/10.1029/WR020i011p01659.

IELPI, A.; LAPÔTRE, M. G. A. A tenfold slowdown in river meander migration driven by plant life. **Nature Geoscience**, v. 13, n. 1, p. 82–86, 2020. Available from: https://doi.org/10.1038/s41561-019-0491-7.

ISLAM, M. N.; KHAN, N. A.; REZA, M. M.; RAHMAN, M. M. Vulnerabilities of river erosion–affected coastal communities in Bangladesh: a menu of alternative livelihood options. **Global Social Welfare**, v. 7, p. 353-366, 2020.

ISLAM, M. N. Community-based responses to flood and river erosion hazards in the active Ganges floodplain of Bangladesh. In: SCIENCE AND TECHNOLOGY IN DISASTER RISK REDUCTION IN ASIA: POTENTIALS AND CHALLENGES. **Proceedings...** 2017. p. 301–325. Available from: https://doi.org/10.1016/B978-0-12-812711-7.00018-3.

ISIKDOGAN, F.; BOVIK, A.; PASSALACQUA, P. RivaMap: an automated river analysis and mapping engine. **Remote Sensing of Environment**, v. 202, p. 88–97, 2017. Available from: https://doi.org/10.1016/j.rse.2017.03.044.

JUNK, W. J.; PIEDADE, M. T. F.; SCHÖNGART, J.; COHN-HAFT, M.; ADENEY, J. M.; WITTMANN, F. A classification of major naturally occurring Amazonian lowland wetlands. **Wetlands**, v. 31, p. 623-640, 2011.

JUNK, W. J.; TERESA, M.; PIEDADE, F.; SCHÖNGART, J.; WITTMANN, F. A classification of major natural habitats of Amazonian white-water river floodplains (várzeas). **Wetlands Ecology and Management**, v. 20, p. 461-475, 2012.

JUNK, W. J. **The central Amazon floodplain:** ecology of a pulsing system. Springer; Ecological Studies, 1997. 126p.

JUNK, W.J.; WELCOMME, R.L. Floodplains. In: WETLANDS AND SHALLOW CONTINENTAL WATER BODIES, 1990, The Hague, The Netherlands. **Proceedings…** SPB Academic Publishers, 1990. p. 491–5241.

JUNK, W.; BAYLEY, P. B.; SPARKS, R. E. The flood pulse concept in river-floodplain systems. In: INTERNATIONAL LARGE RIVER SYMPOSIUM (LARS), 106., 1989, Canada. **Proceedings…** Canadian Special Publication of Fisheries and Aquatic Science, 1989. p. 110-127.

KIEDRZYŃSKA, E.; KIEDRZYŃSKI, M.; ZALEWSKI, M. Sustainable floodplain management for flood prevention and water quality improvement. **Natural Hazards**, v. 76, n. 2, p. 955–977, 2015. Available from: https://doi.org/10.1007/s11069-014-1529-1.

KLEINHANS, M. G.; VAN DEN BERG, J. H. River channel and bar patterns explained and predicted by an empirical and physics-based method. **Earth Surface Processes and Landforms**, v. 36, p. 721–738, 2011. doi:10.1002/esp.2090.

KONDOLF, G. M.. **Sacramento River ecological flows study:** off-channel habitat study results. [S.l.]: The Nature Conservancy. 2007. 190 p. Technical report.

KOTHARI, A.; CAMILL, P.; BROWN, J. Conservation as if people also mattered: policy and practice of community-based conservation. **Conservation and Society,** v. 11, p. 1–15, 2013.

LANGENDOEN, E. J. et al. Improved numerical modeling of morphodynamics of rivers with steep banks. **Advances in Water Resources**, v. 93, p. 4–14, 2016.

LATRUBESSE, E. M. et al. Damming the rivers of the Amazon basin. **Nature**, v. 546, 2017. Available from: https://doi.org/10.1038/nature22333.

LEGLEITER, C. J.; HARRISON, L. R.; DUNNE, T. Effect of point bar development on the local force balance governing flow in a simple, meandering gravel bed river. **Journal of Geophysical Research: Earth Surface**, v. 116, n. 1, 2011.

LEITHÄUSER, H.; HOLZHACKER, R. L. Local experience, knowledge, and community adaptations to environmental change: the case of a fishing village in central Vietnam. **Regional Environmental Change**, v. 20, 2020. Available from: https://doi.org/10.1007/s10113-020-01703-9.

LI, H.; HUANG, C.; LIU, Q.; LIU, G. Accretion–erosion dynamics of the yellow river delta and the relationships with runoff and sediment from 1976 to 2018. **Water (Switzerland)**, v. 12, n. 11, 2020. Available from: https://doi.org/10.3390/w12112992.

LI, Z.; WU, X.; GAO, P. Experimental study on the process of neck cutoff and channel adjustment in a highly sinuous meander under constant discharges. **Geomorphology**, v. 327, p. 215–229, 2019.

LIU, Z.; YAO, Z.; WANG, R. Assessing methods of identifying open water bodies using Landsat 8 OLI imagery. **Environment and Earth Science**, v. 75, n. 10, p. 1–13, 2016.

LUIZE, B. G.; MAGALHÃES, J. L. L.; QUEIROZ, H.; LOPES, M. A.; VENTICINQUE, E. M.; DE MORAES NOVO, E. M. L.; SILVA, T. S. F. The tree species pool of Amazonian wetland forests: which species can assemble in periodically waterlogged habitats? **PLoS ONE**, v. 13, n. 5, 2018. Available from: https://doi.org/10.1371/journal.pone.0198130.

MARQUES, R. O.; CARVALHO, J. A. L. Processos fluviais no Rio Amazonas: erosão lateral e emplicações para a cidade de Parintins. **Revista Geonorte**, v. 10, p. 108–132, 2019.

MARTHA, T. R.; SHARMA, A.; KUMAR, K. V. Development of meander cutoffs: a multi-temporal satellite-based observation in parts of Sindh River, Madhya Pradesh, India. **Arabian Journal of Geosciences**, v. 8, p. 5663–5668, 2015.

MARTINELLI, L. A.; FERREIRA, J. R.; VICTORIA, R. L.; MORTATTI, J.; FORSBERG, B. R.; BONASSI, J. A.; DE OLIVEIRA, E.; TANCREDI, A. C. Fluxo de Nutrientes em alguns Rios do Estado de Rondonia, Bacia do Rio Madeira. **Acta Limnologica Brasiliense**, v. 11, p. 911-930, 1988.

MARTINELLI, L. A.; VICTORIA, R. L.; DEVOL, A. H.; FORSBERG, B. R. Suspended sediment load in the Amazon Basin: an overview. **Geojournal**, v. 14, n. 4, p. 381-389, 1989.

MARTINS, V. S. et al. Seasonal and interannual assessment of cloud cover and atmospheric constituents across the Amazon (2000–2015): insights for remote sensing and climate analysis. **ISPRS Journal of Photogrammetry and Remote Sensing**, v. 145, p. 309–327, 2018.

MATTHEWS, E.; FUNG, I. Methane emission from natural wetlands: global distribution, area, and environmental characteristics of sources. **Global Biogeochemical Cycles**, v.1, p. 61-86, 1987.

MATHWORKS. **Bioinformatics Toolbox: User's Guide** (R2012a), 2012.

MCELWEE, P. et al. Working with Indigenous and local knowledge (ILK) in large-scale ecological assessments: reviewing the experience of the IPBES Global Assessment. **Journal of Applied Ecology**, v. 57, p. 1666–1676, 2020.

MCFEETERS, S. K. The use of the Normalized Difference Water Index (NDWI) in the delineation of open water features. **International Journal of Remote Sensing**, v. 17, p. 1425–1432, 1996. doi:10.1080/01431169608948714.

MCGINNIS, D. F.; RANGO, A. Earth resources satellite systems for flood monitoring. **Geophysical Research Letters**, v. 2, n 4, p. 132–135, 1975. Available from: https://doi.org/10.1029/GL002i004p00132.

MEADE, R. H. Suspended sediments of the modern Amazon and Orinoco Rivers. **Quaternary International**, v. 21, p. 29-39, 1994.

MEITZEN, K. M. **Floodplains:** reference module in Earth systems and environmental sciences. [S.l.]: Elsevier, 2018.

MELACK, J. M.; HESS, L.; SIPPEL, S. Remote sensing of lakes and floodplains in the Amazon basin. **Remote Sensing Reviews**, v. 10, n. 3, 1994.

MELLO, C. F.; CARVALHO, D. R. L.; CRUZ, M. J. M. Erosão/sedimentação e o modo de vida ribeirinho na costa do Arapapá – Rio Solimões (AM). **Revista Geonorte**, v. 2, n. 4, p. 377-384, 2012.

MEJIA ÁVILA, D.; SOTO BARRERA, V. C.; MARTÍNEZ LARA, Z. Spatio-temporal modelling of wetland ecosystems using Landsat time series: case of the Bajo Sinú Wetlands Complex (BSWC)– Córdoba– Colombia. **Annals of GIS**, v. 25, p. 231–245, 2019.

MIRANDA, L. E. Fish assemblages in Oxbow Lakes relative to connectivity with the Mississippi River. **Transactions of the American Fisheries Society**, v. 134, n. 6, p.1480–1489. 2005. Available from: https://doi.org/10.1577/t05-057.1.

MOGHADDAM, M. H. R.; SEDIGHI, A.; FAYYAZI, M. A. Applying MNDWI index and linear directional mean analysis for morphological changes in the Zarriné-Rūd River. **Arabian Journal of Geosciences**, v. 8, p. 8419–8428, 2015.

MONIRUL, A. G. M.; ALAM, K.; MUSHTAQ, S; CLARKE, M. L. Vulnerability to climatic change in riparian char and river-bank households in Bangladesh: implication for policy, livelihoods and social development. **Ecological Indicators**, v. 72, p. 23–32 2017.

MONEGAGLIA, F.; ZOLEZZI, G.; GÜNERALP, I.; HENSHAW, A. J.; TUBINO, M. Automated extraction of meandering river morphodynamics from multitemporal remotely sensed data. **Environmental Modelling and Software**, v. 105, p. 171–186, 2018.

MUKHERJEE, R.; BILAS, R.; BISWAS, S. S.; PAL, R. Bank erosion and accretion dynamics explored by GIS techniques in lower Ramganga river, Western Uttar Pradesh, India. **Spatial Information Research**, v. 25, n. 1, p. 23–38, 2017. Available from: https://doi.org/10.1007/s41324-016-0074-2.

NAKANO, D.; NAKAMURA, F. The significance of meandering channel morphology on the diversity and abundance of macroinvertebrates in a lowland river in Japan. **Aquatic Conservation: Marine and Freshwater Ecosystems**, v. 18, p. 780–798, 2008.

NANSON, G.C.; AND HICKIN, E.J. Channel migration and incision on the Beatton River. **Journal of Hydraulic Engineering**, v. 109, n. 3, p. 327–337, 1983. Available from: https://doi.org/10.1061/(ASCE)0733-9429.

NASCIMENTO, L. N.; BECKER, M. L. Hydro-businesses: national and global demands on the São Francisco River basin environment of Brazil. **International Review of Social History**, v. 55, p. 203–233, 2010.

NGUYEN, U. N. T.; PHAM, L. T. H.; DANG, T. D. An automatic water detection approach using Landsat 8 OLI and Google Earth Engine cloud computing to map lakes and reservoirs in New Zealand. **Environmental Monitoring and Assessment**, v. 191, n. 4, 2019. Available from: https://doi.org/10.1007/s10661-019-7355-x.

OBOLEWSKI, K. Macrozoobenthos patterns along environmental gradients and hydrological connectivity of oxbow lakes. **Ecological Engineering**, v. 37, p. 796–805, 2011.

OGAR, E.; PECL, G.; MUSTONEN, T. Science must embrace traditional and indigenous knowledge to solve our biodiversity crisis. **One Earth**, v. 3, n. 2, p. 162–165, 2020. Available from: https://doi.org/10.1016/j.oneear.2020.07.006.

OKI, T.; KANAE, S. Global hydrological cycles and world water resources. **Freshwater Resources**, v. 313, p. 1068-1072, 2006.

OPPERMAN, J.J.; GALLOWAY, G.E.; DUVAIL, S. The multiple benefits of river-floodplain connectivity for people and biodiversity. In: LEVIN, S. A. (Ed.). **Encyclopedia of biodiversity**. [S.l.]: Academic Press, 2013. p.144-160.

PARDO-PASCUAL, J. E.; ALMONACID-CABALLER, J.; RUIZ, L. A.; PALOMAR-VAZQUEZ, J. Automatic extraction of shorelines from Landsat TM and ETM+ multi-temporal images with subpixel precision. **Remote Sensing of Environment**, v. 123, p. 1–11, 2012. Available from: https://doi.org/10.1016/j.rse.2012.02.024.

PARKER, G.; SAWAI, K.; IKEDA, S. Bend theory of river meanders. part 2. nonlinear deformation of finiteamplitude bends. **Journal of Fluid Mechanics**, v. 115, p. 303–314, 1982.

PARSAPOUR-MOGHADDAM, P.; RENNIE, C. D. Influence of meander confinement on hydro-morphodynamics of a cohesive meandering channel. **Water (Switzerland)**, v. 10, 2018.

PATEL, N.; KAUSHAL, B. K. Improvement of user's accuracy through classification of principal component images and stacked temporal images. **Geo-Spatial Information Science**, v. 13, p. 243–248, 2010.

PAUL, B. K.; RASHID, H. **Climatic hazards in coastal Bangladesh:** non-structural and structural solutions. [S.l.]: Elsevier, 2016. 327p.

PEAKALL, J.; ASHWORTH, P. J.; BEST, J. L. Meander-bend evolution, alluvial architecture, and the role of cohesion in sinuous river channels: a flume study. **Journal of Sedimentary Research**, v. 77, p. 197–212, 2007.

PEARCE, J. Development, NGOs, and civil society: the debate and its future. In: EADE, D.; PEARCE, J. (Ed.). **Development, NGOs and civil society**. [S.l.]: Oxfam Publishing, 2000. p. 15–43. Available from: https://doi.org/10.3362/9780855987015.001.

PEDERSEN, E.; WEISNER, S. E. B.; JOHANSSON, M. Wetland areas' direct contributions to residents' well-being entitle them to high cultural ecosystem values. **Science of the Total Environment**, v. 646, p. 1315–1326, 2019.

PEIXOTO, J. M. A.; NELSON, B. W.; WITTMANN, F. Spatial and temporal dynamics of river channel migration and vegetation in central Amazonian white-water floodplains by remote-sensing techniques. **Remote Sensing of Environment**, v. 113, n. 10, p. 2258–2266, 2009. Available from: https://doi.org/10.1016/j.rse.2009.06.015.

PEKEL, J. F.; COTTAM, A.; GORELICK, N.; BELWARD, A. S. High-resolution mapping of global surface water and its long-term changes. **Nature**, v. 540, n. 7633, p. 418–422, 2016.

PENCZAK, T. et al. Fish assemblage changes relative to environmental factors and time in the Warta River, Poland, and its oxbow lakes. **Journal of Fish Biology**, v. 64, p. 483–501, 2004.

PERUCCA, E.; CAMPOREALE, C.; RIDOLFI, L. Significance of the riparian vegetation dynamics on meandering river morphodynamics. **Water Resources Research**, v. 43, n.3, 2007. Available from: https://doi.org/10.1029/2006WR005234.

PETERMANN, P. The birds. In: JUNK, W. J. (Ed.). **The central Amazon floodplain:** ecology of a pulsing system. [S.l.]: Springer, 1997. p. 126.

PEZZUTI, J. et al. Commoning in dynamic environments: community-based management of turtle nesting sites on the lower Amazon floodplain. **Ecology and Society**, v. 23, 2018.

PRICE, M. F. Navigating social–ecological systems: building resilience for complexity and change. **Biological Conservation**, v. 119, n. 4, p. 581, 2004.

RHOADS, B. L.; SCHWARTZ, J. S.; PORTER, S. Stream geomorphology, bank vegetation, and three-dimensional habitat hydraulics for fish in midwestern agricultural streams. **Water Resources Research**, v. 39, n. 8, 2003. Available from: https://doi.org/10.1029/2003WR002294.

RICHEY, J. E.; NOBRE, C.; DESER, C. Amazon River discharge and climate variability: 1903 to 1985. **Science**, v. 246, p. 101-103, 1989.

RÍOS-VILLAMIZAR, E. A.; PIEDADE, M. T. F.; COSTA, J. G.; ADENEY, J. M.; JUNK, W. J. Chemistry of different Amazonian water types for river classification: a preliminary review. **Water and Society**, v. 178, 2014.

ROWLAND, J. C. et al. A morphology independent methodology for quantifying planview river change and characteristics from remotely sensed imagery. **Remote Sensing of Environment**, v. 184, p. 212–228, 2016.

SABO, J.L.; SPONSELLER, R.; DIXON, M.; GADE, K.; HARMS, T.; HEFFERNAN, J.; JANI, A.; KATZ, G.; SOYKAN, C.; WATTS, J. Riparian zones increase regional species richness by harboring different, not more, species. **Ecology**, v. 86, p. 56–62, 2005.

SALO, J.; KALLIOLA, R.; HÄKKINEN, I.; MÄKINEN, Y.; NIEMELÄ, P.; PUHAKKA, M.; COLEY, P.D. River dynamics and the diversity of Amazon lowland forest. **Nature**, v. 322, p. 254–258, 1986.

SARKER, M. N. I.; WU, M.; ALAM, G. M. M.; SHOUSE, R. C. Livelihood vulnerability of riverine-island dwellers in the face of natural disasters in Bangladesh. **Sustainability (Switzerland)**, v. 11, n. 6, 2019. Available from: https://doi.org/10.3390/su11061623.

SARP, G.; OZCELIK, M. Water body extraction and change detection using time series: a case study of Lake Burdur, Turkey. **Journal of Taibah University for Science**, v. 11, n. 3, p. 381–391, 2017. Available from: https://doi.org/10.1016/j.jtusci.2016.04.005.

SCHONHUTH, M. Negotiating with knowledge at development interfaces. In: SILLITOE, P.; BICKER, A.; POTTIER, J. (Ed.). **Participating in development:** approaches to indigenous knowledge. London; New York: Routledge, 2002. p. 139-161.

SCHWENK, J.; FOUFOULA-GEORGIOU, E. Meander cutoffs nonlocally accelerate upstream and downstream migration and channel widening. **Geophysical Research Letters**, v. 43, n. 12, p. 437-445, 2016.

SCHMITT, D. N.; J. H. HORNSBY. **A fisheries survey of the Savannah River:** final report. Project F-30-12. Atlanta: Georgia Department of Natural Resources, Game and Fish Division, 1985.

SCHMIDT, G.; JENKERSON, C.; MASEK, J.; VERMOTE, E.; GAO, F. Landsat Ecosystem Disturbance Adaptive Processing System (LEDAPS) algorithm description. **Open-file Report**, v. 2013-1057, p. 1–27, 2013.

SCHOOK, D. M.; RATHBURN, S. L.; FRIEDMAN, J. M.; WOLF, J. M. A 184-year record of river meander migration from tree rings, aerial imagery, and cross sections. **Geomorphology**, v. 293, p. 227–239, 2017.

SCHWENK, J.; KHANDELWAL, A.; FRATKIN, M.; KUMAR, V.; FOUFOULA-GEORGIOU, E. High spatiotemporal resolution of river planform dynamics from landsat: the rivMAP toolbox and results from the Ucayali river. **Earth and Space Science**, v. 4, p. 46–75, 2017.

SHAHROOD, A. J. et al. RiMARS: an automated river morphodynamics analysis method based on remote sensing multispectral datasets. **Science of the Total Environment**, v. 719, 2020.

SIDHU, N.; PEBESMA, E.; CÂMARA, G. Using Google Earth Engine to detect land cover change: Singapore as a use case. **European Journal of Remote Sensing**, v. 51, n. 1, p. 486-500, 2018.

SILVA, S. M. et al. A dynamic continental moisture gradient drove Amazonian bird diversification. **Science Advances**, v. 5, 2019.

SIQUEIRA-SOUZA, F. K.; FREITAS, C. E. C.; HURD, L. E.; PETRERE, M. Amazon floodplain fish diversity at different scales: do time and place really matter? **Hydrobiologia**, v. 776, n. 1, p. 99–110, 2016. Available from: https://doi.org/10.1007/s10750-016-2738-2.

SINGH, K. V.; SETIA, R.; SAHOO, S.; PRASAD, A.; PATERIYA, B. Evaluation of NDWI and MNDWI for assessment of waterlogging by integrating digital elevation model and groundwater level. **Geocarto International**, v. 30, p. 650–661, 2015.

SIPPEL, S. J.; HAMILTON, S. K.; MELACH, J. M.; NOVO, E. M. M. Passive microwave observations of inundation area and the area/stage relation in the Amazon River floodplain. **International Journal of Remote Sensing**, v. 19, n. 16, p. 3055-3074, 1998.

SIVANPILLAI, R.; JACOBS, K. M.; MATTILIO, C. M.; PISKORSKI, E. V. Rapid flood inundation mapping by differencing water indices from pre- and post-flood Landsat images. **Frontiers of Earth Science**, 2020. doi:10.1007/s11707-020-0818-0.

SOUSA, M. M.; OLIVEIRA, W. Identifcação de feições anômalas dos sistemas de drenagem na região do Alto Juruá – AC/AM, utilizando dados de sensoriamento remoto. **Revista Brasileira de Geografa Física**, v. 9, n. 4, p. 1254–1267, 2016.

SPADA, D.; MOLINARI, P.; BERTOLDI, W.; VITTI, A.; ZOLEZZI, G. Multi-temporal image analysis for fluvial morphological characterization with application to Albanian rivers. **ISPRS International Journal of Geo-Information**, v. 7, 2018.

STANFORD, C. B. et al. Turtles and tortoises are in trouble. **Current Biology**, v. 30, p. R721–R735, 2020.

STØLUM, H. H. Planform geometry and dynamics of meandering rivers. **Bulletin of the Geological Society of America**, v. 110, p. 1485–1498, 1998.

SUIZU, T. M.; NANSON, G. C. Temporal and spatial adjustments of channel migration and planform geometry: responses to ENSO driven climate anomalies on the tropical freely-meandering Aguapeí River, São Paulo, Brazil. **Earth Surface Processes and Landforms**, v. 43, p. 1636–1647, 2018.

SUN, T.; MEAKIN, P.; JØSSANG, T.; SCHWARZ, K. A. simulation model for meandering rivers. **Water Resources Research**, v. 32, n. 9, p. 2937–2954, 1996. Available from: https://doi.org/10.1029/96WR00998.

SZABÓ, S.; GÁCSI, Z.; BALÁZS, B. Specific features of NDVI, NDWI and MNDWI as reflected in land cover categories. **Landscape & Environment**, v. 10, p. 194–202, 2016.

SYLVESTER, Z.; DURKIN, P.; COVAULT, J. A. High curvatures drive river meandering. **Geology**, v. 47, p. 263–266, 2019.

THOMAZ, S. M.; BINI, L. M.; BOZELLI, R. L. Floods increase similarity among aquatic habitats in river-floodplain systems. **Hydrobiologia**, v. 579, n. 1, 1–13, 2007. Available from: https://doi.org/10.1007/s10750-006-0285-y.

THOM, G.; XUE, A. T.; SAWAKUCHI, A. O.; RIBAS, C. C.; HICKERSON, M. J.; ALEIXO, A.; MIYAKI, C. Quaternary climate changes as speciation drivers in the Amazon floodplains. **Science Advances**, v. 6, n. 11, 2020. Available from: https://doi.org/10.1126/sciadv.aax4718.

TOCKNER, K.; STANFORD, J. A. Riverine floodplains: present state and future trends. **Environmental Conservation**, v. 29, p. 308–330, 2002.

TOMASINI, S.; THEILADE, I. Local ecological knowledge indicators for wild plant management: autonomous local monitoring in Prespa, Albania. **Ecological Indicators**, v. 101, p. 1064–1076, 2019.

VAN DIJK, W. M.; VAN DE LAGEWEG, W. I.; KLEINHANS, M. G. Experimental meandering river with chute cutoffs. **Journal of Geophysical Research: Earth Surface**, v. 117, 2012.

VASCONCELLOS, A. M. DE A.; VASCONCELLOS SOBRINHO, M. The meanings of rural community according to nature of community livelihood in Brazilian Amazonia. **Interações (Campo Grande)**, v. 21–30, 2017. Available from: https://doi.org/10.20435/inter.v18i2.1545.

XIA, H. et al. Changes in water surface area during 1989-2017 in the Huai River Basin using Landsat data and Google earth engine. **Remote Sensing**, v. 11, 2019.

XIE, H.; LUO, X.; XU, X.; PAN, H.; TONG, X. Evaluation of Landsat 8 OLI imagery for unsupervised inland water extraction. **International Journal of Remote Sensing**, v. 37, n. 8, p. 1826–1844, 2016. Available from: https://doi.org/10.1080/01431161.2016.1168948.

XIONG, J.; THENKABAIL, P. S.; GUMMA, M. K.; TELUGUNTLA, P.; POEHNELT, J.; CONGALTON, R. G.; YADAV, K.; THAU, D. Automated cropland mapping of continental Africa using Google Earth Engine cloud computing. **ISPRS Journal of Phogrammetry and Remote Sensing**, v. 126, p. 225-244, 2017.

XU, H. Modification of normalised difference water index (NDWI) to enhance open water features in remotely sensed imagery. **International Journal of Remote Sensing**, v. 27,p. 3025–3033, 2006.

YANG, Y.; LIU, Y.; ZHOU, M.; ZHANG, S.; ZHAN, W.; SUN, C.; DUAN, Y. Landsat 8 OLI image based terrestrial water extraction from heterogeneous backgrounds using a reflectance homogenization approach. **Remote Sensing of Environment**, v. 171, p. 14–32, 2015. Available from: https://doi.org/10.1016/j.rse.2015.10.005.

YANG, X.; QIN, Q.; YÉSOU, H.; LEDAUPHIN, T.; KOEHL, M.; GRUSSENMEYER, P.; ZHU, Z. Monthly estimation of the surface water extent in France at a 10-m resolution using Sentinel-2 data. **Remote Sensing of Environment**, v. 244, 2020.

YOUSEFI, S.; POURGHASEMI, H. R.; HOOKE, J.; NAVRATIL, O.; KIDOVÁ, A. Changes in morphometric meander parameters identified on the Karoon River, Iran, using remote sensing data. **Geomorphology**, v. 271, p. 55–64, 2016. Available from: https://doi.org/10.1016/j.geomorph.2016.07.034.

ZEN, S.; GURNELL, A. M.; ZOLEZZI, G.; SURIAN, N. Exploring the role of trees in the evolution of meander bends: The Tagliamento River, Italy. **Water Resources Research**, v. 53, p. 5943–5962, 2017.

ZHOU, T.; ENDRENY, T. The straightening of a river meander leads to extensive losses in flow complexity and ecosystem services. **Water (Switzerland)**, v. 12, n. 6, 2020. Available from: https://doi.org/10.3390/W12061680.

ZINGER, J. A.; RHOADS, B. L.; BEST, J. L; JOHNSON, K. K. Flow structure and channel morphodynamics of meander bend chute cutoffs: a case study of the Wabash River, USA. **Journal of Geophysical Research: Earth Surface**, v. 118, p. 2468–2487, 2013.

ZHU, Z. Change detection using landsat time series: a review of frequencies, preprocessing, algorithms, and applications. **ISPRS Journal of Protogrammetry and Remote Sensing**, v. 130, p. 370-384, 2017.

WALKER, J. J.; SOULARD, C. E.; PETRAKIS, R. E. Integrating stream gage data and Landsat imagery to complete time-series of surface water extents in Central Valley, California. **International Journal of Applied Earth Observation and Geoinformation**, v. 84, p. 101973, 2020.

WANG, L.; XU, M.; LIU, Y.; LIU, H.; BECK, R.; REIF, M.; EMERY, E.; YOUNG, J.; WU, Q. Mapping freshwater chlorophyll-a concentrations at a regional scale integrating multi-sensor satellite observations with google earth engine. **Remote Sensing,** v. 12, n. 20, p. 1–18, 2020.

WANG, C.; JIA, M.; CHEN, N.; WANG, W. Long-term surface water dynamics analysis based on landsat imagery and the Google Earth Engine Platform: a case study in the middle Yangtze River Basin. **Remote Sensing**, v. 10, 2018.

WANG, C.; JIA, M.; CHEN, N.; WANG, W. Long-term surface water dynamics analysis based on landsat imagery and the Google Earth Engine Platform: a case study in the middle Yangtze River Basin. **Remote Sensing**, v. 10, n. 10, 2018. Available from: https://doi.org/10.3390/rs10101635.

WARD, J. V.; TOCKNER, K.; SCHIEMER, F. Biodiversity of floodplain river ecosystems: ecotones and connectivity. **River Research and Applications**, v. 15, n. 3, p. 125-139, 1999.

WEISSCHER, S. A. H.; SHIMIZU, Y.; KLEINHANS, M. G. Upstream perturbation and floodplain formation effects on chute-cutoff-dominated meandering river pattern and dynamics. **Earth Surface Processes and Landforms**, v. 44, p. 2156–2169, 2019.

WENGER, E. **Communities of practice:** a brief introduction. [S.l.]: Etienne and Beverly, 2011.

WULDER, M. A. et al. Current status of Landsat program, science, and applications. **Remote Sensing of Environment**, v. 225, p. 127-147, 2019.